Provenance and Tectonic Setting of Sandstone Unit in Both Tanjero and Gercus Formations: Implication by Geochemistry and Geochronology, Kurdistan Region, Northeastern Iraq

A thesis
Submitted to the Council of College of Science at the University of Sulaimani in Partial Fulfillment of the Requirements for the Degree of Doctor of Philosophy in Geology
(Sedimentology)

By
Derin Muhammad Sadiq
B.Sc. Geology (1998), University of Sulaimani
MSc. Sedimentology (2010), University of Sulaimani

Supervised By
Dr. Nabaz Rashid Hama Aziz
Assistant Professor

February 2020 **Reşeme 2719**

Supervisors' Certification

I certify that this thesis entitled (Provenance and Tectonic Setting of Sandstone Unit in Both Tanjero and Gercus Formations: Implication by Geochemistry and Geochronology, Kurdistan Region, Northeastern Iraq) was prepared under my supervision at the Department of Geology, College of Science, University of Sulaimani in partial fulfillment of the requirements for the degree of Doctor of Philosophy in Sedimentology.

Signature:

Supervisor: Dr. Nabaz Rashid Hama Aziz

Scientific Title: Assistant Professor

Date:

In view of the available recommendations, I forward this thesis for debate by the examining committee.

Signature:

Name: Dr. Mushir Mustafa Baziany

Head of Geology Department

Date:

ACKNOWLEDGEMENTS

Thanks to Almighty God for giving me this opportunity to complete this thesis, my appreciate goes to the Presidency of Sulaimani University, College of Science and department of Geology for giving me this opportunity to obtain the degree of Doctor of Philosophy in Science.

My sincere gratitude goes to my supervisor Dr. Nabaz Rashid Hama Aziz for his guidance, continued support, engorgement and his professional advice throughout the whole process of my thesis writing. I would like to thank Prof. Dr. Khalid Jalal Aswad, Dept. of Geology, university of Mosul for his critical reading of my thesis and his valuable discussion.

My warmest thanks go to, Dr. Yousif Osman Mohammad who gave me unlimited supports for his suggestion and comments during the field work and during preparation of my Thesis.

I would like to express my thanks to Prof. Kamal Haji for his support from their critical disscutions.

Special thanks go to head of Department of Geology, Dr. Mushir Baziany for providing available facilities and administrative support.

I am also very grateful to Mr. Hiwa Jamal for his help of computer programing.

My appreciation also goes to my collegue Parween for her entire assistance throughout my study and writing my thesis.

I am seriously in to my family who helped me through to pass the most difficult time during my study. It is their presence who urged me to be where I am today.

Thereby, I dedicate this work to my parents and my lovely daughter Mina.

ABSTRACT

Detrital zircon (DZ) U-Pb geochronology,petrography and whole-rock geochemistry were used to characterize Upper Cretaceous and Middle Eocene clastic rocks from the Tanjero flysch and Gercus molasse, NE Iraq. These data were also used to constrain provenance of the lithified clasts and to evaluate the tectonic evolution of the Northern Zagros Orogenic Belt. The petrography of the sandstone rocks of the Tanjero Formation reveals poor sorting and rapid deposition. The LILE concentration in the studied samples is lower than the corresponding values for the upper continental crust (UCC). Post-Archean Australian Shale (PAAS) indicating the dominant sources have mafic and ultramafic signatures, with some of the cratonic material. Major and trace element geochemical data reveal that Tanjero samples show slight chemical maturity than Gercus samples and both were subjected to moderate weathering. The youngest zircon age population in Tanjero flysch yields,an age of 93Ma which coincides closely in age with Albian-Cenomanian arc -dominated magmatic event (i.e. 106–92 Ma). In addition to later age, however, the detrital zircon U-Pb data set shows a strong episodic age distribution: 400, 448, 511, 553, 646, 779, 878, 996 and 1121 Ma sggest multicycle derivation from mostly Neoproterozoic basement of the Arabian-Nubian Shield that were at some point hosted by Early Pliensbachian - Turonian Qulqula radiolarite basin which was located along Arabian passive margin. The DZ U-Pb measurements revealed that the Gercus Molasse fall into several separable age population ranges from 92-102 (Albian-Cenomanian), 221 (Upper Triassic), 395-511 (Cambrian), 570-645 (Neoproterozoic), 1111 (Mesoprotrozoic), and lesser numbers of Paleoproterozoic (1622-1991 Ma) ages. The source of Proterozoic detrital Zircons is enigmatic; the age peaks at 1.1, 1.5, 1.6, and 1.9 Ga (Proterozoic) which may sugges that these analyses is interpreted as indicating that the zircons are derived from Arabian crystalline basement. The detrital zircons

with age populations at 0.63–0.86 Ga probably originated from the Arabian-Nubian Shield. The age peak at 0.55 Ga correlates with Cadomian Magmatism reported from north Gondwana. The age peaks at ~0.4 Ga is interpreted to represent Gondwana rifting and the opening of Paleotethys. The youngest ages populations at 93 Ma indicate that fraction of DZ were transported directly from the contemporaneously active magmatic arc. The DZ U-Pb age spectra from the Gercus Formation suggess that the foreland sediments either influx from multiple mixed provenances or the result of recycling from the accretionary complex terrane (Qulqula Radiolarite 221Ma).

LIST OF CONTENTS

Content		Page No.
Acknowledgements……		I
Abstract……..		II
List of Content……		IV
List of figure……...		VII
List of table……		XIII
CHAPTER ONE: INTRODUCTION		
1.1	Preface…….....	1
1.2	Location of the study area……..	2
1.3	Previous…….	4
1.4	Aim of Study…….	6
1.5	Tectonic setting…….	6
1.6	Geology of the studied areas……..	9
1.6.1	Tanjero Formation…….	9
1.6.2	Gercus Formation……..	13
1.7	Material and Methods……	15
1.7.1	Sampling…….....	15
1.7.2	Methodology……..	18
CHAPTER TWO: PETROGRAPHY AND MINERALOGY		
2.1	Preface……	21
2.2	Petrography of Tanjero……..	22
2.3	Petrography of Gercus……	25
2.4	Mineralogy…….	27
2.4.1	Quartz…….	27
2.4.2	Calcite……	27
2.4.3	Dolomite……	27
2.4.4	Feldspar……..	28

2.4.5 Rock fragmets…… 29
2.4.6 Matrix……. 31
2.4.7 Cement……... 31
2.4.8 Heavy Minerals…….. 33

CHAPTER THREE: GEOCHEMISTRY

3.1 Preface…… 43
3.2 Geochemistry of major oxides……... 44
3.2.1 SiO_2…… 44
3.2.2 TiO_2 ……... 46
3.2.3 Al_2O_3…….. 46
3.2.4 Fe_2O_3 ……. 47
3.2.5 MnO……... 47
3.2.6 MgO……... 47
3.2.7 CaO…… 48
3.2.8 K_2O…… 48
3.2.9 Na_2O……... 50
3.2.10 P_2O_5…… 50
3.2.11 LOI……. 51
3.3 Trace elements……... 53
3.3.1 High field strength elements (HFSE)……. 53
3.3.2 Large ion lithophile elements (LILE)…… 55
3.3.3 Transition trace elements (TTE)…… 57
3.4 Geochemical Classfication…….. 61
3.5 REE elements……. 62
3.6 Spider diagrams…….. 65

CHAPTER FOUR: GEOCHRONOLOGY

4.1 Preface…… 73

4.2 Detrital Zircon U-Pb Geochronology…… 73
4.3 Data integration and geological implications…… 76

CHAPTER FIVE: PROVENANCE

5.1 Preface…… 85
5.2 Provenance …… 85
5.2.1 Major elements chemistry and tectonic setting…….. 85
5.2.1.1 Total alkalis-Silca (TAS) diagram for the Sandstone of both Tanjero and Gercus Formations …… 85
5.2.1.2 Zr/TiO_2-SiO_2…… 86
5.2.2 Trace elements chemistry and tectonic setting…… 87
5.2.2.1 Y/Ni vs. Cr/V diagram……... 87
5.2.2.2 Th vs Sc diagram…… 89
5-2-3 Source area weathering…….. 91
5.3 Tectonic Setting……. 93
5.4 Provenance demarcations……. 97
5.5 Timing and duration of Tanjero and Gercus clastic rocks……... 98
5.5.1 Tanjero Flysch……... 98
5.5.2 Cercus Molasse …… 100
5.6 Tectonic implication …… 102

CHAPTER SIX: CONCLUSIONS AND RECOMMENDATIONS

6.1 Conclusions…… 106
6.2 Recommendations…….. 109
References……. 110

LIST OF FIGURES

Figure No.	Figure Title	Page No.
1.1	Regional tectono-stratigraphic map for NE Iraq shows the location of the study area…….	3
1.2	Tectonic Zones and structural elements of the Unstable Shelf (Jassim and Goff, 2006)……...	6
1.3	Lithological section of the Tanjero Formation A: Chwarta section, B: Dokan section. Fm-formation, Thic-thickness…	10
1.4	Lithological section of Gercus Formation……...	12
1.5	Regional tectonostratigraphic map for the NW Zagros belt across Iraq shows distribution of the upper Cretaceous and Palogene succession. After Koshnaw et al., (2017); A-A$^{/}$ and D-D$^{/}$ indicate the studied sections of the Tanjero clastic; H-H$^{/}$ and Q-Q$^{/}$ indicate the studied section of the Gercus clastic rocks……..	14
1.6	a- Field photograph of sandstone beds of Tanjero Formation in Chwarta section 2 km west of Mokaba village. B- Coarse sandstone parasequence about 10m thick, 2 km west of Dokan town……	16
1.7	a- Field photograph of sandstone beds of Tanjero Formation in Chwarta section, near Tagaran village…….	16
1.8	Field photograph of a- Alternation of red claystone, sandstone and marl of Gercus Formation along road cut in Jabal Habiat-Sultan. Koya area; b- Red sandstone layer within Gercus Formation……..	17

1.9 Field photograph of a- sandstone layer within Gercus Formation in Haibat-Sultan area; d- view of Gercus Formation near Wazyara village. Qaradax Mountain…….. 17

2.1 Photomicrographs of Tanjero lithic-arenite; A- Coarse lithic-arenite; B- mono- and poly-Quartz grains; texture sand with fossil debris; C-D Lithic arenite with plagioclase and chert rock fragment……... 24

2.2 Photomicrographs of Gercus lithic-arenite rocks; A- lithic-arenite rocks were poorly sorted and angular to subrounded grain morphology; B- Chert fragment; C- deformed plagioclase; D- dolostone RF; E&F- plutonic RF…… 26

2.3 Photomicrographs of A-monoQuartz;B-polyquartz;C-Calcite; D-Deformed Plagioclase…… 29

2.4 Mineralogical classification of the clastic rocks in the Tanjero and Gercus Formation (Pettijohn, 1975); Q: Total quartz; F: Total Feldspar; RF: Total rock fragments…… 32

2.5 Backscattered image of Cr-spinel; a & b Tanjero lith-arenite, c & d; Gercus lith-arenite……. 35

2.6 Photomicrographs of Zircon in Tanjero and Gercus (A and B), Apatite in Tanjero and Gercus (C and D), respectively……. 37

2.7 Photomicrograph of Tourmaline in Gercus Clastic rocks……. 38

2.8 Photomicrographs of selected Rutile minerals in the Tanjero clastic rocks (A-D) and Gercus clastic rocks (E and F)…… 39

2.9 Epidote minerals in A-Tanjero; B- Gercus clastic rocks….. 39

2.10 Photomicrograph of pyroxene in a-Tanjero; B-Gercus……. 41

2.11 Photomicrograph of Serpentine minerals in A- Tanjero; B-Gercus……. 42

3.1 Binary relationship diagram SiO_2, TiO2, Fe_2O_3 and MnO Vs. Al_2O_3…….. 45

3.2 Binary relation diagram of MgO, CaO, K_2O and Na_2O vs. Al_2O_3……. 49

3.3 Binary relation diagram of P_2O_5 and LOI vs. Al_2O_3…….. 51

3.4 Variation diagram of HFSE vs. La for Tanjero and Gercus clastics……... 54

3.5 Variation diagram of LILE in Tanjero and Gercus clastics... 56

3.6 Variation diagram of TTE vs. La for Tanjero and Gercus clastics……. 59

3.7 Geochemical classification of Tanjero and Gercus clastic rocks using Log (SiO_2/Al_2O_3 vs. Log (Na_2O/K_2O) ratios (Pittijohn, et al., 1987)……. 61

3.8 Chondrite-Normalized REE pattern of the Tanjero (T). Normalizing values (after sun and McDonugh, 1989). PAAS and UCC normalizing values (after Taylor and McLennan, 1985)…… 64

3.9 Chondrite-normalized REE pattern of the Gercus (G) clastics. Normalizing values (after sun and McDonugh, 1989). PAAS and UCC normalizing values (after Taylor and McLennan, 1985)……..... 65

3.10 NMORB normalized plots for Tanjero clastic samples. Normalizing values (after sun and McDonough, 1989)……... 67

3.11 NMORB normalized plots for Gercus clastic samples. Normalizing values (after sun and McDonough, 1989)……. 68

4.1 Concordia age of the analyzed zircons standards; A- Plesovice Reference Age 337Ma and B- Temora 2 Reference Age 416 Ma…… 69

4.2 Concordia diagram of dated detrital zircons from Tanjero Formation shows different concordant points indicates a wide spectrum of Concordia age (Ma). These data excluded the highly discordant analyses…… 72

4.3 Concordia diagram of dated detrital zircons from Gercus Formation shows different concordant points indicate a wide spectrum of Concordia age (Ma). These data excluded the highly discordant analyses……..... 75

4.4 Age probability distribution diagram depicting detrital zircon U-Pb ages of Tanjero Formation…….. 77

4.5 Age probability distribution diagram depicting detrital zircon U-Pb ages of Gercus Formation ……... 78

5.1 A) Total alkalis-silica source rock classification diagram (TAS; Lebas et al., 1986). B) Zr/TiO_2-SiO_2 after Winchester and Floyd (1977)…….. 80

5.2 Plot Cr/V versus Y/Ni ratios (Hiscott, 1984) showing the ultramafic and felsic sediment supply to the foreland basin. The diagram shows a mixing line of ultrabasic (Cr/V = 45; Y/Ni = 0.001) and granitic (Cr/V = 0.093; Y/Ni = 8.889) rocks (Turekian and Wedepohl 1961; Dinelli et al. 1999). Percentages show the extent of ultrabasic addition to the mixture……... 82

5.3 Th vs. Sc for Tanjero and Gercus clastic samples (after McLennan et al., 1993)…….. 83

5.4 A) V-Ni-Th ternary diagram for Tanjero and Gercus clastic rocks (from Bracciali, et al., 2007). CaO + MgO- Na_2O+ K_2O- SiO_2/10 after Taylor and McLenan 1985.B) CaO + MgO- Na_2O+ K_2O- SiO_2/10 after Taylor and McLenan 1985…… 85

5.5 A)Major element plots (SiO_2 vs Al_2O_3+ Na_2O+K_2O) of the Tanjero and Gercus samples to recognize chemical maturity as a function of palaeoclimatic conditions, after (Suttner & Dutta, 1986). B) Al_2O_3 - CaO + Na_2O - K_2O ternary diagram after Nesbitt and Young (1984), showing the relationship between Tanjero……... 86

5.6 The Plot of the trace element composition of Tanjero and Gercus clastic rocks on the Th-Sc-Zr/10 tectonic setting discrimination diagram (After Bataia and Crook, 1986). OIA: Oceanic Island Arc; CIA: Continental Island Arc; ACM: Active Continental Margin; PM:Passive continental Margin……... 88

5.7 Tectonic interpretation diagram (Ternary plots) of detrital components in Tanjero and Gercus sandstones on the tectonic provenance discrimination diagram of (Dickinson, 1983). B) Tectonic interpretation diagrams (A) Ternary plots of detrital components in the Tanjero and Gercus sandstones on the tectonic provenance discrimination diagram of Dickinson et al. (1983). Qt is the total quartz, F is the feldspar, and RF is the total rock fragments. The solid lines mark the major fields of provenance in terms of tectonic setting……

91

5.8 Nb/Yb vs Th/Yb diagram for Tanjero and Gercus clastic rocks, after (Pearce, 2008). SZ—subduction zone enrichment; CC—crustal contamination; F—fractional crystallization; WPE—within plate enrichment…… 92

5.9 Summary of detrital zircon age spectra of the Tanjero clastic NE Iraq versus the main tectono-magmatic events of Arabian Plate……. 95

5.10 Summary of detrital zircon age spectra of the Gercus clastic, NE Iraq versus the main tectono-magmatic events of Arabian Plate……. 98

5.11 Schematic diagram presenting the tectonic evolution model (Hypothesis A) of the Tanjero clastic rocks within the Foreland basin……. 101

5.12 Simplified tectonic evolution model (Hypothesis B) showing erosion in the both of Ophiolite material and Qulqula Radiolarite transported directly to the Tanjero flaych basin……. 101

LIST OF TABLES

Table No.	Table Title	Page No.
1.1	The latitude, longitude and location of the selected sections of the Tanjero (T) and the Gercus (G) clastic samples……..	3
2.1	Modal analyses of the Tanjero and Gercus samples……..	23
2.2	Percentage and average of the heavy minerals in both Tanjero and Gercus samples…….	33
3.1	Major oxide (Wt. %) concentrations of the Tanjero and the Gercus clastic rocks……	53
3.2	Trace concentration (ppm) of the Tanjero and the Gercus clastic rocks……	61
3.3	Concentration (ppm) of REEs in Tanjero and Gercus clastics……...	69
3.4 A	Correlation coefficient matrix and scatter diagram of major elements in the Tanjero samples…….	70
3.4 B	Correlation coefficient matrix and scatter diagram of major elements in the Gercus samples…….	71
3.5 A	Correlation coefficient matrix and scatter diagram of major elements in the Tanjero samples……	72
3.5 B	Correlation coefficient matrix and scatter diagram of major elements in the Gercus samples……	73

4.1 DZ U–Pb isotopes of the Sandston samples in Tanjero Formation…… 80

4.2 DZ U–Pb isotopes of the Sandston samples in Gercus Formation……. 83

Chapter One

Introduction

1.1 Preface

Clastic sediment packages are geological archives that record and preserve signatures of past geological events in source provinces, during transport, at the depocentre (Dickinson and Suczek, 1979; Bhatia, 1983).

Flysch and molasse facies are well known orogenic sediments and recognized on the basis of difference of lithology, depositional environment and time relation tectonics uplift (Karim, 2004). Flysch sediments is comprised deep marine sediments (mainly turbidites and other gravity flow sediments) which deposited during syn-tectonic phase of orogeny, while molasse sediments consist mainly of sandstone and conglomerate with predominance of red color which deposited in nonmarine or shallow marine environment during post-tectonic phase of orogeny (Pettijohn, 1975; Potter and Pettijohn, 1987; Bate and Jackson, 1980; Mial, 1990).

The Upper Cretaceous Tanjero and the Middle Eocene Gercus Formations are typical flysch and molasse facies. Both flysch and molasse facies were deposited in the foreland basin of the Zagroside Orogeny (Ditmar et al., 1972; Buday, 1980; Al-Qayim, 1993 and 1995a; Kamal et al., 2007). The Foreland basins in Iraq is located between the Arabian craton and the Alpine orogen which is now commonly called the Zagros Fold Zone. The flysch to molasse transition in peripheral foreland basins has been interpreted as recording the passage of the thrust wedge over the passive margin of the under-thrust plate (Stockmal and Beaumont, 1987). Heavy minerals typically comprise ~1% of clastic sediments. Each heavy mineral grain is a

unique messenger of coded data, carrying the details of its' ancestry and the vicissitudes of its sedimentary history (Mange and Maurer, 1992; Mange and Wright, 2007). Analysis of heavy minerals in foreland basin sequences may thus prove valuable in constraining the structural histories of both the basin and the tectonic hinterlands (Mange and Maurer, 1992).

This study considers the source and petrogenesis of the Sandstone rocks within both Tanjero and Cercus Formations in the Foreland basin using the heavy minerals, new detrital zircon U-pb geochronology and whole rock major, trace and rear earth elements geochemistry.

1.2 Location of the Study Area

The study area is located within Sulaimani and Erbil Governorate in northeastern Iraq (Fig. 1.1). Two representative sections (Dokan and Mawat-Chwarta) were sampled for the Tanjero clastic rocks (Table 1). The Dokan section placed with longitude E 44° 57$^{/}$ 28$^{//}$ – E 44° 55$^{/}$ 10$^{//}$ and latitude N 35° 55$^{/}$ 45$^{//}$- N 35° 56$^{/}$ 45$^{//}$and is situated along Qashqoli river. The Chwarta-Mawat section placed with longitude (E 45° 26$^{/}$ 44$^{//}$- E 44° 52$^{/}$ 49$^{//}$) and latitude (N 35° 46$^{/}$ 33$^{//}$- N 35° 59$^{/}$ 19$^{//}$) and situated within Kuna-Masi and Tagaran villages. The Gercus sections are situated between longitude (E 44° 39$^{/}$ 28$^{//}$- E 44° 54$^{/}$ 58$^{//}$) and latitude (N 36° 06$^{/}$ 43$^{//}$- N 35° 55$^{/}$ 28$^{//}$) from Kilka-Smaq area stretching south to Qaradagh mauntain. The Qaradagh section is situated between longitude (E 45° 21$^{/}$ 21$^{//}$- E 45° 21$^{/}$ 8$^{//}$) and latitude (N 35 16$^{/}$ 02$^{//}$- N 35 16$^{/}$ 33$^{//}$).

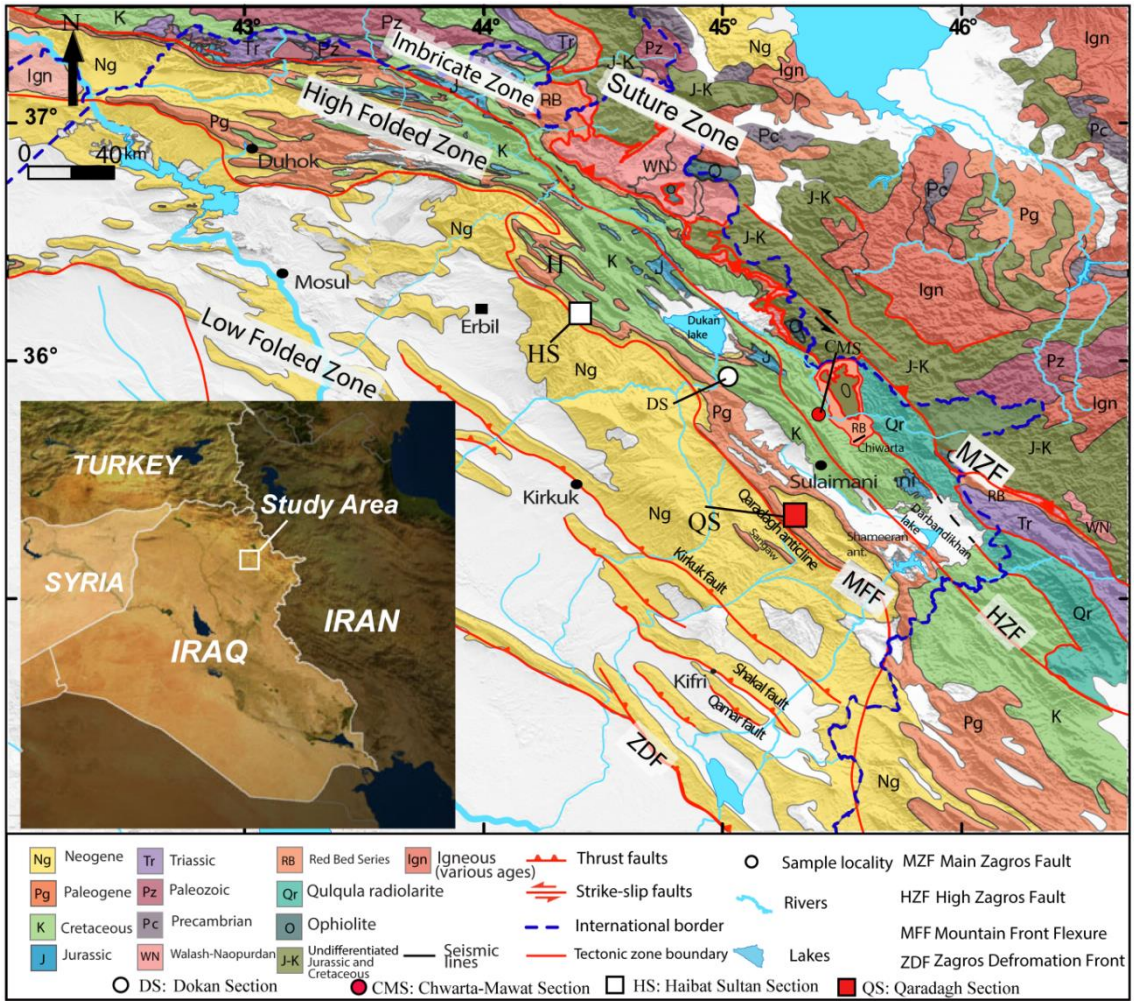

Fig. (1.1) Regional tectonostratigraphic map for the NW Zagros belt across Iraq shows distribution of the upper Cretaceous, Palogene succession and the location of the selected sections for Tanjero and Gercus Formation, After Koshnaw et al., (2017).

Table (1.1): The latitude, longitude and location of the selected sections of the Tanjero (T) and the Gercus (G) clastic samples

Sample	Section	Locality	Latitude	longitude
T1- T10	Dokan (D-D′)	Sara Anticline Qashqoli River	N 35º 55′ 45″ - N 35º 56′ 45″	E 44º 57′ 28″ - E 44º 55′ 10″
T11-T20	Mawat-Chwarta (A-A′)	Kuna Masi-Tagaran villages	N 35º 46′ 33″- N 35º 59′ 19″-	E 45º 26’ 44’’- E 44º 52’ 49’’-
G1-G10	Koya-Dokan H-H′	Hiabat Sultan klka-smaq	N 36º 06′ 43″ - N 35º 55′ 28″ -	E 44º 39’ 28’’- E 44º 54’ 58’’-
G11-G20	Qaradqgh Q-Q'	Wazyara	N 35º 16′ 02″ - N35º 16′ 33″	E 45º 21′ 21″ - E 45º 21′ 38″

1.3 Previous studies

The clastic rock parts of both flysch (Tanjero Formation) and molasse (Gercus Formation) of the Kurdistan foreland basin, NE Iraq were limited to geochemical and geochronological investigations. The Tanjero Formation is well studied in most aspects of sedimentology and paleontology by many researchers (Bellen et al., 1959; Kassab, 1972; 1975, Buday, 1980; Al-Rawi, 1981; Buday and Jassim, 1987; Saadallah and Hassan, 1987; Jaza, 1992; Lawa et al., 1998; Al-Rawi and Al-Rawi, 2002; Karim, 2004; Karim and Surdashy, 2005; Jassim and Goff, 2006).

A few and limited geochemical studies have been done by Al-Nakib and Dhannoun (2014) in where they, have studied the impact of sharp changes in source rocks on the geochemistry of Tanjero formation in Dokan district, northeast Iraq. They have concluded that a sharp increase in the mafic and ultramafic source rocks elements (Cr, Ni, Co, Sc and V), and an obvious

decrease in the felsic source rocks elements (Y, Rb, Zr, Hf, Th) changes in the geochemical characteristics of the formation occur. The changes involved the emplacement of island arc volcanics and ophiolites onto the ridge separating the foreland basin to the west and southwest from the Neo-Tethys to the east and northeast in which the emplacement of these mafic and ultramafic rocks is undoubtedly related to the different stages of the collision of the Arabian Plate with Eurasian Plate.

Koshnaw et al (2017), has studied Neogene shortening and exhumation of the Zagros fold-thrust belt and foreland basin in the Kurdistan region of northern Iraq. The only single grain detrital zircon U-Pb age signature of the Tanjero Formation shows a unimodal population centered at ~100 Ma, indicative of ophiolitic derivation. Ali and Mohammed (2018) has studied the geochemistry and provenance of sandstone unit in Tanjero Formation in Sulimania and Pira-Magron Area, NE-Iraq. He concluded that Geochemical classification of the an Upper Cretaceous Tanjero sandstone clastic rocks are lithic arenites to Fe-Sand and indicates that they were mainly derived from Albian-Cenomanian Gimo–Qandil sequence ophiolite-bearing terrane and Hemipelagic sediments (Parautochthonous Qulqula rocks).

Previous investigation of the Middle Eocene Gercus formation included the study of sedimentology, stratigraphy and palaeontology (Dhannoun et al., 1988; Ameen, 2006; Karim et al., 2007; Al-Qayimet al., 2007; Sa’ad et al., 2013; 2014; Hussain & Aghwan, 2015; Karim et al., 2018). there have been no Whole-rock geochemical and detrital zircon geochronology studies.

1.4 Aims of the study

The main aim of the present thesis can be summarized in the following points:

1- Separation and identification of heavy minerals in siliciclastic rocks within the Tanjero flysch and the Gercus molasse sediments.
2- Petrography and mineralogy of detrital heavy minerals.
3- Whole-rock geochemistry of major, trace and REE elements of both Tanjero Flysch and Gercus molasse sediments
4- Age determination of detrital zircon by U-Pb dating.
5- Provenance study of flysch and molasse units in the Kurdistan foreland basin.
6- Tectonic setting of flysch and molasse sediments.

1.5 Tectonic Setting

Jassim and Buday (2006) have divided Iraq into three tectonically different areas, **the Stable Shelf** with major buried arches and antiforms but no surface anticlines; **the Unstable Shelf** with surface anticlines, and the **Zagros Suture Zone** which comprise thrust sheets of radiolarian chert, igneous and metamorphic rocks (Fig 1.2). These three areas contain tectonic subdivisions which trend N-E in the Stable Shelf and NE-SW or E-W in the Unstable Shelf and the Zagros Suture. The N-E trend is due to Palaeozoic tectonic movements. The E-W and NE-SW trends are due to Cretaceous-Recent Alpine orogenesis. The Unstable Shelf is subdivided into Foothill Zone; High folded Zone and Imbricate Zone. The Tanjero Formation crops out in the high folded and also in the Imbricate Zone (Fig. 1.2).

The Zagros Suture formed within the Neo-Tethys were thrusted over the Arabian Plate during two distinct phases of obduction and collision, during Late Cretaceous and Miocene-Pliocene. Aswad (1999) has presented a new tectonic subdivision of the Zagros Suture Zone in the Mawat-Chwarta area based on Allochthony versus Autochthony criteria (plate tectonic and sea floor spreading theory). He has subdivided the area into five successions from bottom to the tope:

1- Para autochthon unit (Qulqula Radiolarite).
2- Neo-autochthon (Upper Cretaceous Tanjero flysch).
3- Tertiary Sedimentary Cover (Red bed series).
4- Nappe Walash-Naopurdan Allochthon
5- Nappe Mawat Allochthone.

According to Aswads' subdivision, the Tanjero flysch comprise part of the unstable zone (high folded and imbricate Zone), while the Gercus molasse comprise the Tertiary sedimentary Cover.

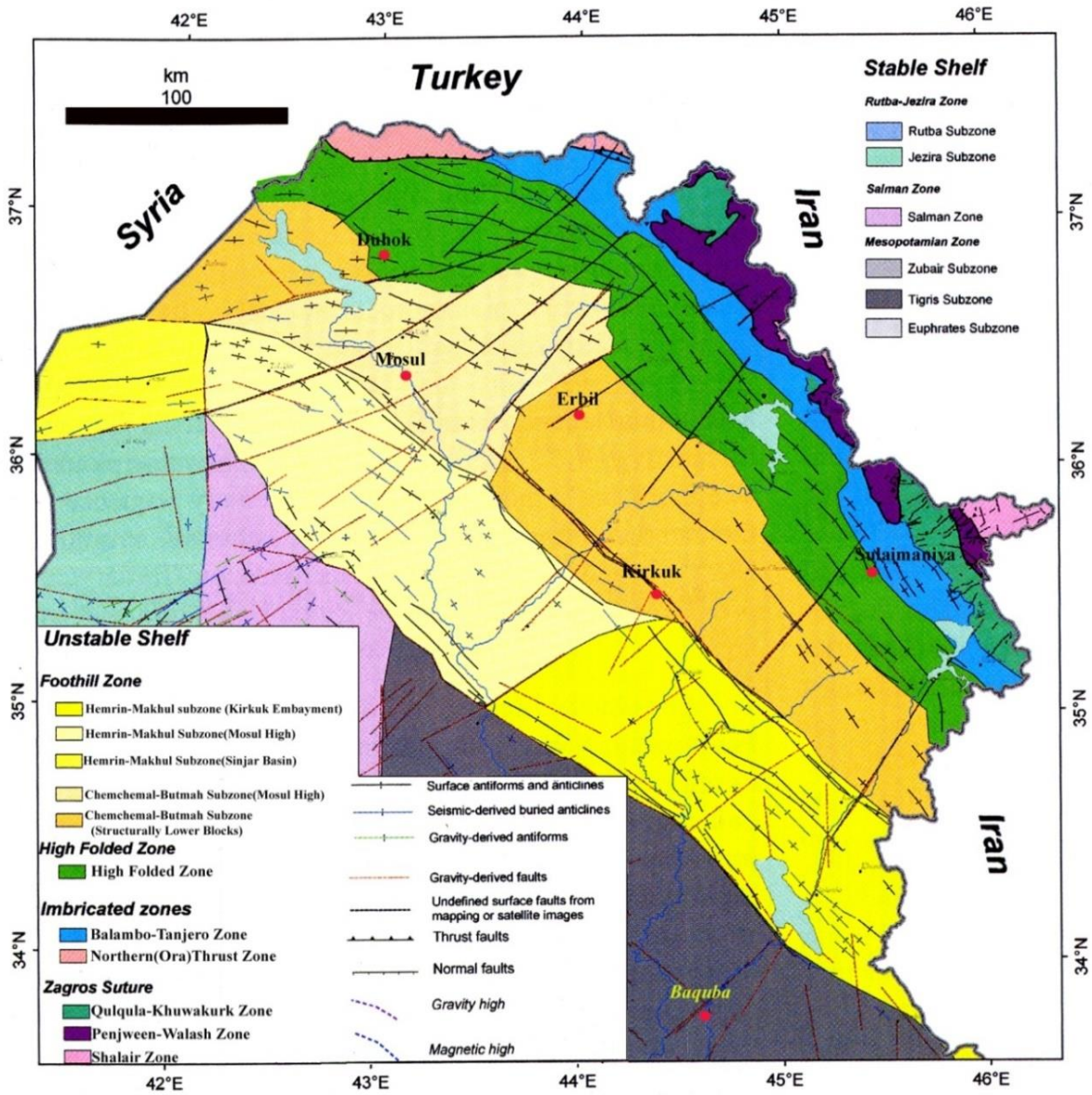

Fig. (1.2) Tectonic Zones and structural elements of the Unstable Shelf (Jassim and Goff, 2006)

1.6 Geology of the study area:

The flysch and molasse facies are represented by Tanjero (Upper Cretaceous) Formation, while the Gercus (Middle –Late Eocene) Formation is typical molasse facies in the study area (Buday, 1980; Buday and Jassim, 1987).

1.6.1 Tanjero Formation (flysch facies)

Tanjero Formation stretches as narrow northwest-southeast belt near and parallel to the Iranian border, which developed during the early stage of collision between the Arabian margin and the Tethyan subduction complex to the northeast (Buday1980; 1987).

The lower part of the Tanjero was intensively deformed and folded. It consist of thin beds of brown silty laminated sandstone repeated several times with dark greenish calcareous gray shale reflected active tectonic alternation of pebbly sandstone and siltstone. The upper part of the formation contains reddish pebbly sand interbedded with brown siltstone with ripple mark structure (Fig 1.3). In the Chwarta-Mawat section, 10 samples were collected in Kuna-Masi and Tagaran localities. The Tanjero Formation in this area is very close to the contact of the Red Bed Series.

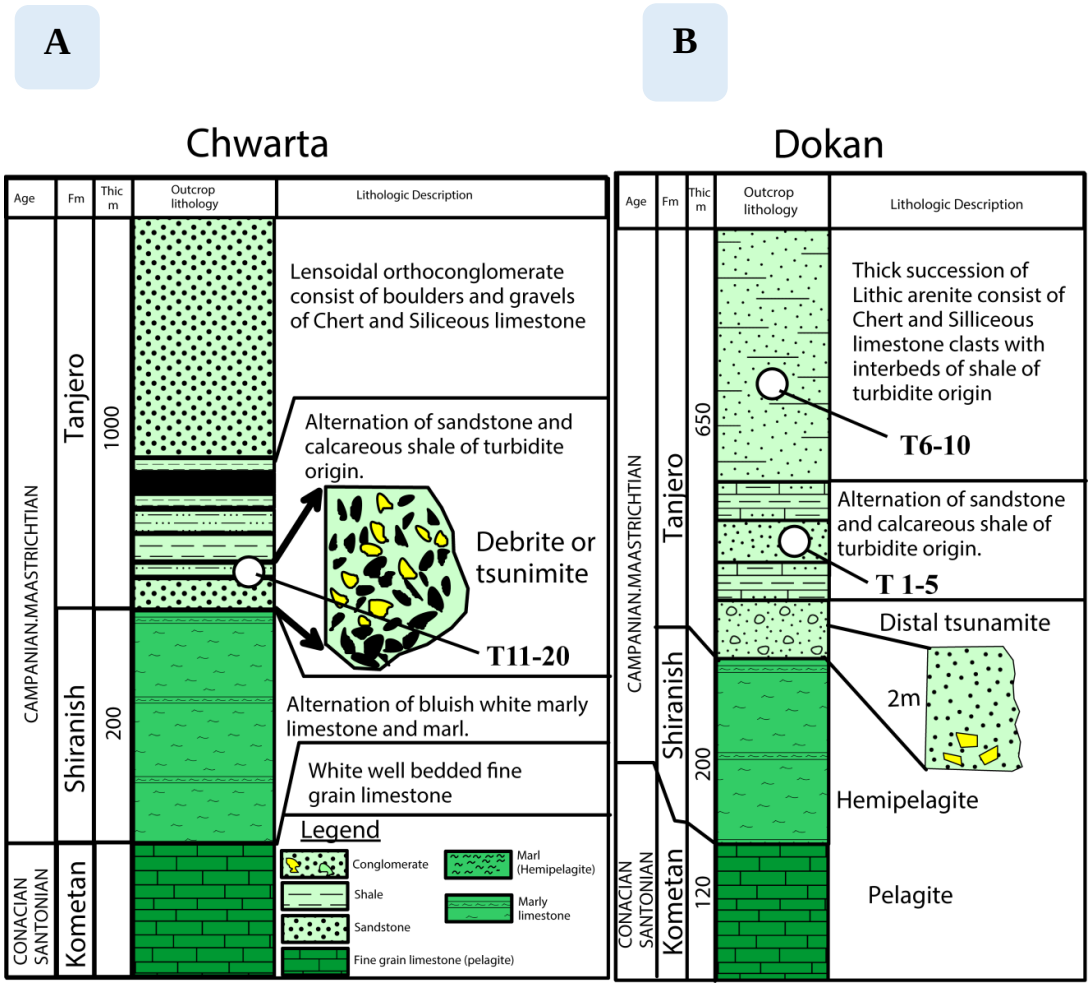

Fig. (1.3) Lithological section of the Tanjero Formation A: Chwarta section, B: Dokan section. Fm-formation, Thic-thickness

Bellen et al. (1959) have defined the Tanjero Formation for the first time and has described it under the name of Tanjero clastic Formation at Sirwan Valley, 1 km to the south of Kani Karweshkan village, near Halabja Town. Dunnington (1952 in Bellen et al. 1959) has divided the formation based on lithology in the type section, into lower and upper parts. The upper part consists of silty marls, siltstone, sandstone, conglomerate and sandy biogenic detrital limestone; this part is 1532 meters thick. The lower part is 484 meters thick and composed of pelagic marl with some siltstone and rare

marly limestone. The forementioned division is based only on the lithologic variation of the type section in the Sirwan valley and has not taken into consideration the other areas. This division is later, followed by all other researchers such as Buday (1980), Al-Rawi (1981), Abdul-Kireem (1986), Jaza, (1991) Saaddlla and Hassan (1987).

Kassab (1972 and 1975) has studied biostratigraphy of the formation and gave the age of Late Campanian -Maastrichtian to the formation. Al-Mehaidi (1975) has discussed briefly the stratigraphy and tectonic of the formation within the Chuarta area and the occurrence of the Aqra Formation in the upper part of Tanjero Formation as a lentil. Al-Rawi (1981) studied in detail the sedimentology, and petrology of the formation in selected section (Sulaimaniya, Dokan and Rawandoz sections). He has mentioned that the lower part at Sulaimaniya has a shallow environment of deposition and concluded that the paleocurrent is toward northwest and flow parallel to the axis of the Tanjero trough. He has studied in detail the clay mineralogy and sandstone of the formation. He has also classified the sandstones according to Pettijohn (1975) and plotted them on triangles.

Abdul-Kireem (1986 a) has studied the formation within stratigraphy of Upper Cretaceous and Lower Tertiary of Sulaimani- Dokan Region. He suggests that removing the word “clastic” from the name of the formation and to put the lower part with Shiranish Formation. Abdul-Kireem (1986 b) studied planktonic forams and stratigraphy of Tanjero Formation. He has assigned, for the formation, the age of Middle-Late Maastrichtian in Dokan area.

Saadallah and Hassan (1987) have made sedimentological analysis of the formation in selected sections from Dokan and Sulaimaniya areas. They have concluded that the paleocurrent is toward west and southwest. The

most recent and detailed study is that of Jaza (1992) which is concerned with sedimentary facies analysis of the formation in the selected sections from Sulaimaniya district. He has recognized the turbidite and submarine fan (as depositional feature of the basin) in the formation. He divides the rock body of the formation into sixteen lithofacies and suggests further detailed study of the formation to reconstruct depositional model for the whole basin and its relation to tectonics. Minas (1997) studies sequence stratigraphy of the formation and puts Tanjero Formation in deeper environment than Shiranish Formation.

Al–Rawi and Al-Rawi (2002) have studied the formation as turbidite example of flysch type in northeast and north of Iraq. They concluded that the formation deposited in deep environment except the limestone beds which are deposited in shallow one.

Karim (2004) and Karim and Surdashy (2005) have put Tanjero Formation in Early Zagros Foreland basin for the first time and have concluded that paleo-current direction was toward south and southwest during Maastrichtian. They have found a very thick succession of conglomerate (500m thick) at Chwarta, Mawat and Qandil area and have correlated this conglomerate with lower part of Tanjero Formation (Fig.1.3). They have further added that the foreland basin formed by continental colliding of Arabian and Iranian during Campanian.

Sharbazheri (2008) has studied the upper boundary of the formation with Kolosh Formation and has proved a gradational (conformable) contact between the two formations by planktonic foraminifera boizonation.

According to Ali et al., 2014 the Tanjero Formation is equivalent in age to the Amiran Formation in Iran, and they are considered to represent typical peripheral foreland deposits.

1.6.2 Gercus Formation:

The Gercus Formation forms part of the Paleogene successions in northern Iraq, have been represented by a thick section of Middle-Late Eocene clastic sediments. A complete section of these rocks form an outcrop in the northeastern side of Jabal Hiabat Sultan in the Unstable Folded Zone (Al-Rawi, 1980; Ai-Qayim, 1994; Jassim & Goff, 2006). Typical molasse facies of the Middle Paleocene–Eocene Megasequence (Jassim & Buday, 2006), are predominantly distinctive Gercus of continental clastic sediments consisting of conglomerates, sandstones and mudstones with some carbonates and evaporites (Fig. 1.4).

The name of the Gercus Formation was first introduced by Maxson (1936, in van Bellen et al., 1959). The type section is approximately 20 km north of Midayat in southern Turkey. In northeastern Iraq, the formation crops mainly several kilometers north of the boundary between High and Low Folded Zones. It extends along a relatively narrow belt in the northwest-southeast direction from eastern to northern Iraq (Buday, 1980; Al-Rawi, 1983; Buday & Jassim, 1987, Jassim & Goff, 2006; Hussain & Aghwan, 2015) and continues northwest into southeast Turkey (Tasman, 1949). To the southeast, the Kashkan Formation in Iran (James & Wynd, 1965) seems to be similar, in most aspects, to the Gercus Formation, including its age (Fig. 1.4). A detailed sedimentological study reveals that this rock accumulated in three main distinct facies associations: aeolian, fluvial and lacustrine. Al-Qayim and Al-Shaibani (1991) have suggested that sediments in the Gercus Formation are deposited in a clastic-dominated tidal flat. On the basis of main lithological distribution, the formation was divided by Ameen (1998) into three parts (lower, middle, upper). The Gercus Formation was deposited in a foreland basin type. This basin (north-northeast Iraq) is a

peripheral flexural foreland basin bordering the Accretionary Complex Terrane (ACT). The ACT developed during the protracted plate convergence between the Arabian and Eurasian Plates due to subduction-collision episodes is composed of serpentinite matrix-mélange and Qulqula radiolarites (Aswad et al., 2011).

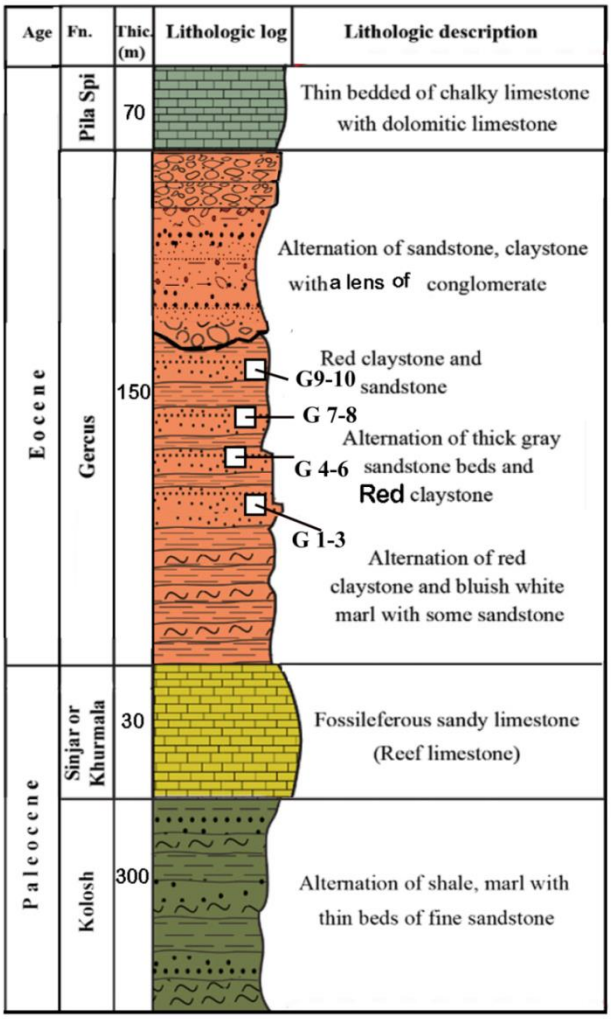

Fig. (1.4) Lithological section of Gercus Formation

1.7 Material and Method

1.7.1 Sampling

Extensive field work has determined the occurrence and spatial distribution of clastic rocks within the Tanjero and Gercus formation in different localities Northeastern Iraq (Fig. 1.1). A total of 10 samples were collected along a vertical section of Tanjero Formation (given the symbol T) exposed at Dokan district in northeast Iraq at the southwest flank of Sara anticline and across the Qashqoli river in the High Folded Zone. The samples are systematically collected near the contact of the Shiranish Formation trough the appearance of thick beds of sandstone (Fig. 1.5 and 1.6).

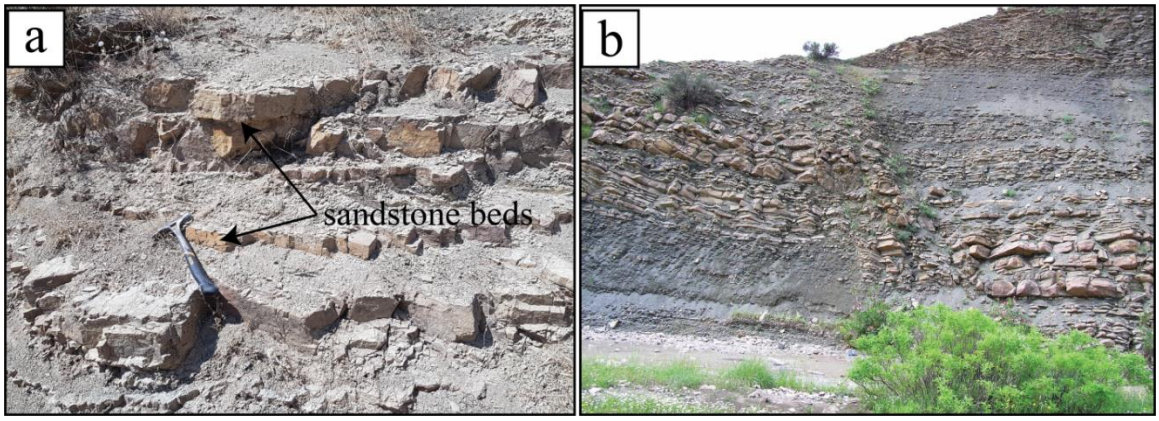

Fig. (1.5) a- Field photograph of sandstone beds of Tanjero Formation in Chwarta section 2 km west of Mokaba village. B- Coarse sandstone parasequence about 10m thick, 2 km west of Dokan town.

Fig. (1.6) Field photograph of sandstone beds of Tanjero Formation in Chwarta section, near Tagaran village.

A well exposed Gercus clastic section cropping out above Chenarook village, NE side of Hiabat Sultan Mountain, Erbil district, in NE Iraq (Fig.1.7 and 1.8). Ten samples of the Gercus clastic rock were collected from Dokan (klka-smaq) and Koya (Hiabat Sultan) locality, while in Qaradqgh (Wazyara), and Garmian (Basara) sections, ten samples were collected (given the symbol G). The latituiude, longitude and location of samples were given in the (Table 1).

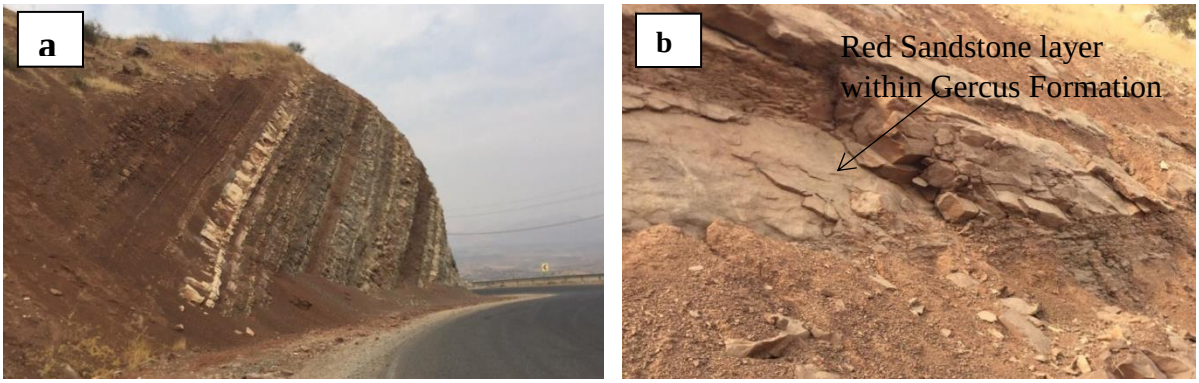

Fig. (1.7) Field photograph of a- Alternation of red claystone, sandstone and marl of Gercus Formation along road cut in Jabal Habiat-Sultan. Koya area; b- Red sandstone layer within Gercus Formation.

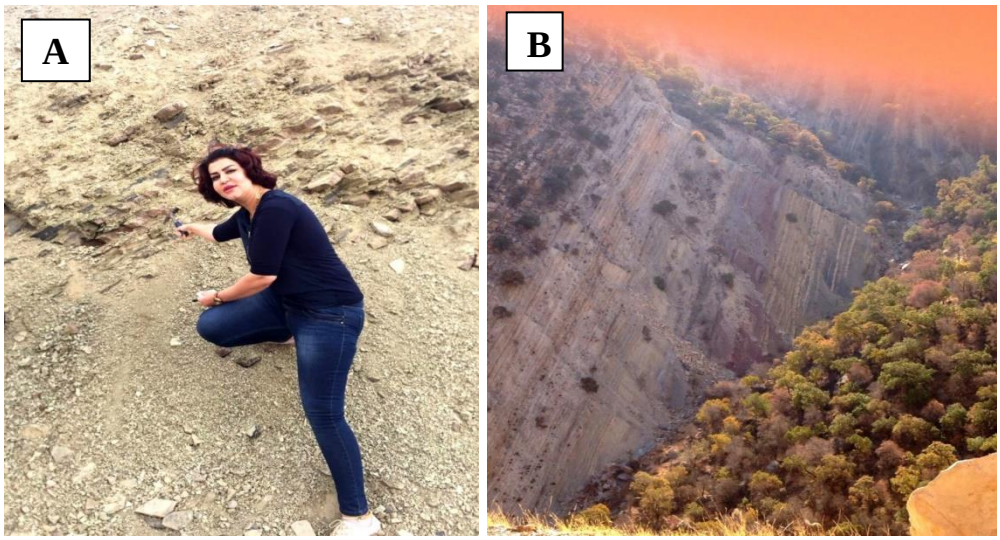

Fig. (1.8) Field photograph of a- sandstone layer within Gercus Formation in Haibat-Sultan area; d- view of Gercus Formation near Wazyara village. Qaradax Mountain.

1.7.2 Methodology

In the current study, various conventional analytical techniques were used for extraction, petrographical, geochemical and chronological studies as follows:

1- Extraction of the detrital heavy minerals at both geochemical laboratory, University of Sulaimani and ORIGINANAL YTICAL Ltd. At Welsh pool city, Great Britain. The procedures for heavy mineral separation was followed according to Carver (1971), these procedures to are outlined below:

a- Concentrated diluted acetic acid (10%) was added to each sample in order to remove the carbonates, and then, to leave the sample for 24 hrs, the samples were washed by water.

b- Concentrated H_2O_2 (20%) was added to each sample in order to remove the organic materials and for disintegration of the small sandstone chips. The samples were washed by decantation for several times.

c- Each sample was washed by water through a 230 mesh sieve (63 microns) in order to remove all the silts and clays.

d- The 2.5Ø, 3Ø, 3.5Ø and 4Ø size graded which were obtained by dry sieving were mixed together.

e- 5 grams of these sizes were used for heavy / light mineral separation.

f- Using heavy liquid Bromoform ($CHBr_3$) with a specific gravity of 2.89. The separation was accelerated by centrifuging for 20 minutes with a speed of 3000c/s.

g- After centrifuging sink sample in ice at the time it will be freeze.

h- The heavy mineral fraction was then washed on filter paper with acetone, dried out and part of them mounted on glass slides with Canada balsam for petrographic study.

i- The heavy minerals were identified using a binocular microscope and polarizing petrographic microscope in the petrography laboratory, department of geology, University of Sulaimani.

2- Identification of all detrital heavy minerals use semi-automated SEM- with backscattered images for each heavy mineral for the Tanjero and Gercus siliciclastic rocks at the Ltd in Welshpool, United Kingdom .

a- An aliquot of ca. 2000-4000 grains from each sample were mounted into epoxy resin, polished and carbon coated.

b- Each sample was then analyzed using the Zeiss EVO MA10 SEM, coupled with an Oxford Instruments 80mm^2 EDS detector with Aztec software

c- Heavy mineral identification used the "Feature" module of Aztec.

3- Petrographic point counting:

Twenty thin sections of representative samples (Ten for each Tanjero and Gercus clastic rocks) were examined to achieve mineralogical classification of the Tanjero and the Gercus clastic samples at original analytical Ltd in Welshpool, United Kingdom. Using high resolution petrography approach, in which all of the particles are carefully and forensically classified. The analysis includes full descriptions, determination of mineralogical abundances based on traditional or Gazzi-Dickinson's point counting approaches which was described by Ingersoll & Suczek(1979), and involves

counting of 300 points per slide (300 points at 0.04 mm intervals on each sample). This method puts fine-grained lithic fragments that do not have individual crystals larger than 0.0625 mm in the lithic fragment pole.

4- Whole-rock geochemical analysis:

Bulk-rock major, trace and rare earth elements (REEs) for twenty clastic rocks (10 samples for each Tanjero and Gercus) were determined at the ALS Laboratory Group SL Seville Spain, using ICP-MS with the Lithium Borate fusion method as a whole rock package encoding ME-MS 81d.

5- U-Pb geochronology:

Detrital zircon grains in a mixture samples (T1, T5, T10, T12, T16 and T20) of the Tanjero and (G1, G5, G10, G12 and G15) of the Gercus clastic rocks were separated using conventional density and magnetic separation techniques. This was repeated several times due to the low zircon content in the samples. Zircon U-Pb dating was determined by the use of an Analytik Jena PQ Elite ICP-MS coupled with an ASI resolution 193-nm excimer laser ablation system on 30 and 35 zircon grains in the mixture samples of Tanjero and Gercus , respectively. Analytical parameters and standardization approach followed by detailed in Papapavlou et al., (2017), Precambrian Research. Zircon analyses were normalized to the BB9 zircon RM, with Plesovice and Temora 2 run as secondary standards. All results and concordia diagrams are presented in tables 4.1 and 4.2.

CHAPTER TWO

PETROGRAPHY

2.1 Preface

Sandstone petrography is a classical technique for characterizing constitute of sandstones and describing their porosity and permeability. It also provides valuable insights into transport history, depositional setting and diagenetic alterations of sediments and sedimentary rocks. Traditional petrographic studies typically involve the point counting of quartz, feldspar and lithic fragments together with the distribution of authigenic phases and diagenetic studies. The varieties of quartz grains (monocrystalline (undulose, non undulose) and poly-crystaline (2-3 crystal units per grain, Unstretched >3 crystal units per grain and Stretched >3 crystal units per grain), feldspar composition, heavy mineral/opaque types and shape, and specific count of lithic clast varieties are all used to provide invaluable provenance information and sandstone classification. In the present study, we have used high resolution petrography approach, in which all of the particles are carefully and forensically classified and the analysis includes full descriptions, determination of mineralogical abundances based on traditional or Gazzi-Dickinson's point counting approaches which was described by Ingersoll et al. (1984). This method is important for deducing the provenance of arenite in relation to tectonic and magmatism. The results are presented in tables 2.1.

2.2 Petrography of Tanjero sandstone rocks

The Petrographic study of the Tanjero clastic rocks revealed diverse mineralogical constitutes based on point- counting results (Table 2.1). The Tanjero lithic vary from fine to coarse grained (Fig. 2.1 A). The average quartz content was 9.53 % in the 10 Tanjero samples (Table 2.1). Monocrystalline and poly-crystalline quartz grains were proportionally minor in the samples. The monocrystalline quartz grains were angular to sub-rounded whereas ploy-crystalline grains were sub-angular to sub-rounded (Fig. 2.1 B). The rock fragments found in the sandstones were diverse with some proportional constituent differences. The common fragments were limestones (typically micritic, very finely peloidal or foraminiferal; Fig. 2.1 E&F), chert, intermediate volcanic and plutonic rocks (Fig. 2.1 C&D), undifferentiated metamorphic fragments and a few clastic mudstones. Feldspars were comparatively common and dominantly represented by plagioclase (including relatively fresh/tabular grains; Fig. 2.1 E). Phyllosilicate grains have occurred as a common biotite mica with lesser chlorite and rare muscovite mica. The accessory grains were mostly represented by very common benthic foraminifera (mostly larger forms that were possibly reworked/recycled; Fig. 2.1 D&F), rare phosphatic grains/fragments, and rare opaque detrital grains and rare traces of both rutile and hypersthene heavy minerals. Note that the interstitial detrital clays were locally intermixed with organic and probably at least in part, represent a pseudomatrix. Metamorphic lithic grains are common and represented by serpentine minerals. The authigenic cement was dominated by pervasive, pore-filling, non-ferroan calcite, typically occurring as relatively coarse pore-filling spar and very rarely as grain-coating isopachous crusts, partially surrounding some lithic grains/foraminifera. Rare microcrystalline siderite, hematite and pyrite were also very finely disseminated locally.

Table (2.1) Modal analyses of the Tanjero and Gercus samples

Sample ID	Quartz%		Feldspar	Rock fragment					Phyllosilicate & Accessories	Matrix	Cement	Clays	Porosity
	Mono	Poly		Sed	Meta	Ign	Chert	Total RF					
T2	2.6	3.43	6.19	29.66	2.95	6.25	14.7	53.56	4.62	6.29	19.82	0.95	2.54
T3	3	1.42	10.5	36.4	2.5	7.3	10.2	56.4	6.08	6.1	13.1	0.9	2.5
T4	6	2.9	6.5	35.5	3.3	8.1	9.7	56.6	1.15	5.5	18.2	0.82	2.33
T6	5	3.3	9.7	34.9	2.7	9.2	10.2	57	5.28	6.8	10.2	0.31	2.41
T8	7.9	4	8.4	32.7	2.4	9.5	11.38	55.98	3.59	7.2	10.5	0.43	2
T10	10	4	6.6	30.5	3.2	7.55	10.8	52.05	7.43	5.5	11.4	0.93	2.1
T11	7.1	2.2	5.6	35.7	2.5	7.4	12.8	58.4	2.26	6.9	13.9	0.64	3
T13	11	5.8	8.7	29.5	4.8	7.1	10.8	52.2	1.87	7.3	10.5	0.51	2.12
T16	4	1	8.3	37.8	2	6.7	10.3	56.8	4.59	7.4	14.7	0.55	2.66
T19	7.3	3.3	6.5	37.3	2.6	9.9	9.9	59.7	1.45	6.1	12.6	0.95	2.1
Av.	6.39	3.14	7.699	33.996	3.3	8.31	11.078		4.74	6.75	14.54	0.68	2.54
Sample ID	Quartz%		Feldspar	Rock fragment					**Phyllosilicate & Accessories**	Matrix	Cement	Clays	Porosity
	Mono	Poly		Sed	Meta	Ign	Chert	Total RF					
G2	8.3	2.3	4.3	35.24	1.3	9.4	8.2	54.14	2	9.4	18.43	0.8	0.33
G4	11.3	1.42	5,1	33.4	2.5	8.3	8.5	52.7	2.3	6.1	17.68	0.9	2.5
G6	10.5	2.9	4.2	40.2	3.3	8.1	10.4	62	1.8	5.5	11.95	0.82	2.33
G5	17.8	4.3	3.8	30.7	2.7	7.2	9.7	50.3	1.12	6.8	13.16	0.31	2.41
G10	13.9	4	5.6	35.5	2.4	7.5	8.38	53.78	2.2	7.2	10.89	0.43	2
G12	9.4	4	3.6	34.9	3.2	5.5	8.6	52.2	3.3	7.5	15.84	0.93	2.83
G14	10.1	2.2	5.3	41.4	2.5	7.4	12.6	63.9	1.1	6.9	8.56	0.44	3.5
G16	9.9	5.8	4.9	37.9	4.8	8.5	7.7	58.9	1.9	6.7	9.27	0.51	2.12
G18	7.9	1	4.5	38.9	2	4.7	9.2	54.8	1.6	7.4	19.59	0.55	2.66
G19	8.3	3.3	3.9	43.4	2.6	9.9	9.5	65.4	2.4	6.1	7.74	0.96	1.9
Av.	10.74	3.122	4.46	37.154	2.73	7.65	9.278		1.972	6.96	13.311	0.665	2.258

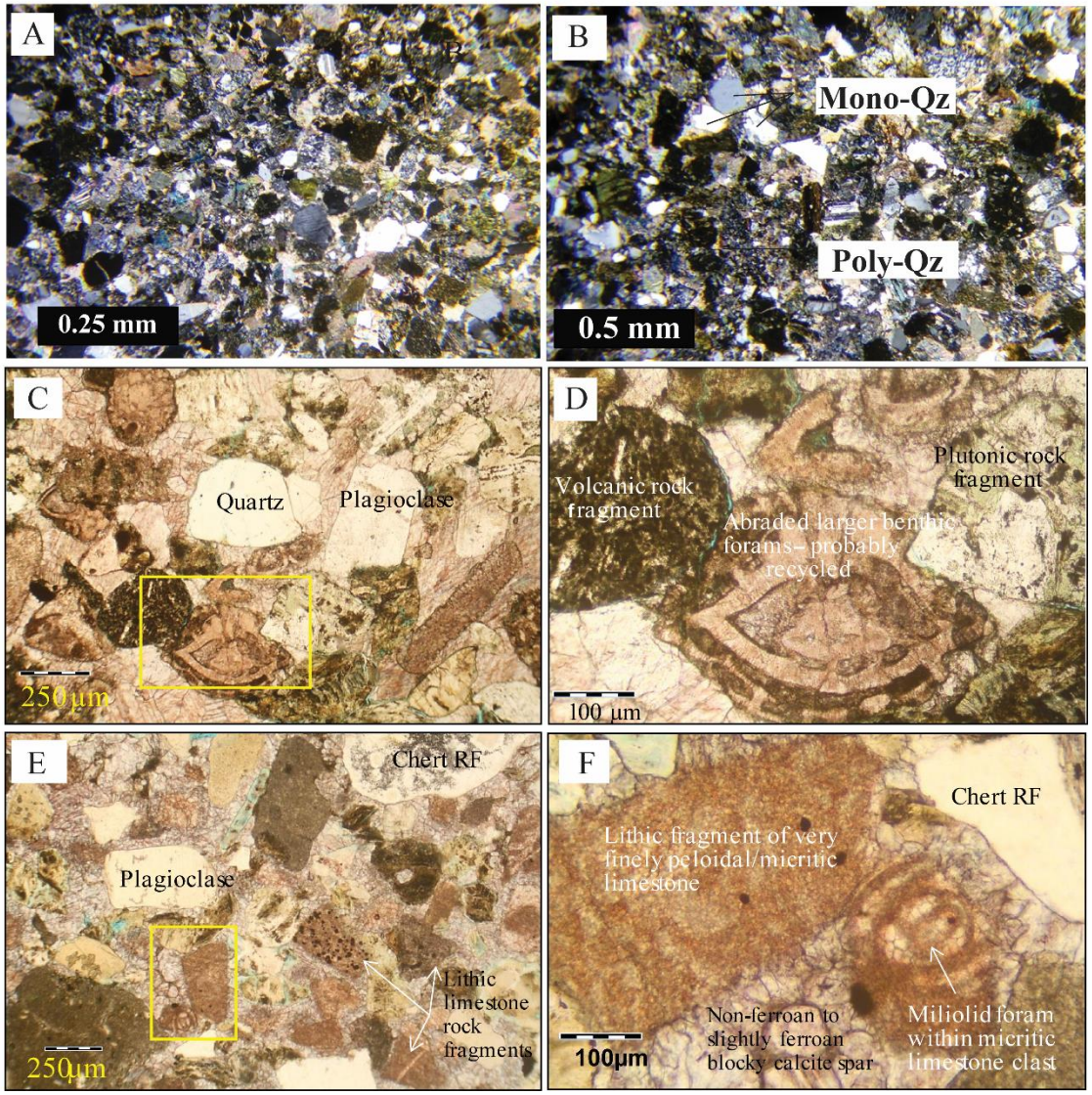

Fig. (2.1) Photomicrographs of Tanjero lithic-arenite; A- Coarse lithic-arenite; B- mono- and poly-Quartz grains; texture sand with fossil debris; C-D Lithic arenite with plagioclase and chert rock fragment

2.3 Petrography of Gercus sandstone rocks

The texture and mineralogy of the Gercus formation were highly variable between locations due in part to the formation length of more than 1,000 km along the Zagros and Taurus belts inside Iran, Iraq and Turkey. Due to textural and mineralogical diversity, the Gercus sandstone had several classifications, including chert-carbonate and Quartz-chert lithic wacke and, less commonly, chert-carbonate and Quartz-chert lithic arenite (Ameen, 2006; Al-Mashaikie et al., 2014). (1982) and as lithic-arenites Pettijohns (1975) classification chart (Fig. 2.4). The lithic-arenite rocks were poorly sorted and angular to subrounded grain morphology (Fig. 2.2 A) Matrix-supported, which was massive at a thin section scale, demonstrated possible rare lamellar fenestral voids, suggestive of some degree of lamination. Compaction was impossible to determine, as the samples were matrix-supported. Detrital grain mineralogy was characterized primarily as monocrystalline quartz and rarely as polycrystalline quartz or feldspar (plagioclase coarse deformed grains; Fig. 2.2 C). Very common lithic rock fragments were predominantly chert (including silicified limestone clasts (Fig. 2.1 B) and dolostone rock fragments (DRF – Fig. 2.2 D). Additional lithic grains included rare fragments of limestone, siliciclastic mudstone, phyllite/schist, and plutonic and volcanic fragments (Fig. 2.1 F). Phyllosilicate grains occurred as rare biotite mica, rare chlorite and rare muscovite mica (grading to an unresolvable illitic/sericitic matrix). Accessory grains such as moderately common detrital opaque grains, phosphatic grains/pellets, rutile and hypersthene/orthopyroxene heavy minerals were observed.

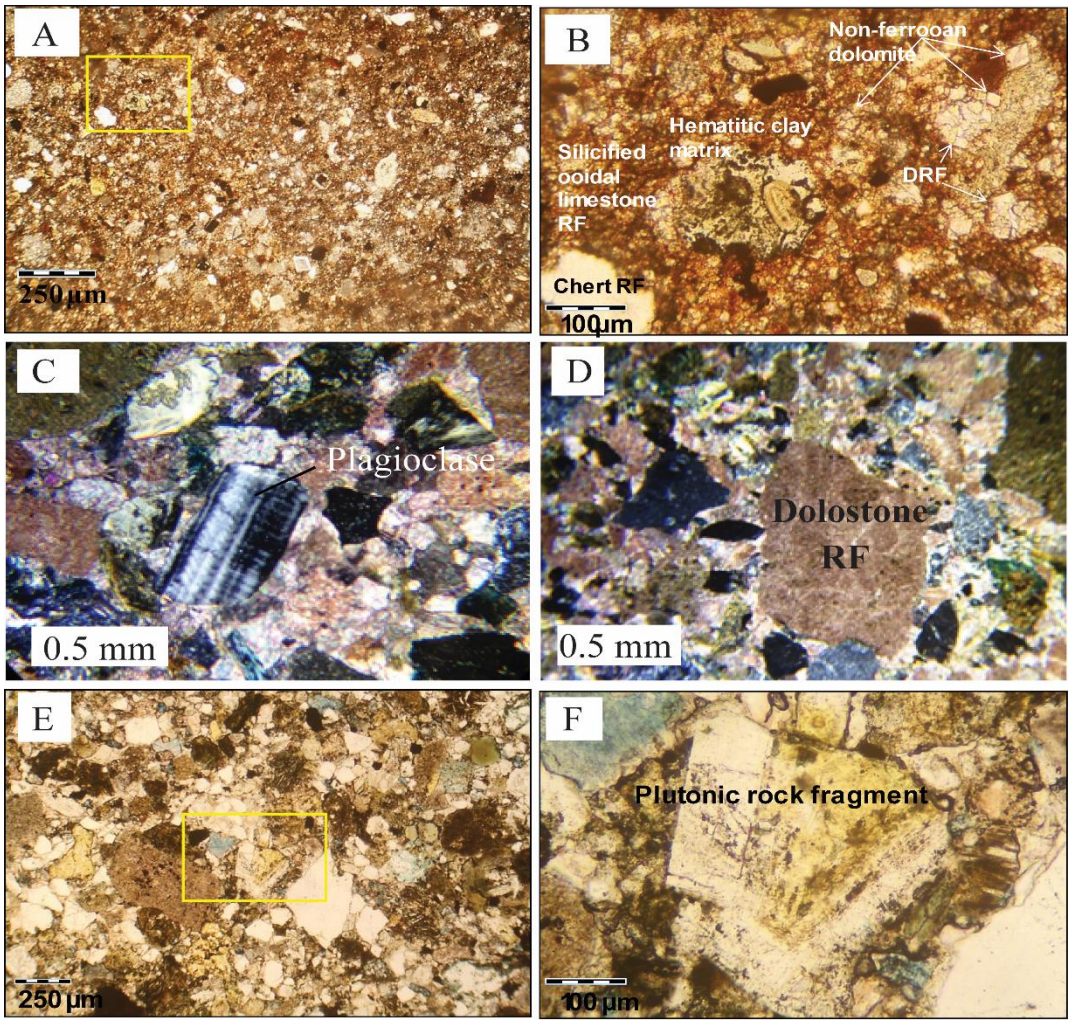

Fig. (2.2) Photomicrographs of Gercus lithic-arenite rocks; A- lithic- arenite rocks were poorly sorted and angular to subrounded grain morphology; B- Chert fragment; C- deformed plagioclase; D- dolostone RF; E&F- plutonic RF

2.4 Mineralogy of both Tanjero and Gercus Sandstone rocks

2.4.1 Quartz

Quartz is the less dominant framework grain in the Tanjero sandstones, constituting an average of 9.53 % of the rock volume, and occurring as monocrystalline (average 6. %; range 3-11 % Table 2.1). In Tanjero samples the monocrystalline quartz grains are angular to sbu-rounded, usually has straight extinction but occasionally shows undulose extinction suggesting a metamorphic origin (Folk,1980),whereas, polycrystalline quartz grains are subangular to sbu-rounded, with poor rounding reflecting a short distance of transportation (Johusson et al., 1988) (average 3.14 %; range 1-5.8 %) grains. Generally, in the Gercus sandstones, the quartz grains are of monocrystalline type (Fig 2.3 A), fairly common (average 12.74 %; range 9.9-19.8 %), and persistent in their distribution.

2.4.2 Calcite

Calcite mineral are dominated by carbonate rock fragment in the Tanjero sandstones (average 33.9 %; range 29.5-37.8 % table 2.1), typically micritic (Fig. 2.1F), very finely peloidal or foraminiferal, whereas,The Gercus formation are characterized by high content of carbonate fragments (average 37.15 %; range 30.7- 43.4% table 2.1), including dolostone rock fragments and rare fragments of limestone (Fig. 2.3 C).

2.4.3 Dolomite

The Dolomite mineral are mainly restricted to the Gercus sandstones. The presence of dolomite may be related to the dolomitization processes and/or a high content of Mg minerals such as olivine, pyroxene and amphibole, as

well as the occurrence of dolomite precipitation environments as a result of presence of hydrothermal fluids and CO_2 gases in the bottom of sedimentary basin (Pichler and Humphrey, 2001). The elevation of Mg/Ca ratio and the PH of the sea water are common as a result of $CaSO_4$ precipitation and iron oxide dissolution (Pichler and Humphrey, 2001).

2.4.4 Feldspar

The Tanjero sandstones have dominantly feldspathic composition (average 7.7 %; range 5.6-10.5 % table 2.1).The feldspars include K-feldspars and plagioclase feldspar with deformed polythenthitic twining (Fig. 2.3 D). The total feldspar minerals in the Gercus samples are lower than the Tanjero samples (average 4.46%; rang 3.6-5.6 %) which are coarse grained, sub-angular in shape, and mainly of plagioclase feldspar. The presence of feldspars indicates igneous or metamorphic source rocks (Pittman, 1970).

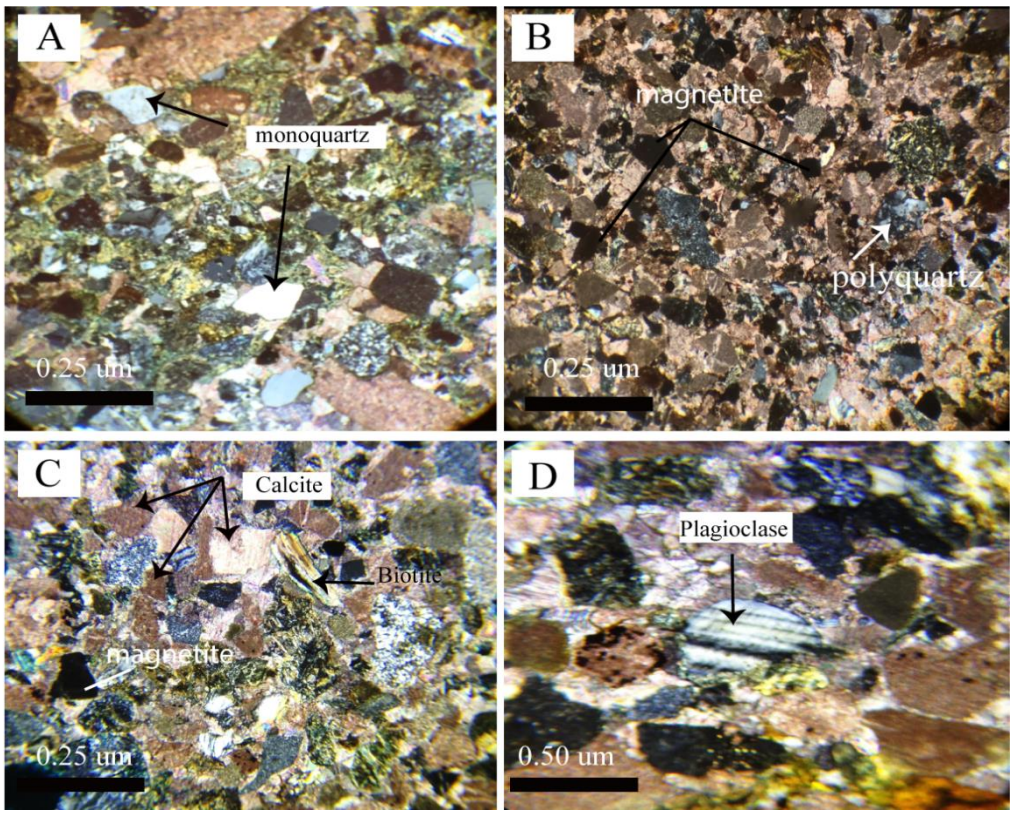

Fig. (2.3) Photomicrographs of A-monoQuartz;B-polyquartz;C-Calcite; D-Deformed Plagioclase.

2.4.5 Rock fragmets

Dominantly, the rock fragments within Tanjero and Gercus clastic rocks comprising very common rock fragments that were derived from older source rocks and survived destruction. They are significantly important in the study provenance. The amount of total rock fragments in Tanjero clastic samples ranges between 52.05% to 59.7%, table 2.1, while the total rock fragments in Gercus clastic samples range between 50.3wt.% to 65.4wt.%. They consist of the following types.

2.4.5.1 Sedimentary rock fragments

Sedimentary rock fragments are the most abundant lithics in Tanjero and Gercus ranging in amount between 29.5- 37.8% with an average of 33.99% table 2.1 in Tanjero clastic samples. The sedimentary rock fragments in the Gercus samples range between 30.7-43.4% with an average of 37.15% table 2.1. The sedimentary rock fragments in both Tanjero and Gercus clastics are of different types including chert, carbonates and clastics. The chert lithics of Tanjero and Gercus (an average of 11.08% and 9.28% respectively table 2.1) are probably derived from the radiolarian beds of Qulqula radiolarite. The carbonate lithics in Tanjero are limestones (typically micritic, very finely peloidal or foraminiferal). The sedimentary lithics in Gercus are common and dominantly comprise dolostone rock fragments and rock fragments of limestone.

2.4.5.2 Igneous Rock fragments

The Tanjero and Gercus clastics are characterized by its content of igneous rock fragments (average of 8.31% and 7.65% table 2.1). Commonly, the igneous rock fragments in Tanjero are volcanic and plutonic rock fragments.

The igneous rock fragments in Gercus are rare volcanic fragments. The existence of igneous lithics is attributed to igneous source rocks present in igneous and Ophiolite in the Zagros Suture Zone.

2.4.5.3 Metamorphic rock fragments

The metamorphic lithics are present as minor amounts with an average of 3.3% and 2.73% table 2.1 in Tanjero and Gercus samples, respectively. Metamorphic lithics in Tanjero and Gercus are mostly serpentines derived

from serpentinites body associated with Qulqula Radiolarite and the serpentinites part of the Ophiolite in the Zagros Suture Zone.

2.4.6 Matrix

The matrix represents ligament materials that are filling void between particles which generally consists of formed clay and micritic materials (Dickinson, 1970). It is produced as a result of disintegration and decomposition of unstable constituents especially rock fragments and feldspars. The matrix amount is in the Tanjero samples, ranging between 5.5 % -7.4%, with average 6.75% table 2.1. The Matrix of Tanjero clastic rocks are interstitial detrital clays is locally intermixed with organic matter and probably, at least in part, represent pseudomatrix. In the Gercus clastic samples, the matrix is ubiquitous, and primarily comprises intermixed (and largely unresolvable) clay/hematite with rare patches of remnant interspersed organic matter (partially pyritized in places). The clay component of the matrix appears to be largely Illicit in composition but is uneasily resolvable in thin section.

2.4.7 Cement

Authigenic cements in the Tanjero clastics are dominated by pervasive pore-filling non-ferroan calcite, typically occurring as relatively coarse pore-filling spar and very rarely as grain-coating isopachous crusts partially surrounding some lithic grains/foraminifera. Rare microcrystalline siderite, hematite and pyrite are also locally finely disseminated.

In Gercus clastic rocks, Matrix is ubiquitous and primarily comprises intermixed (and largely unresolvable) clay/hematite with rare patches of remnant interspersed organic matter (partially pyritized in places). Note that

the clay component of the matrix appears to be largely Illitic in composition but is uneasily resolvable in thin section.

2.5 Mineralogical classification of Tanjero Sandstone rocks.

There are number of mineralogical classifications of sandstone and most use a triangular diagram Q: Total quartz; F: Total Feldspar; RF: Total rock fragments. According to Pettijohn, (1975) classifications both the Tanjero and Gercus samples are lithic arenites (Fig.2.4).

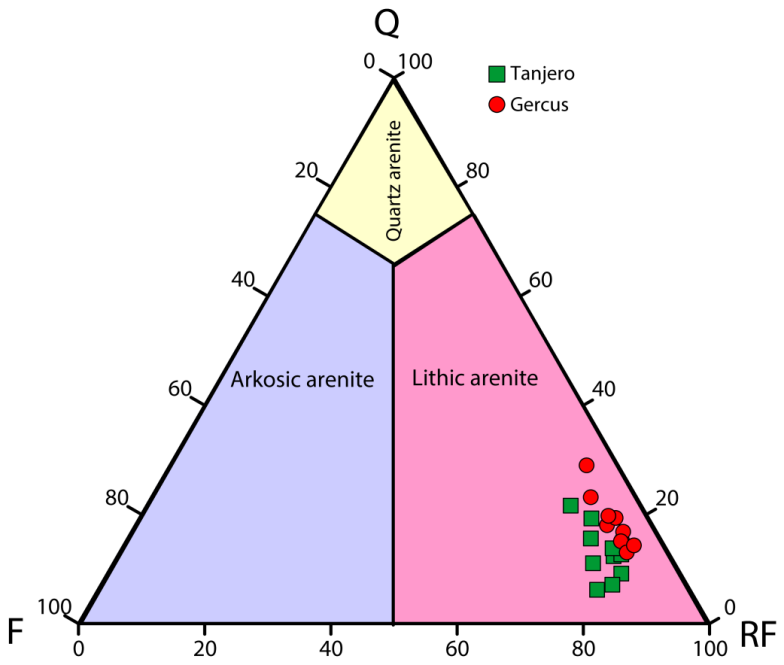

Fig. (2.4) Mineralogical classification of the clastic rocks in the Tanjero and Gercus Formation (Pettijohn, 1975); Q: Total quartz; F: Total Feldspar; RF: Total rock fragments.

2.6 Heavy Minerals

The importance of heavy minerals in sedimentary studies, despite their low abundances (<1.0%), is that they allow an assess of the source and environmental conditions of deposition of the sediment (Pettijohn, et al., 1987; Garzanti, et al., 2013, Ali et al., 2017). Each heavy mineral grain is a unique Recorder of data, carrying the details of its Provenance, destance of the source rocks and re-sedimentation processes (Mange, & Wright, 2007). Thus, the analysis of heavy minerals in foreland basin sequences can prove valuable in constraining the structural histories of both extra-basin and intra-basin (e.g., hydraulic) processes that influenced the formation of clastic rocks (Dill, 1998). These minerals are devided into two groups; the first group is Opaque Heavy Minerals which includes Goethite, Magnetite, Hematite and Chromite; the second group is Non opaque heavy minerals. Neumerous reseachers have studied the satability of the heavy mnierals against weatheing processes. Zircon is stable during chemical and physical weathering, while Pyroxene and Amphiboles are strongly affected by weathering (Nickle, 1973; Morton, 1985). Based on the stabilty of heavy minerals, Folk (1974) has classified heavy minerals into three groups; firstly Ultra-stable Heavy Minerals, include Zircon, Tourmaline and Rutile; secondly Meta-stable Heavy Minerals include Garnet, Epidote and Kayanite; thirdly Unstable Heavy Minerals incude pyroxene, Amphible ans Serpentine. In the present study, the heavy minerals were separeted from 10 sandstone samples of each Tanjero and Gercus clastic rocks following the method of Carver (1971) and their identifications was carried out and confirmed under high resolution microscope copled with semi-automated

SEM-EDS prope. Backscattered images were prepared for some heavy mineral grains.

2.6.1 Opaque minerals

2.6.1.1 Cr-Spinel

Chromian spinel occurs as an accessory mineral in sedimentary rocks in which it preserves its compositional signature after burial in sedimentary strata which has mechanical stability, and is easy to recognize. It has immense geodynamic implications and is known to be a provenance marker of mafic and ultramafic rocks, especially Alpine-type peridotites (Arai and Okada 1991; Cookenboo et al. 1997; Lee 1999). The chemistry of the spinel group minerals is expressed by $AB2O_4$, in which (A) represents divalent cations(R^{+2}) and (B) trivalent cations(R^{+3}). Deer et al (1992) have subdivided spinel group into three series, namely spinel series (Al) that includes Spinel, Hercynite, Gahnite and Galaxite. Magnetite series (Fe^{+3}) includes Magnesioferrite, Magnetite, Franklinite, Jacobsite and Trevorite, and chromite series (Cr) that includes Magnesiochromite and chromite, according to whether the trivalent ion is Al, Fe, or Cr.

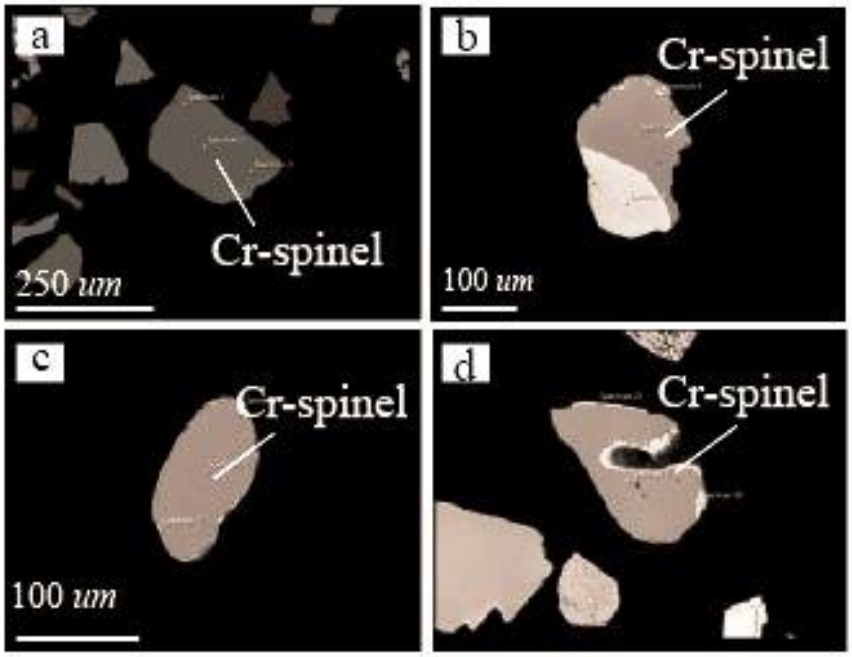

Fig. (2.5) Backscattered image of Cr-spinel; a & b Tanjero lith-arenite, c & d; Gercus lith-arenite

Cr-Spinel shows subhedral to anhedral shapes in the Tanjero Sandstone samples, usually without traces of abrasion on their surfaces (Figure 2.6 A and B). Cr-Spinel extracted from the clastic samples of the Gercus exhibit rounded and corroded surface which indicate sorting due to the distance from the source rocks (Fig 2.6 C and D). Detrital Cr-spinels have been recognized in the Upper Cretaceous Tanjero clastics and have been interpited and derived from Ophiolite. An ophiolite source consists of the harzburgitic mantle Peridotite developed mainly in a supra-subduction zone setting.

2.6.1.2 Magnetite

Sub-rounded to sub-angular opaque magnetites were identified in all the samples (Fig. 2.5 B). In comparison between the two formations, both seem to be dominated by the occurrence of opaque minerals. The opaque content is forming 79.83-87.04 % of the heavy mineral suite in the Tanjero clastic samples. Accessory grains of detrital opaque minerals were highly common in the clastic samples of the Gercus molasse, forming 93.73% of the heavy mineral suite. These minerals include magnetite, Cr-spinel and ilmenite.

2.6.1.3 Ilmenite

The mineral Ilmenite (Titanium magnetite) comprises the opaque group. The existence of Ilmenite among the opaque minerals was determined based on the semi-quantitative estimation of SEM-EDS results. The Tanjero litharenite samples are characterized by the presence of high content (19.66 wt. %) of ilmenite mineral among the opaque group, while in the Gercus clastic samples, the ilmenite content range between 5.81-9.52 wt. %. The high content of ilmenite within Tanjero samples indicates the mafic source of these rocks.

2.6.2 Non Opaques

The non-opaque heavy minerals are represented in the present study by three groups; ultrastable, metastable, and unstable (Folk, 1974).

2.6.2.1 Ultra Stable Heavy Minerals

Ultra Stable Heavy Minerals include zircon, rutile and tourmaline. Their presence is an evidence of involvement of metamorphic and acidic igneous rocks (Chaodong et al., 2005; Ruiz et al., 2007).

2.6.2.1.1 Zircon

Zircon is found as fine subhedral to anhedral grains in the Tanjero clastic samples, Zircon is characterized by its colorless**,** pale yellow or pale pink colors and high relief. The zircon content is significantly low in the Tanjero clastic rocks. It comprises only 0.11 wt. % of the Ultra stable heavy minerals. Zircon occurs as very finely, rounded grain in the Gercus clastic rocks (Fig. 2.6 A and B).

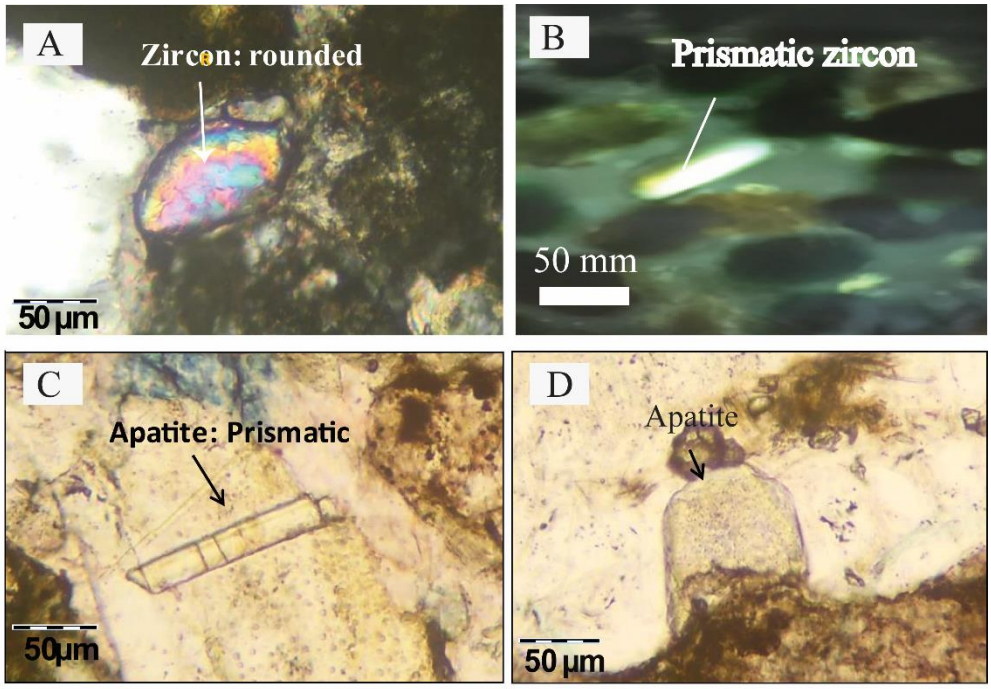

Fig. (2.6) Photomicrographs of Zircon in Tanjero and Gercus (A and B), Apatite in Tanjero and Gercus (C and D), respectively.

2.6.2.1.2 Tourmaline

Tourmaline is a group of minerals with complex chemical compositions and various colors. The variation in colors is due to the complexity of chemical composition and show paleochroism under ordinary light. Tourmaline minerals occur only in the Gercus clastic rocks indicating that the mineral has been derived from the granitic part of the Zagros Ophiolite (Mohammad et.al.2016). It occurs as fine rounded to sub-rounded grains, display pale-green to pale yellow color (Fig. 2.7).

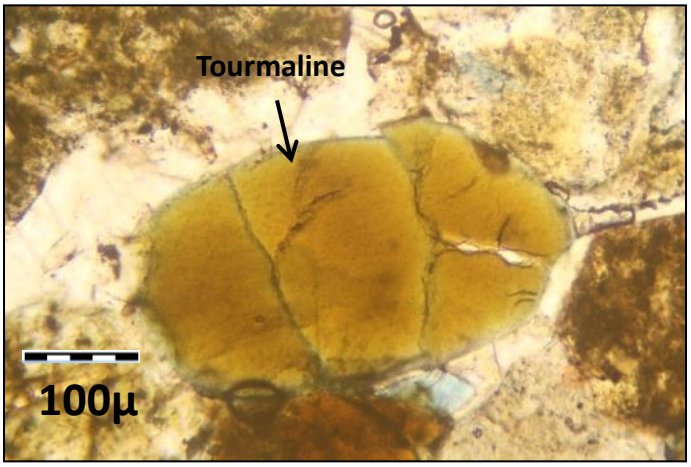

Fig. (2.7) Photomicrograph of Tourmaline in Gercus Clastic rocks

2.6.2.1.3 Rutile

Rutile is identified by its high relief**,** red or brown to yellowish orange color, display pleochroism from yellow to reddish brown (Kerr, 1959). In the Tanjero clastic samples, the rutile exhibit different forms, it occurs as corroded sub-rounded fine grains, angular, or prismatic crystals (Fig. 2.8 A-D). The rutile mineral in the Tanjero clastic samples comprises 0.3 wt. % of the heavy mineral contents. In the Gercus samples, rutile grains occur as

sub-rounded to prismatic fine grains (Fig. 2.8 E and F). The Gercus samples are characterized by its high content of rutile (3.36 wt. % of the total heavy minerals). This can be attributed to the corporation of mafic source rock.

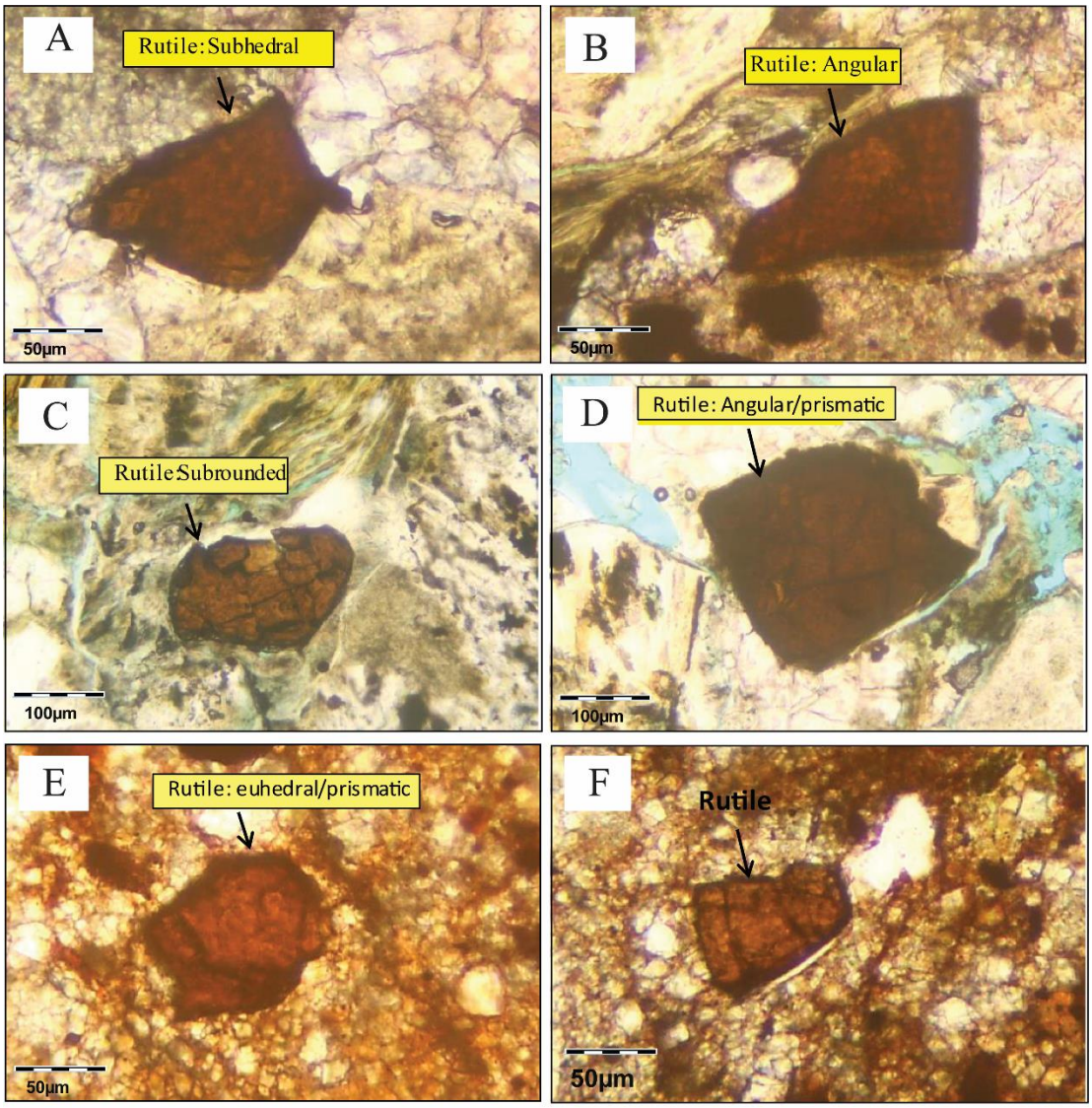

Fig. (2.8) Photomicrographs of selected Rutile minerals in the Tanjero clastic rocks (A-D) and Gercus clastic rocks (E and F)

2.6.2.2 Metastable Heavy Minerals

This subgroup includes Garnet, Epidote, Apatite and Kyanite, only Apatite and Epidote are recognized in the studied clastic rocks. Epidote presents as Euhedral-Subherdral grains in the Tanjero clastics, while Epidote in Grecus clastics are present as subrounded grains (Fig. 2.9).

Apatite occurs in Igneous, Metamorphic and Sedimentary rocks. It may present in veins and pegmatites, and may be with hydrothermal origin (Hurlbut, 1971). Apatite occursas prismatic grains in the Tanjero clastic samples in very minor grains. The Apatite grains were found as Euhedral-subhedral grains in the Gercus clastic samples in greater amount as compared to Tanjero samples (Fig 2.6 C and D).

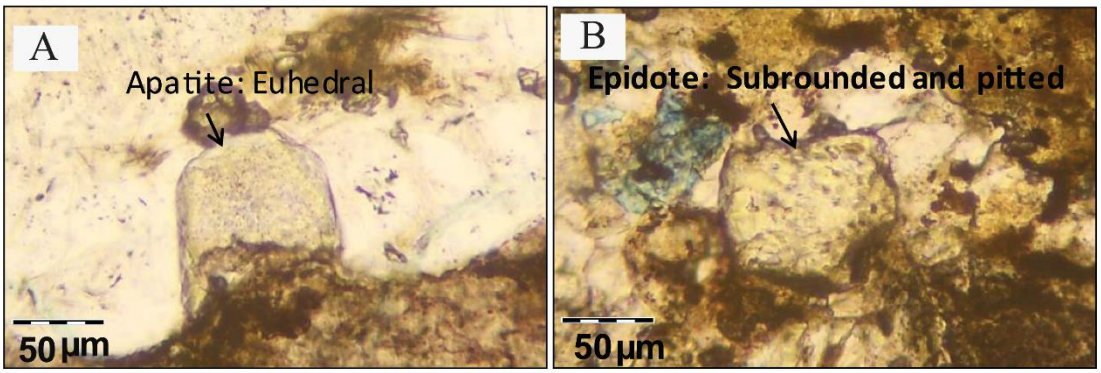

Fig. (2.9) Epidote minerals in A-Tanjero; B- Gercus clastic rocks

2.6.2.3 Unstable Heavy Minerals

The unstable heavy minerals recognized in the studied sandstones are pyroxene and serpentine.

2.6.2.3.1 Pyroxene

Pyroxene occurs as colorless or pale green in color. In Tanjero and Gercus clastics pyroxene is present as Orthopyroxene type (Hypersthene). The Orthopyroxene occurs as subhedral / subrounded grains in Tanjero samples, while the Orthopyroxene in Gercus samples exhibit subhedral crystal shapes (Fig. 2.10).

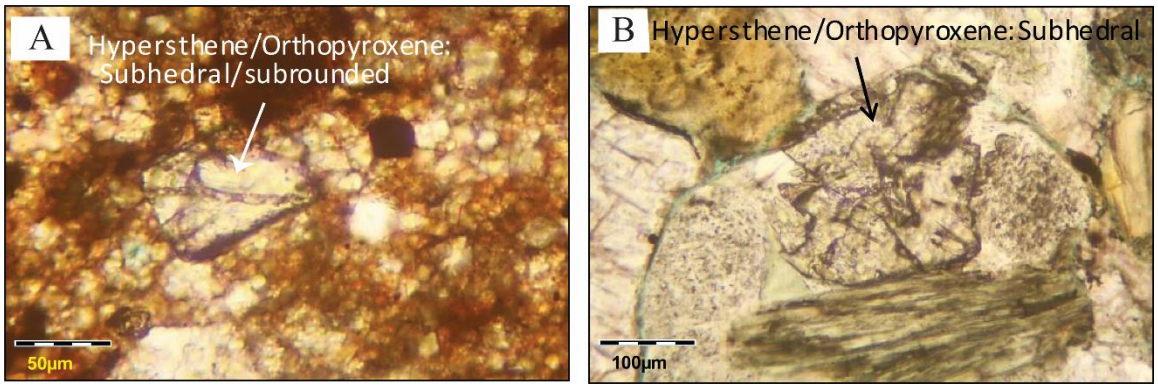

Fig. (2.10) Photomicrograph of pyroxene in a-Tanjero; B-Gercus

2.6.2.3.2 Serpentine

Serpentine is a common minerals in igneous and metamorphic rocks. It occurs as a result of serpentinisation process from Olivine, Proxene and Amphibole minerals. Both Tanjero and Gercus are characterised by its high content of serprntine minerals (Fig. 2.11). The serpentine minerals are coorporated to the Tanjero and Gercus from the Igneous rocks in the

Zagros Ophiolites because the Ophiolite belts contain high amount of serpentinte rocks.

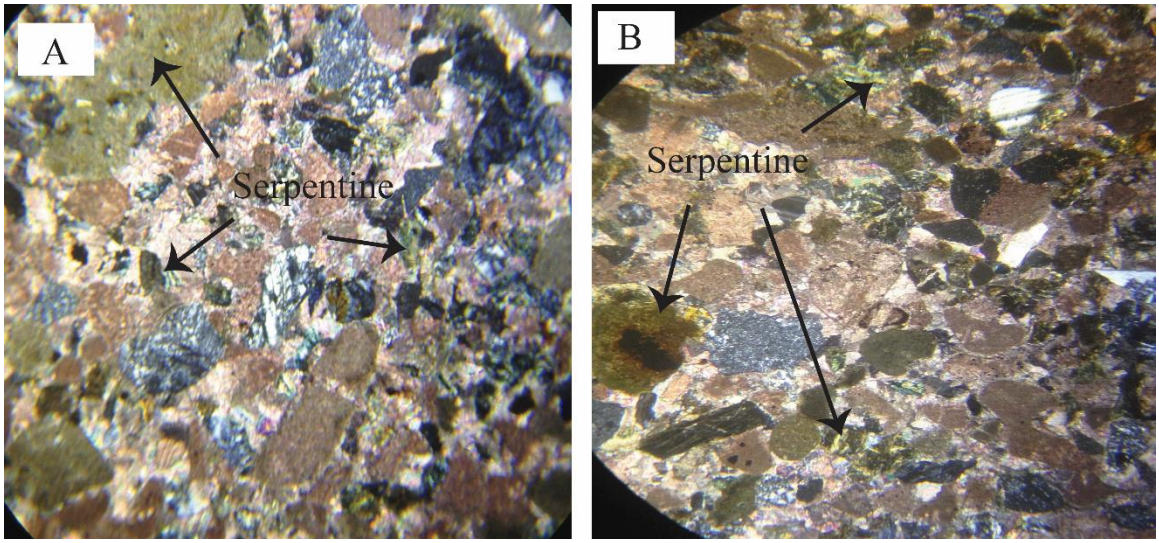

Fig. (2.11) Photomicrograph of Serpentine minerals in A- Tanjero; B- Gercus.

CHAPTER THREE

GEOCHEMISTRY

3.1 Preface:

The geochemical composition of clastic rocks represents their primary mineralogy and the effect of a complex result of various variables such as source material (provenance), weathering, transportation, and depositional setting (Nesbitt and Young, 1982; Bhatia, 1985; McLennan, 1989; McLennan, et al,. 1993; Cox and Lowe, 1995, Peterson, 2009) Therefore, sandstone geochemistry has a number of important applications (e.g. Potter 1978; Bhatia 1983, 1985; Roser & Korsch1988; Floyd et al. 1991; McLennan et al. 1993; Dinelli et al.1999; Getaneh 2002; Lacassie et al. 2004; Rahman & Suzuki2007; Dey et al. 2009). For instance, major-element chemistry can provide information about the tectonic setting of sedimentary basins, allowing distinction between sandstones derived from oceanic island arc, continental island arc, active continental margin, and passive margin settings (Bhatia 1983; Roser & Korsch 1986; Kroonenberg 1994). Major- and trace element chemistry have been used to evaluate sedimentation rates and depositional environments in orogenic belts (Sugisaki1984).

In the present study, geochemical analyses were undertaken on sandstone samples of Tanjero and Gercus formation. A total of 20 samples 10 samples were selected from each section and analyzed for whole-rock major, trace and REE elements using X-ray fluorescence and inductively coupled plasma–mass spectrometer (ICP–MS) at the ALS Laboratory Group SL Seville, Spain. The individual major

trace and REE element analyses of the sandstones of the Tanjero and Gercus clastic rocks are presented in Tables 3.1, 3.2and 3.3.

3.2 Geochemistry of major oxide:

Major-element chemistry has been utilized to infer the original clastic assemblages in deeply buried and altered sedimentary rocks and to clarify the processes that produced the sediments (Argast & Donnelly 1987). The Major element distributions reflect the mineralogy of the studied samples. The major element composition of both Tanjero and Gercus samples are quite variable. For reference mean values of the post-Archean Australian shale (PAAS) and the Upper Continental Crust (UCC) are included in tables and figures (Taylor and McLennan, 1985). Variations in the major element geochemistry of the Tanjero and Gercus sandstones are shown using Al_2O_3 abundances as normalization factor to make comparisons among the different lithologies, because of its immobile nature during weathering, diagenesis, and metamorphism (e.g., Bauluz et al., 2000; Etemad-Saeed et al., 2011). Major element concentrations are presented in Tables 3.1.

3.2.1 SiO_2

Generally the clastic rocks are characterised by their high content of detrital silica transported to the sedimentary basin as free silica (detrital quartz) or as silicate tetrahedral in the structure of clay minerals and also may precipitate as colloidal with clay minerals (Goldschmidt. 1962). The Tanjero sandstone sample shows low content of SiO_2 (34.5-48.1wt. %; average 41.52 wt. %) as compared to both PAAS and UCC, while the SiO_2 content in the Gercus molasse is strongly variable and higher than the Tanjero samples. It ranges 42.9-58.6 wt. % with an average of 47.07 wt.%. - 68.7 Wt.%. The SiO_2 content of silica in the Gercus samples is also lower as compared to PAAS and UCC. The invariant diagram

between Al_2O_3 and SiO_2 used to investigate the elemental relationship. In general Al_2O_3 shows a weak negative correlation within SiO_2 in the Gercus samples (R=0.34) while no clear correlation observed in Tanjero samples. This indicates that the SiO_2 content concentrated in Quartz and Feldspars (fig.3.1 A and table 3.4A&B).

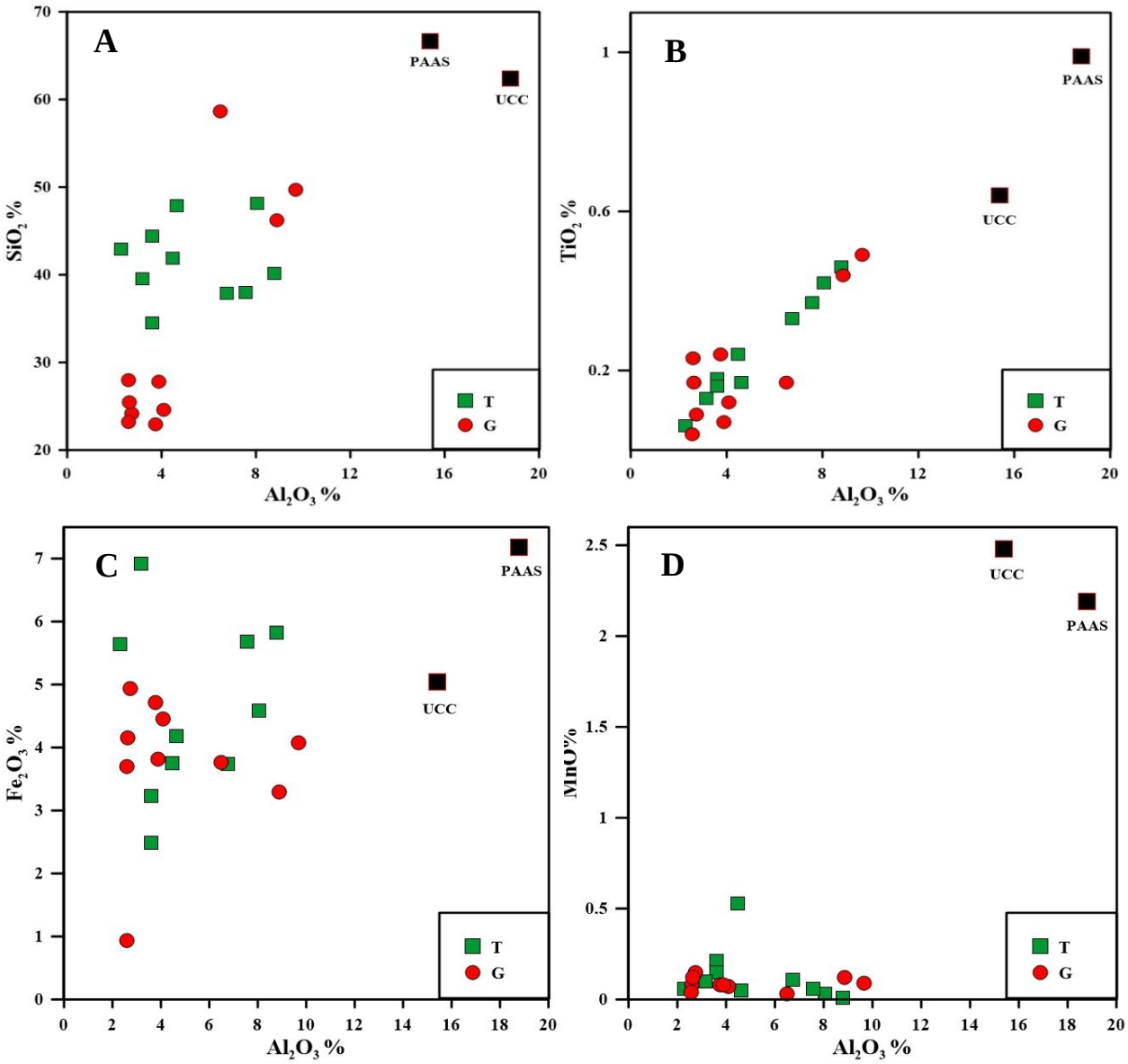

Fig. (3.1) Binary relationship diagram SiO_2, TiO_2, Fe_2O_3 and MnO Vs. Al_2O_3.

3.2.2 TiO_2

The TiO_2 occurs in the clay minerals replacing Al and Fe^{+3} or it enter the chemical composition of opaque heavy minerals such as Rutile (TiO_2), Ilmenite ($FeTiO_3$) and Sphene ($CaTiSiO_5$) (Goldschmidt, 1962). The TiO_2 content in the Tanjero samples range between 0.06 wt.% to 0.46 wt% with an average of 0.25 wt.%, while the TiO_2 content in the Gercus samples range between 0.07 wt.% to 0.49 wt.% with an average of 0.21 wt.% (Table 3.1). The TiO_2 content is variable and lower as compared to the PAAS and UCC in both Tanjero and Gercus samples. The Tanjero samples show strong positive correlation (R=0.99) with Al_2O_3, k_2O, Na_2O and P_2O_5 which indicate entering the TiO_2 in the Clay minerals, Phylosilicates (Chlorite and Biotite) and Sphene (Fig. 3.1 B and table 3.4A&B). The Gercus samples show the same strong correlation within the above mentioned oxides.

3.2.3 Al_2O_3

The Clay minerals are characterised by its high content of Al_2O_3 as compared to other minerals and the Al_2O_3 are concentrate in Feldspar minerals. The Al_2O_3 content in the Tanjero samples range between 2.3wt.% to 8.78 wt.% with an average of 5.29 wt.%, while the Al_2O_3 content in the Gercus samples range between 4.08 wt.% to 9.67 wt.% with an average of 6.13 wt.%. The Tanjero and Gercus Al_2O_3 contents are lower as compared to the average PAAS and UCC content. This attributed to the low content of clays in the Tanjero and Gercus sandstones. Al_2O_3 is positively correlated with K_2O and Na_2O in both Tanjero and Gercus samples (Fig. 3.2 C and D and table 3.4 A & B) indicating Al_2O_3 concentrations in Clay, Feldspar and Mica minerals (McLennan et al., 1999).

3.2.4 Fe_2O_3

The Fe_2O_3 are present in high quantity in the iron oxide minerals such as Magnetite, Hematite, Chromite and Ferromagnesian minerals in the mafic and ultramafic such as pyroxene, amphibole and micas rocks. The Fe_2O_3 content in the Tanjero clastics range between 2.49 wt.% to 6.92 wt.% with an average of 4.6wt.%, while the Fe_2O_3 content in the Gercus clastics range between 3.29 wt.% to 4.94 wt.% with an average of 3.78 wt.%,. The Fe_2O_3 concentrations in both Tanjero and Gercus clastics are low as compared to its content in PAAS. Bivariate diagram between Fe_2O_3 and Al_2O_3 in the Tanjero and Gercus samples, show very weak correlation (Fig. 3.1 C) probably reflecting the low content of chlorite in the matrix and rock fragment.

3.2. 5 MnO

The MnO enter the structure of ferromagnisum minerals (Olivine, Pyroxene and Amphiboles) replacing Fe and Mg. It replaces Ca and Mg in Calcite and Dolomite. The MnO content in the Tanjero samples range between 0.06 to 0.53 wt.% with an average of 0.13 wt.%, while the MnO content in the Gercus samples range between 0.03 to 0.15 wt.% with an average of 0.09 wt.%. Both Tanjero and Gercus samples are characterised by its vlow content of MnO if compared to its content in PSSA (2.19 wt.%) and UCC (2.48 wt.%) in (Fig. 3.1 D). MnO show weak negative correlation with Al_2O_3 in both Tanjero and Gercus Formations (Fig.3.1D).

3-2-6 MgO

Generally there is a notable enrichment of MgO in both Tanjero and Gercus samples. The Tanjero MgO content range between 2.04 wt.% to 9.92 wt.% with an average of (5.98 wt.% table 3.1). The Gercus samples contain 2.52 wt.% to 13.35 wt.% with an average of 7.85 wt.% (table 3.1). The MgO content in Tanjero and

Gercus samples are high as compared to its content in PASS and UCC. The unusual higher content of MgO and MnO are related to the higher content of ferromagnesian related elements as a reflection of the high contribution of mafic-ultramafic (pyroxene, Amphibole) weathered clastics during sedimentation. This probably can be confirmed by the presence of serpentine clastics in the Tanjero samples. The MgO content in the Tanjero and Gercus samples show negative correlation within CaO (-0.6) because the MgO concentrate in the ferromagnesian minerals, while the MgO content in the Gercus samples show moderate negative correlation within K_2O (-0.66) and Na_2O (-0.7) indicating concentration of the MgO in the ferromagnesian minerals rather than the clays (Fig. 3.2 A).

3.2.7 CaO

The CaO is highly distributing in the carbonate sedimentary rocks rich in calcite and dolomite. The CaO is variable in the Tanjero and Gercus samples. CaO contents in the Tanjero range between 16.7 wt.% to 27.8 wt.% with an average of 21.6 wt.% and in the Gercus samples the CaO contents range between 7.05 wt.% to 19.8 wt.% with an average of 16.7 wt.% (table 3.1). This indicates by the high content of rock fragment in the Tanjero and Gercus clastic rocks. CaO also presents in silicate minerals such as plagioclase and Epidote as carbonate cement. The CaO content in Gercus clastics shows weak correlation (Fig 3.2 B) within the Al_2O_3 indicating concentration of CaO in the carbonate phases rather than the clay minerals.

3.2.8 K_2O

The k-feldspar mineral and the micas as well as cay minerals (illite) are rich in K_2O. The K_2O content in the Tanjero samples range between 0.06 wt.% to 1.24 wt% with an average of 0.5 wt.% (table 3.1). Its content in the Gercus samples range between 0.12 wt.% to 1.48 wt.% with an average of 0.47wt.%. The K_2O

content of Tanjero and Gercus samples are characterised by its low content as compared to its average content in UCC (Fig. 3.2 C).K_2O show positive correlation with Al_2O_3, TiO_2, and Na_2O in both Formations (table 3.4 A & B).

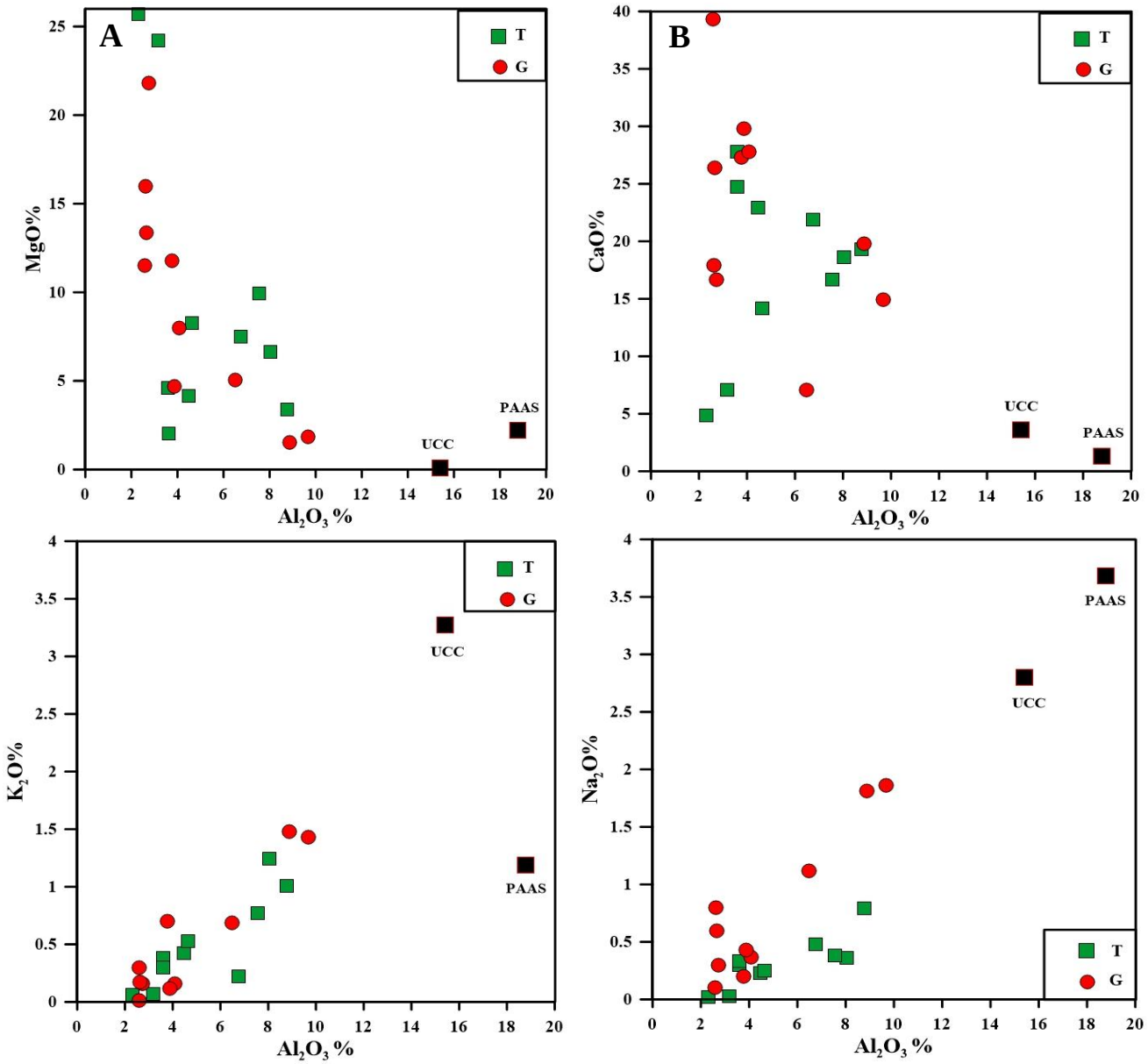

Fig. (3.2) Binary relation diagram of MgO, CaO, K_2O and Na_2O vs. Al_2O_3

3.2.9 Na_2O

The Na_2O content in the Tanjero and Gercus clastic rocks can be indicated by the content of Plagioclase Feldspars (Albite) in the samples. The content of Albite is increased with in the increasing of Albitization process. The Na_2O content in the Tanjero samples range between 0.02 to 0.48 wt.% with an average of 0.42 wt.%, while the Na_2O content in the Gercus samples range between 0.3 to 1.86 wt.% with an average of 0.71 wt.%. The Na_2O content in both Tanjero and Gercus samples indicate the presence of Na-plagioclase. The Na_2O content of both Tanjero and Gercus clastics shows strong positive correlations (0.89 and 0.9) within the Al_2O_3 content which indicates that the Na_2O is present in the Plagioclase mineral (Fig 3.2 D).

3.2.10 P_2O_5

Phosphor is considered as a secondary lithophile element in the earth crust and it is concentrated in the Apatite mineral during meddle and late fractional crystallization process and the most common phosphor minerals in sedimentary rocks. It is also present in some other additional minerals such as Monazite and Xenotime (Degens, 1965). The P_2O_5 content in the Tanjero samples range between 0.01 to 0.11 wt. % with an average of 0.05 wt.%, while its content in the Gercus samples range between 0.01 to 0.12 wt.%, with an average of 0.046 wt.%. This low content of P_2O_5 in Tanjero and Gercus samples are related to the low content of Apatite in the samples as compared to its content in PASS (0.16 wt.%) and UCC (0.15 wt.%), respectively (fig. 3.3 A). P_2O_5 show positive correlation K_2O, TiO_2, and Na_2O in both Formations (table 3.4 A & B).

3.2.11 LOI

LOI represents the content of H_2O and other gases in the clastic rocks of Tanjero and Gercus. The Clastic rocks are characterized by its high content of water. The LOI content in the Tanjero samples range between 11.9 to 24.9 wt.% with an average of 19.7 wt.% while in the Gercus samples the LOI content range between 13.9 t0 20.3 with an average of 19.3 wt.%. The H_2O content concentrates in the Phyllosilicate and Clay minerals (Fig. 3.3 B).

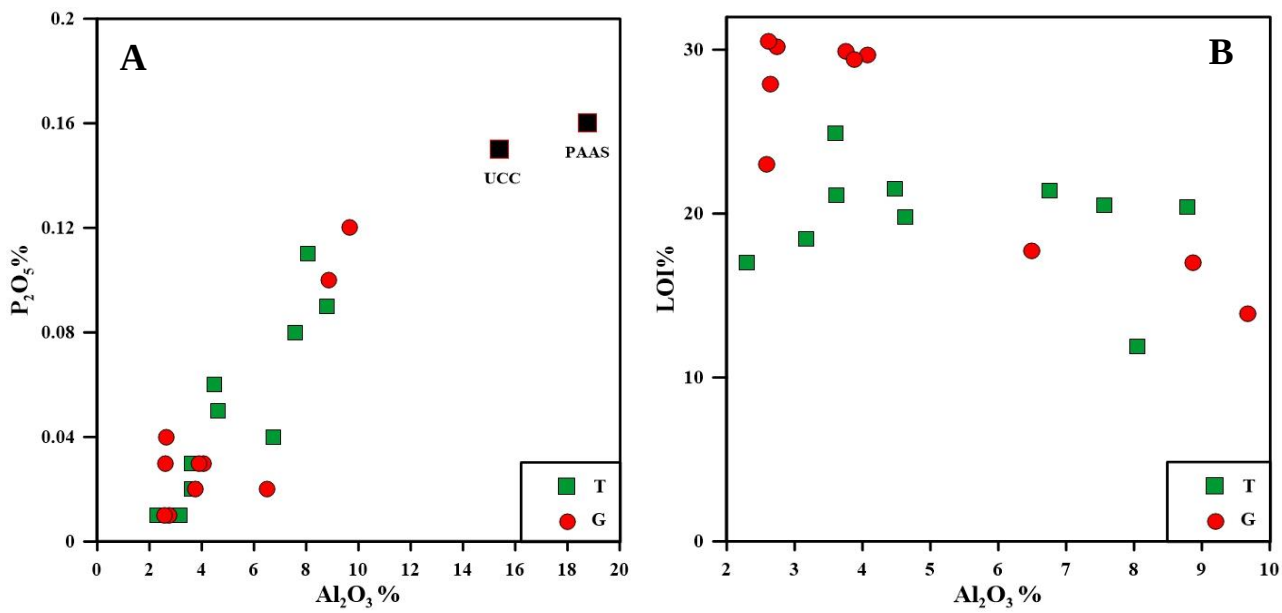

Fig. (3.3) Binary relation diagram of P_2O_5 and LOI vs. Al_2O_3

Table (3.1) Major oxide (Wt. %) concentrations of the Tanjero and the Gercus clastic rocks

SAMPLE	SiO_2	TiO_2	Al_2O_3	Fe_2O_3	MnO	MgO	CaO	K_2O	Na_2O	P_2O_5	LOI	Total
T1	34.5	0.18	3.6	3.23	0.21	4.58	27.8	0.38	0.3	0.03	24.9	99.71
T5	37.9	0.33	6.75	3.74	0.11	7.5	21.9	0.22	0.48	0.04	21.4	99.89
T7	41.9	0.24	4.48	3.75	0.53	4.16	22.9	0.42	0.23	0.06	21.5	100.17
T9	44.4	0.16	3.61	2.49	0.15	2.04	24.7	0.3	0.33	0.02	21.1	99.3
T12	39.5	0.13	3.17	6.92	0.1	7.05	24.2	0.07	0.03	0.01	18.45	99.63
T14	42.9	0.06	2.3	5.64	0.06	4.88	25.7	0.06	0.02	0.01	17	98.63
T15	47.9	0.17	4.63	4.18	0.05	8.27	14.18	0.53	0.25	0.05	19.8	100.01
T17	48.1	0.42	8.05	4.59	0.03	6.62	18.63	1.24	0.36	0.11	11.9	100.05
T18	40.1	0.46	8.78	5.82	0.01	3.37	19.3	1.01	0.79	0.09	20.4	100.13
T20	38	0.37	7.56	5.68	0.06	9.92	16.7	0.77	0.38	0.08	20.5	100.02
Ava.	41.52	0.252	5.293	4.6	0.131	5.98	21.601	0.5	0.42	0.05	19.7	-
G1	44.2	0.09	4.74	4.94	0.15	11.8	16.7	0.16	0.3	0.01	18.2	101.29
G3	48	0.23	5.61	3.7	0.08	6	17.9	0.3	0.8	0.03	17.5	100.15
G5	42.9	0.24	4.76	4.72	0.08	11.8	17.3	0.4	0.3	0.02	18.4	100.92
G7	58.6	0.17	6.49	3.76	0.03	5.04	7.05	0.45	0.52	0.02	18.75	100.88
G9	46.2	0.44	8.87	3.29	0.12	2.52	19.8	1.48	1.81	0.1	17	101.63
G11	49.7	0.49	9.67	4.08	0.09	3.85	14.9	1.43	1.86	0.12	13.9	100.09
G13	43.17	0.04	5.58	0.93	0.04	11.5	19.3	0.1	0.2	0.01	20.3	101.17
G15	45.5	0.17	6.64	4.15	0.12	13.35	16.4	0.17	0.46	0.04	17.9	104.9
G17	44.6	0.12	4.08	4.46	0.07	7.99	17.8	0.16	0.37	0.03	19.7	99.38
G20	47.8	0.07	4.88	3.81	0.08	4.68	19.8	0.12	0.43	0.03	18.4	100.1
Ava.	47.067	0.21	6.132	3.78	0.09	7.853	16.695	0.477	0.705	0.046	19.21	-
PAAS	62.4	0.99	18.78	7.18	2.19	2.2	1.29	1.19	3.68	0.16	-	-
UCC	66.6	0.64	15.4	5.04	2.48	0.1	3.59	3.27	2.8	0.15	-	-

3.3 Trace elements

Trace elements are usually less affected than major elements during chemical and/or physical alteration (White, 2005), hence they are very useful tool to provide a clear picture of the source area (Lopez et al. 2005). In the present study, the selected samples from all the studied sections from different areas of the Tanjero and Gercus clastic rocks were analysed and the result are presented in Table (3.2).

3.3.1 High field strength elements (HFSE)

High field strength elements (HFSE) such as Zr, Hf, Ta, Y, and Nb preferentially partitioned into melts during fractional crystallization of magma (Feng and Kerrich, 1990) and have high ionic charges. They become insoluble and immobile during weathering, metamorphism and they are essentially unaffected by hydrothermal alteration, weathering and low to medium grade metamorphism (Grosch et al., 2007; Koralay, 2010; White et al., 2002). They tend to concentrate in felsic rocks more than mafic rocks (Etemad-Saeed et al., 2011). Generally, the low content of the HFSE in the Tanjero clastics reflect the composition of the original parent material to be mafic and ultramafic. Zirconium is a high field strength element that is largely immobile during alteration and metamorphic processes (Pearce and Cann, 1973). Zr contents in the Tanjero samples range between 9-61 ppm and Gercus samples range between 12-28 ppm, reflecting its low concentrations in mafic and ultramafic source rocks (Mason and Moore, 1982; Wilson, 1989). According to the proposition by Taylor and McLennan (1985), Zr occurs predominantly in heavy minerals. It shows increase with an increase of La due to its concentration in the heavy minerals (Fig. 3.4 A and table 3.5A and B).

Yttrium tends to be enriched more in felsic than in mafic rocks. Yttrium values in the Tanjero clastic is lower than the upper continental crust (3-18 ppm) that

showed by McLennan (2001); Ranjan and Banerjee (2009). The Y content in the Gercus samples range between 17-23 ppm (fig. 3.4 B). It shows negative correlation with Ni, Cr and V in the Tanjero samples while no clear correlation observed in Gercus samples see table 3.5A and B.

Niobium concentrations are low in the Tanjero samples that range from 1.1 to 8.8 ppm (table 3.2). The Nb content in the Gercus samples range from 3-9 ppm. The low Nb values reflect little impact from a felsic source to the Tanjero and Gercus (Andersen, 1995; Krauskof, 1979). The Hf content in the Tanjero range between 0.2-1.6 ppm, while in the Gercus samples, it ranges between 0.2-3.4 ppm. The Hf content of Tanjero and Gercus is low if compared to PAAS and UCC (fig. 3.4 C).

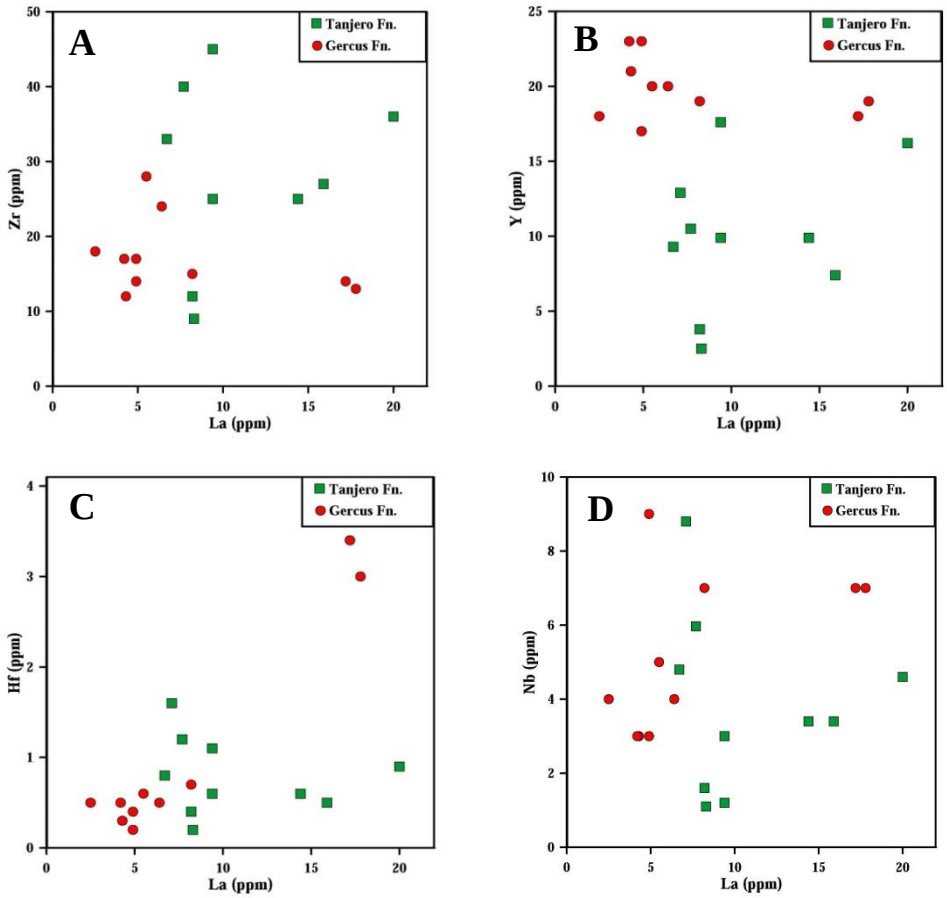

Fig. (3.4) Variation diagram of HFSE vs. La for Tanjero and Gercus clastics

3.3.2 Large ion lithophile elements (LILE)

Large ion lithophile elements (LILE) are mainly represented by Rb, Ba, Sr, Th, U and Pb that are characterized by their high solubility in water. Therefore, they are considered to be generally mobile elements during metamorphism and weathering processes (Pearce and Peate 1995; Grosch et al., 2007) . They have the ability to be absorbed onto clay mineral surfaces. The LILE concentration in the Tanjero clastics is very low if compared to its content in UCC and PAAS (see table 3.2).

The LILE content in Tanjero and Gercus ranges between; Ba (25-120 ppm; 11-48 ppm), Sr (107-386 ppm) and Rb (3-15 ppm; 4-31 ppm), respectively. Most of Ba and Sr are present in carbonate. The distribution of Ba in the sedimentary rocks is different from Sr because of the lower stability of Ba. There is no clear correlation between Sr with any other trace elements except Ba due to the presence of Sr in multiple minerals including feldspars, clays and carbonates.

Rb concentrates in the K-feldspars, Mica Phyllosilicates and Clay minerals. The Ba, Sr, and Rb show high correlations together that indicate its close relations in their minerals. The Ba and Sr content in the Tanjero and Gercus samples are depleted if compared to its content in PAAS (650 ppm) and UCC (700 ppm). The Rb content in the Gercus samples is close and comparable with the average of Granodiorite. This suggests a greater crustal source for Gercus within the mafic and ultramafic source. The U content of the Tanjero ranges between 0.4-1.68 ppm and in the Gercus samples it ranges between 0.23-3.35 ppm. Tanjero samples contain 0.23-1.9 ppm Th, while in the Gercus samples the Th content is between 0.6-4.42 ppm (table 3.2). The Tanjero and Gercus samples are with low U and Th content if compared to PAAS and UCC. This indicates that the impact of felsic component is low.

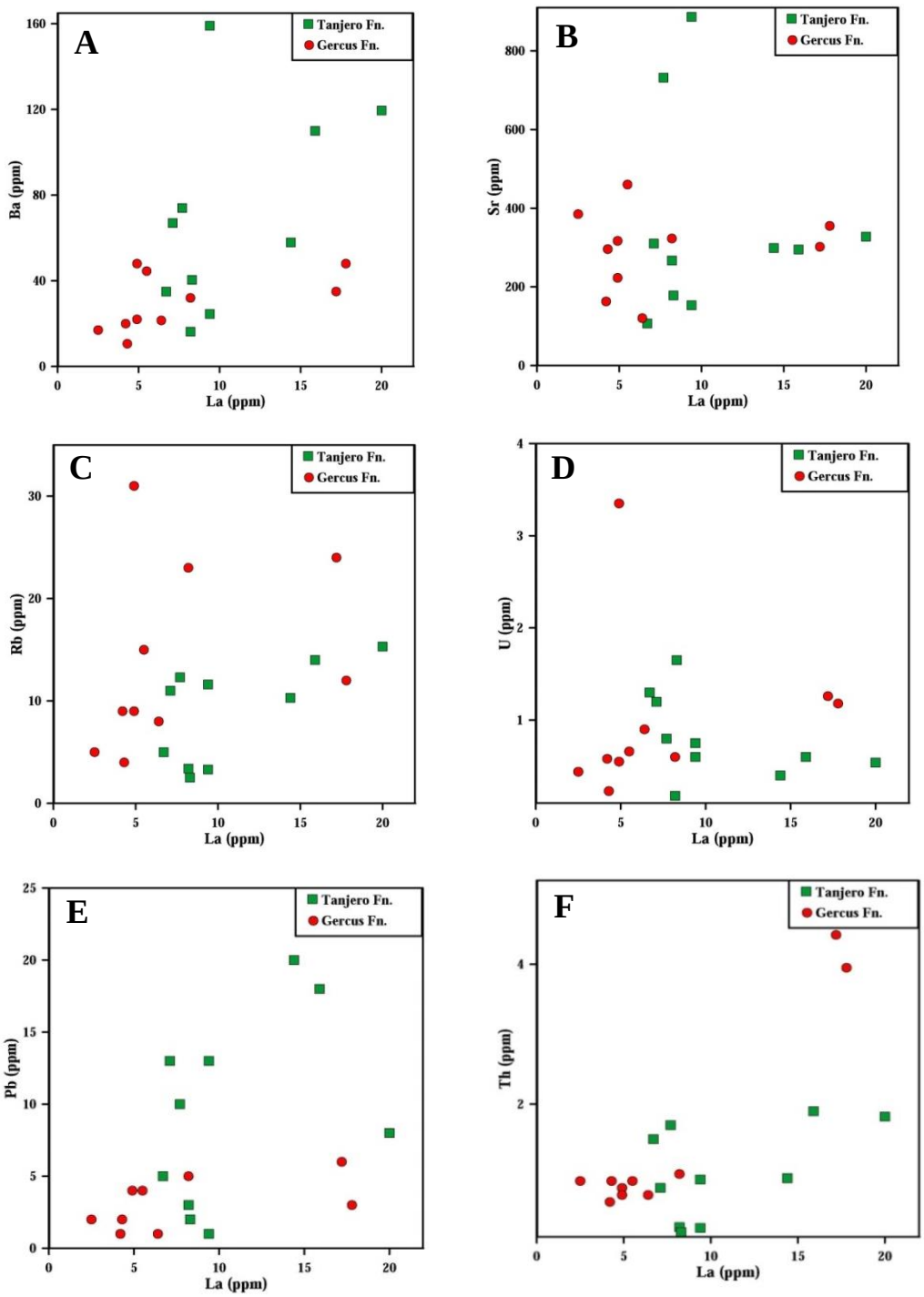

Fig. (3.5) Variation diagram of LILE in Tanjero and Gercus clastics

The Pb content in Tanjero samples ranges between 1-20 ppm (table3). Its content in Gercus ranges between 1-6 ppm. The Pb enters the structure of Zircons and Sulfides minerals, as the presence of these minerals are confirmed by petrological studies.

3.3.3 Transition trace elements (TTE)

Transition trace elements (TTE) also called ferromagnesian trace elements include V, Sc, Co, Ni, and Cr. They show convergent behavior during the evolutionary processes of volcanic rocks which are very important for determining provenance and tectonic setting (Armstrong-Altrin et al. 2004). It is well known that these elements concentrate in Olivine, Cr-spinel, Pyroxene and some Clay minerals such as Chlorite and Simictite.

The V content in the Tanjero samples range between 132-192 ppm, in the Gercus samples, it ranges between 39-84 ppm. This element occurs in the structure of pyroxene, amphibole, biotite and oxides that have titanium in their structures (Mason and Moore, 1982). Therefore, V has high values in samples that are rich in Pyroxene (Fig. 3.6 A).

Cr occurs in igneous rocks in spinel minerals, such as chromites, and it also occurs in ferromagnesian minerals such as pyroxene and olivine. In ultramafic igneous rocks Cr content is more than 2000 ppm in basalt, it ranges between 150 and 200 ppm; it reduces to 25–80 ppm in intermediate rocks and to less than 20 ppm in granitic rocks. The Cr content in the Tanjero samples range between 632-1790 ppm. In the Gercus samples the Cr content ranges between 800-2410 ppm.

The high values of Cr within the Tanjero and Gercus samples attributed to the impact of mafic-ultramafic source rocks and indicate the contribution of the Ophiolites and serpentines association within Qulqula in the source area, as Cr occurs in chromite and spinel is generally resistant to geochemical weathering

(Wodepohl, 1978). Therefore, Cr is transported from the source area to the sedimentary environments in the resistant minerals. Cr show strong positive correlation with Ni in the Gercus samples while it shows weak correlation with Ni in the Tanjero samples (Fig. 3.6 B and table 3.5A and B).

Ni and Co concentrate in olivine (Wilson, 1989; Winter 2001). They show weak negative correlations with Nb, Zr, Ba, Sr and Rb and La in the Tanjero and Gercus clastic samples. Ni is a lithophilic element but behaves as siderophilic (Miyashiro and Shido, 1975). Cobalt is less abundant than Ni with a range of 17-69 ppm in Tanjero and 8-45 ppm in Gercus. An increase of Co and a decrease of other transition elements do not always reflect a mafic rock origin but could be due to sedimentary sorting processes (Wani and Mondal , 2010) in (fig. 3.6 C).

The Ni content in Tanjero clastic samples ranges between 112-1450 ppm. The Ni content in Gercus clastic samples ranges between 310-898 ppm. According to Garver et al. (1996), if Cr and Ni > 100 ppm, they show a high correlation that probably indicate derivation from ultramafic components in the source area, Thus the Tanjero clastic were impacted with more mafic-ultramafic source rocks, compared to Gercus (Table 3.2).

Scandium occurs in mafic and intermediate igneous rocks. It is mainly present in Pyroxenes, Amphiboles and Micas (Wodepohl, 1978). The Sc content in the Tanjero samples ranges between 10-19 ppm, while in the Gercus samples, they range between 16-28 ppm. The Sc content in the Gercus samples are higher that their values PSSA and UCC indicating contribution of felsic component associated within the Ophiolite sequences (fig. 3.6 E).

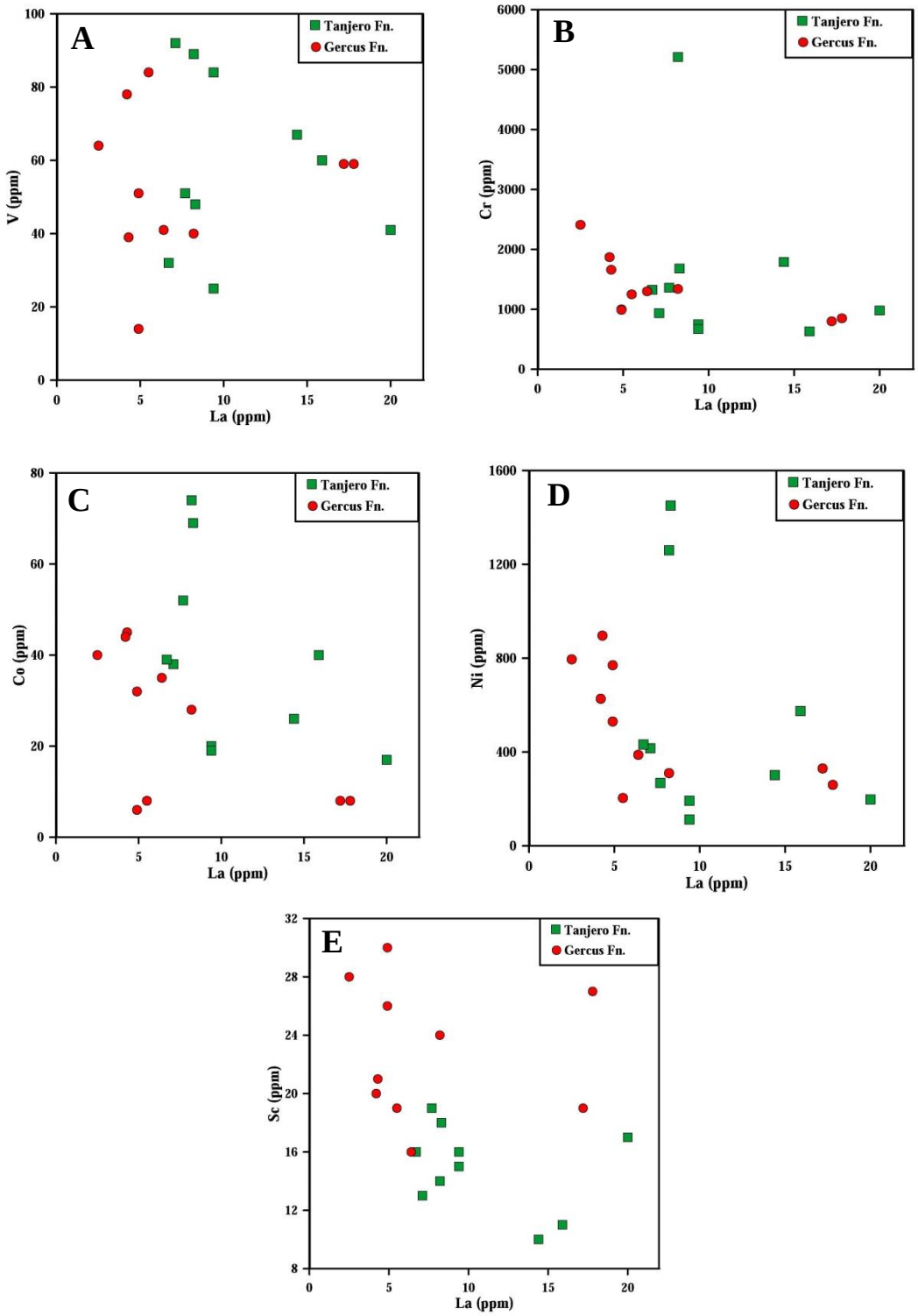

Fig. (3.6) Variation diagram of TTE vs. La for Tanjero and Gercus clastics.

Table (3.2) Trace concentration (ppm) of the Tanjero and the Gercus clastic rocks

SAMPLE	**T1**	**T5**	**T7**	**T9**	**T12**	**T14**	**T15**	**T17**	**T18**	**T20**
Ni	302	192	198	112	260	450	575	416	268	432
Co	26	20	17	19	74	69	40	38	52	39
Cr	1790	750	980	670	1210	1680	632	934	1359	1325
Sc	10	15	17	16	14	18	11	13	19	16
V	167	184	141	125	189	148	160	192	151	132
Ba	57.9	24.5	119.5	159	16.2	40.4	110	67	74	35
Rb	10.3	3.3	15.3	11.6	3.4	2.5	14	11	12.3	5
Sr	299	153.5	328	886	267	178.5	295	310	732	107
Zr	25	45	36	25	12	9	27	61	40	33
Y	10	18	16	10	13.8	3	7	13	11	9
Nb	3.4	1.2	4.6	3	1.6	1.1	3.4	8.8	5.97	4.8
Ga	4.1	5.6	5.9	2.9	2.5	0.7	4.1	5.2	4.6	2.2
Hf	0.6	1.1	0.9	0.6	0.4	0.2	0.5	1.6	1.2	0.8
Cu	53	18	42	22	15	9	50	42	26	10
Zn	72	23	71	71	50	23	63	58	37	42
Pb	20	1	8	13	3	2	18	13	10	5
Li	20	10	20	30	10	10	22	17	15	10
Cs	0.52	0.18	0.78	0.73	0.23	0.14	0.5	0.25	0.15	0.24
Th	0.94	0.23	1.82	0.92	0.24	0.17	1.9	0.8	1.7	1.5
U	0.4	0.6	0.54	0.75	0.18	1.65	0.6	1.2	0.8	1.3
SAMPLE	**G1**	**G3**	**G5**	**G7**	**G9**	**G11**	**G13**	**G15**	**G17**	**G20**
Ni	896	388	627	204	226	333	177	795	523	412
Co	45	35	44	8	8	8	6	40	32	28
Cr	1660	1300	1870	1250	850	800	1000	2410	990	1340
Sc	21	16	20	19	27	19	30	28	26	24
V	39	41	78	84	59	59	44	64	55	77
Ba	10.6	21.5	20	44.5	48	35	48	17	22	32
Rb	4	8	9	15	12	24	9	5	31	23
Sr	296	120.5	163	460	355	302	317	385	223	323
Zr	12	24	17	28	13	14	14	18	17	15
Y	21	20	23	20	19	18	17	18	23	19
Nb	3	4	3	5	7	7	3	4	9	7
Ga	1.1	1.9	2.5	2.8	9	9.8	0.1	2.2	2.1	5
Hf	0.3	0.5	0.5	0.6	3	3.4	0.2	0.5	0.4	0.7
Cu	4	10	15	14	13	22	7	12	16	21
Zn	24	27	31	27	39	51	50	30	29	32
Pb	2	1	1	4	3	6	4	2	4	5
Li	10	10	10	20	20	30	10	10	15	15
Cs	0.07	0.31	0.26	0.75	0.8	2.64	0.01	0.23	0.42	0.36
Th	0.9	0.7	0.6	0.9	3.95	4.42	0.8	0.9	0.7	1
U	0.23	0.9	0.58	0.66	1.18	1.26	3.35	0.44	0.55	0.6

3.4 Geochemical classification

The clastic rocks of Tanjero and Gercus has been determined by several petrographical procedures, including quartz, feldspar and rock fragments. They are classified geochemically as lithic-arenites when plotted on the SiO_2/Al_2O_3 vs Na_2O/K_2O diagram (Fig. 3.7) (Pittijohng3, et al., 1987). The low total quartz content in the Tanjero samples, together with major quantities of chert fragments and the high proportion of volcanic detritus confirm the principal source of mafic-ultramafic.

The relative enrichment of plagioclase within Tanjero and Gercus sediments, shifting towards a higher Na_2O/K_2O ratio (0.4–0.03) is shown in Fig. 3.7. Hence, the limited development of mature quartz-rich sediments in Tanjero clastic sediments attributed to less abundant K-feldspar.

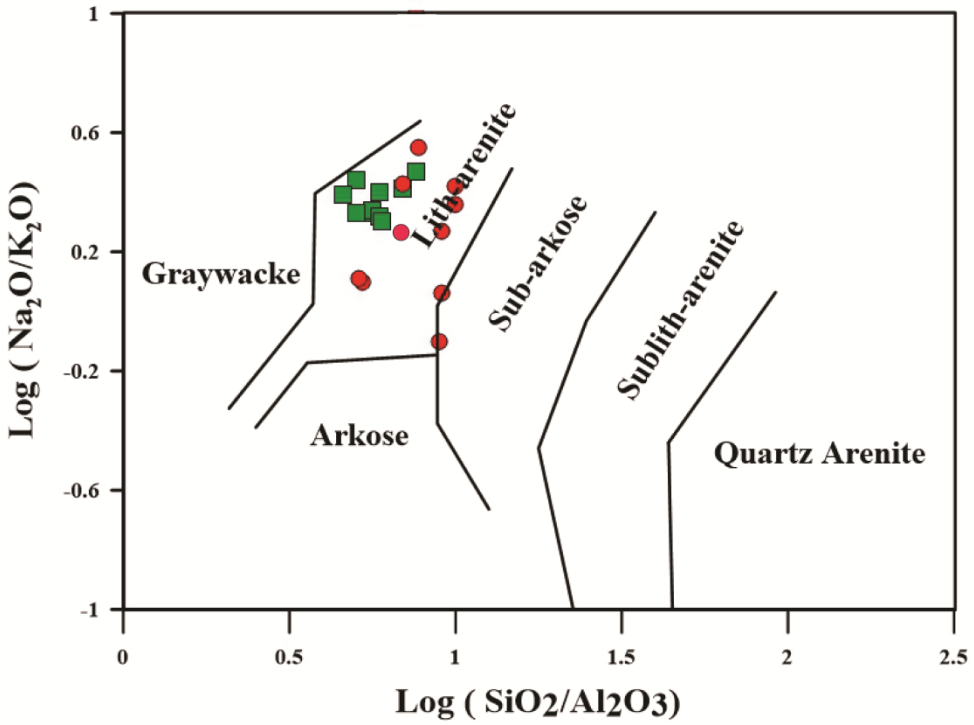

Fig. (3.7) Geochemical classification of Tanjero and Gercus clastic rocks using Log (SiO_2/Al_2O_3 vs. Log (Na_2O/K_2O) ratios (Pittijohn, et al., 1987).

3.5 REE elements

Rare earth element is concise by REE to form those elements that are not massive with solid which represent a group of elements with atomic number ranging between 57-71 these are called lanthanides group which have similar chemical and physical behaviors, but they are different in ionic radius which decreases regularly from Lanthanum (La) with ionic radius 1.03A° to Lutetium (Lu) 0.86A°. REE is classified into light rare earth element (LREE) with lower atomic number which includes La, Ce, Pr, and Nd elements and a heavy rare earth element (HREE) with higher atomic number includes Dy, Ho, Er, Tm, Yb, and Lu. Elements that stand with intermediate atomic number Pm, Sm, Eu, Gd, and Tb called middle REE (MREE) (Wilson, 1989; and White, 2001). They are also trivalent under most geological condition, except Europium Eu^{+3} and Cerium Ce^{+3} that are both possibly gain other valance like Eu^{+2} and Ce^{+4} in the case of high oxidation (Henderson, 1984). LREE enriched samples are referred to by $(La/Sm)_n>1$ and (MREE) enrichment if the $(Gd/Yb)_n$ ratios for all samples are >1. The enrichment and depletion of REE in any type of rocks are inspected by normalizing the concentrations of individual REE in a rock to their abundances in chondrite or primitive mantle.

In the study of clastic rocks, the REE abundance and the distribution pattern of the analytical data are useful in understanding the petrogenesis of different types of arenites (Bhatia and Crook 1986; Condie 1991; McLennan and Taylor 1991). REEs are among the most important group of elements in terms of provenance indicator. In the present study, the REE concentrations of the Tanjero and Gercus sandstones were normalized using normalizing values of Sun and McDonough (1989) and the representative REE analyses are listed in (Table 3.3). The overall chondrite-normalized REE patterns of the Tanjero samples display one package

REE variability, may reflect source-rock geochemistry variation (ultramafic and mafic rocks from Iraqi Zagros Ophiolites and mafic terrains within Qulqula). Accordingly, the REE pattern displays enrichment in the total REEs of 10X chondrite (CI) to 30X chondrite (Fig. 3.8). All the distribution patterns of the Tanjero samples display LREE (light REE) enrichment La_n/Sm_n range between 6.89-2.97 and flat HREE (heavy REE) Gd_n/Yb_n with values ranging between 1.88-1.27. Eu anomaly is apparent in the REE patterns of the Tanjero samples (Eu/Eu*) varies between 0.65-0.93, similar to the PAAS and UCC Eu anomaly pattern which are normally interpreted as resulting from removal of plagioclase (Ali et al.,2013).

The rare earth elements (REE) concentrations of the sandstone rocks within the Gercus Formation are shown as chondrite-normalized patterns in Fig. 3.9. All the distribution patterns of the Gercus shows light REE enrichment La_n/Sm_n range between 3.34 to 5.24 with flat HREE, Gd_n/Yb_n range between 1.23 to 1.99. Eu anomaly is apparent in the REE patterns of the Gercus samples (Eu/Eu*) varies between 0.69-1.01, with slight negative Eu anomaly. The Gercus sandstones shows a variable total REE content (9.4- 82.92) ppm. This ratio is variable as compared to UCC (143 ppm; Taylor & McLennan 1985) and PAAS (183; Taylor & McLennan 1985).

The REE pattern displays enrichment in the total REEs of 4X to 20X chondrite. The distribution pattern partitioned into three groups; the first display REE of 4X chondrite (sample G15), with low total REE (9.14); second group display REE variability of 6X-12X chondrite; the third group display high REE variability of 20X chondrite (sample G9 and G11) close to the REE content of PAAS and UCC. The three group's package of the Gercus REE pattern with increasing the total REE contents indicate multiple source-rock geochemistry variation and exhumation of different source terrains within the uplifting of the source area.

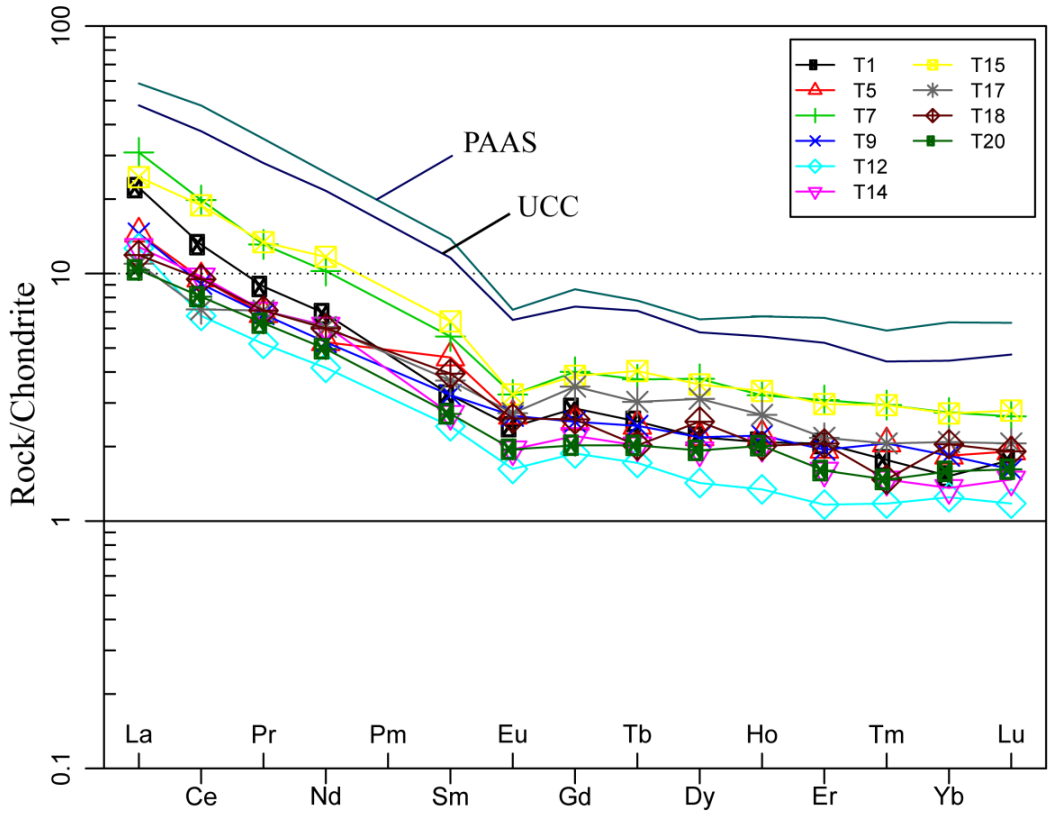

Fig. (3.8) Chondrite-Normalized REE pattern of the Tanjero (T). Normalizing values (after sun and McDonough, 1989). PAAS and UCC normalizing values (after Taylor and McLennan, 1985)

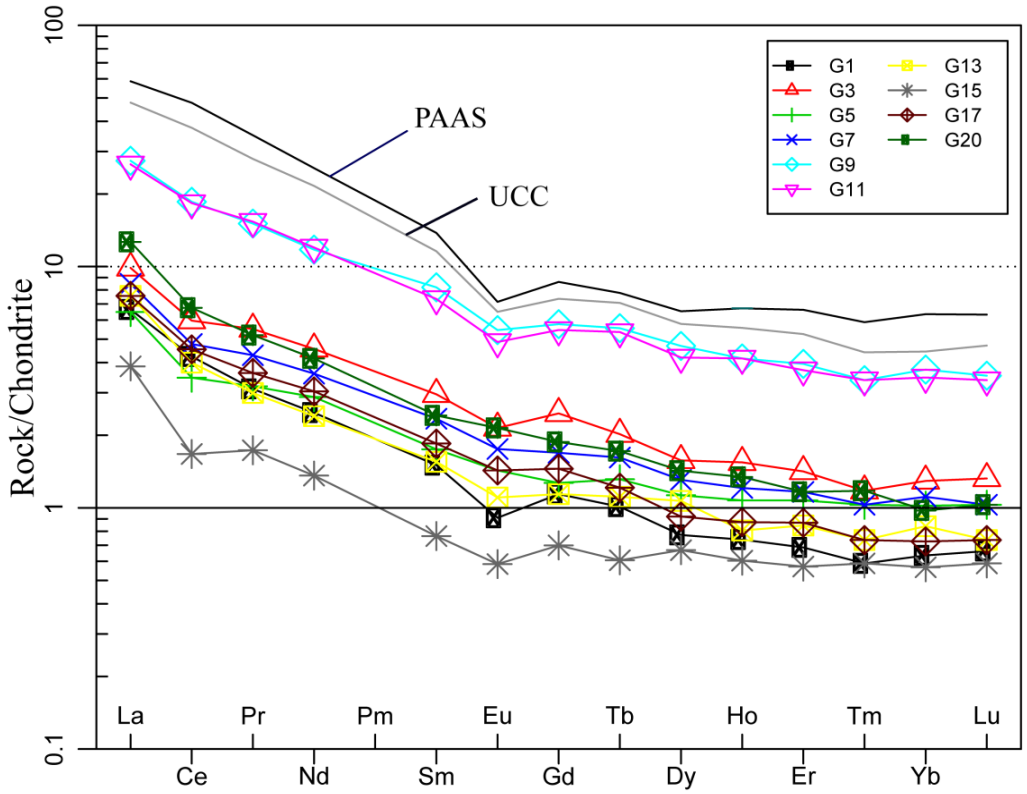

Fig.(3.9) Chondrite-normalized REE pattern of the Gercus (G) clastics. Normalizing values (after sun and McDonough, 1989). PAAS and UCC normalizing values (after Taylor and McLennan, 1985).

3.6 Spider diagrams for Sandstone rocks in both Tanjero and Gercus Formations

Multi-elements diagrams (Spider diagrams) normalized against N-MORBs can be used to constrain the source and melting properties of rocks (Pearce, 1983). In this kind of diagrams , elements arranged along a horizontal axis on which elements mobile in aqueous fluids occupy the left hand (as far as Ba) and immobile elements in aqueous fluids occupy the right hand from Nb (Ali et al.,2012).

N-MORBs normalized trace elements pattern for both Tanjero and Gercus Formations show enrichment in the large ion lithophile elements (LILEs e.g. U,Ph Cs) and depletion in high field strength elements (HFSEs e.g. Nb, Ba, Ti Sun and McDonough,1989,see Figs 3.10 and 3.11). These characteristics are common in the arc setting and broadly attributed to subduction enrichment and fluid metasomatism processes in subduction zones (Pearce et al., 1995).

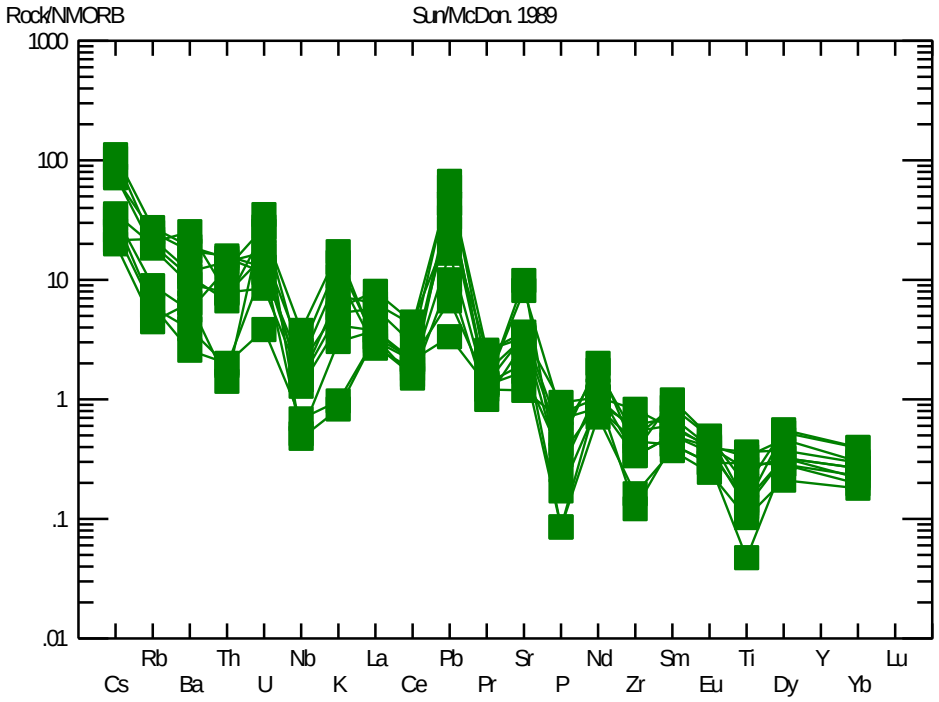

Figure 3.10 NMORB normalized plots for Tanjero clastic samples. Normalizing values (after sun and McDonough, 1989).

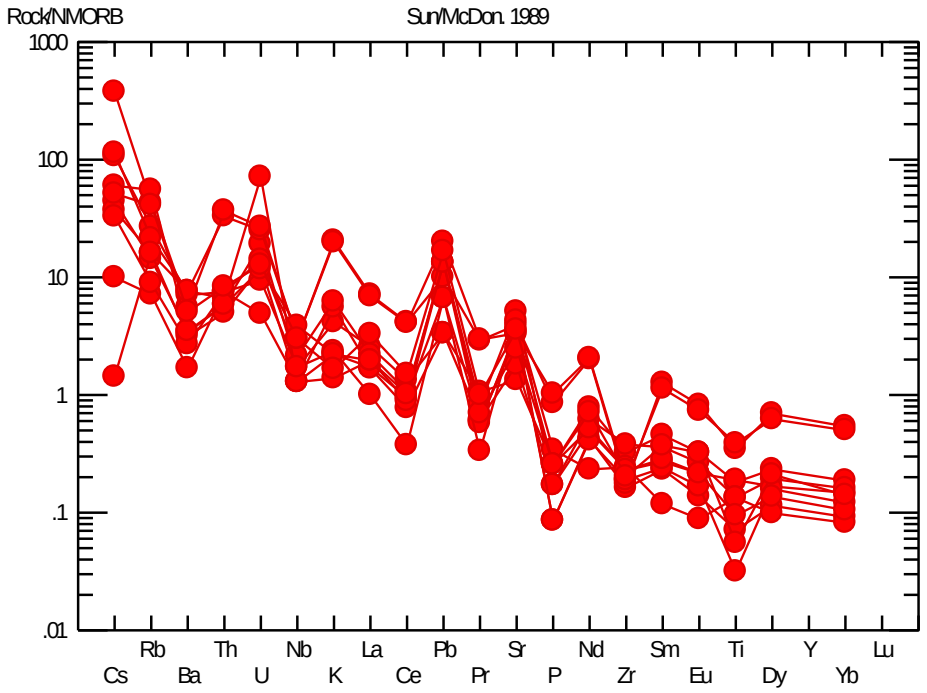

Figure 3.11 NMORB normalized plots for Gercus clastic samples. Normalizing values (after sun and McDonough, 1989).

Table (3.3) Concentration (ppm) of REEs in Tanjero and Gercus clastic rocks

Sample	**T1**	**T5**	**T7**	**T9**	**T12**	**T14**	**T15**	**T17**	**T18**	**T20**
La	14.4	9.4	20	9.4	8.2	8.3	15.9	7.1	7.7	6.7
Ce	21.9	16	33.2	15.2	11.3	16.3	31.6	12	15.9	13.5
Pr	2.25	1.74	3.33	1.74	1.32	1.8	3.4	1.8	1.8	1.6
Nd	8.6	6.6	12.8	6.6	5.2	7.7	14.6	7.6	7.5	6.2
Sm	1.31	1.86	2.26	1.31	0.98	1.1	2.6	1.5	1.6	1.1
Eu	0.37	0.41	0.5	0.41	0.25	0.3	0.5	0.42	0.4	0.3
Gd	1.55	1.37	2.18	1.37	1.02	1.2	2.1	1.9	1.4	1.1
Tb	0.25	0.24	0.37	0.24	0.17	0.2	0.4	0.3	0.2	0.2
Dy	1.47	1.47	2.53	1.47	0.96	1.3	2.4	2.1	1.7	1.3
Ho	0.31	0.33	0.48	0.33	0.2	0.3	0.5	0.4	0.3	0.3
Er	0.9	0.85	1.35	0.85	0.51	0.7	1.3	0.95	0.9	0.7
Tm	0.12	0.14	0.2	0.14	0.08	0.1	0.2	0.14	0.1	0.1
Yb	0.67	0.81	1.21	0.81	0.55	0.6	1.2	0.92	0.9	0.7
Lu	0.12	0.13	0.18	0.11	0.08	0.1	0.19	0.14	0.13	0.11
La_N/Sm_N	6.89	3.17	5.54	4.5	5.24	4.73	3.83	2.97	3.02	3.82
Gd_N/Yb_N	1.88	1.37	1.46	1.37	1.5	1.62	1.42	1.28	2.73	1.27
Eu/Eu*	0.79	0.78	0.69	0.93	0.76	0.8	0.65	0.76	0.82	0.83
Σ REE	54.22	41.35	80.59	39.98	30.82	40	76.89	37.27	40.53	33.91
Sample	**G1**	**G3**	**G5**	**G7**	**G9**	**G11**	**G13**	**G15**	**G17**	**G20**
La	4.3	6.4	4.2	5.5	17.8	17.2	4.9	2.5	4.9	8.2
Ce	7.1	10	5.8	8	31.1	30.7	6.7	2.8	7.6	11.3
Pr	0.79	1.4	0.81	1.09	3.83	3.9	0.76	0.44	0.92	1.32
Nd	3.1	5.7	3.6	4.5	14.7	15	3	1.7	3.8	5.2
Sm	0.61	1.2	0.71	0.95	3.33	2.98	0.63	0.31	0.75	0.98
Eu	0.14	0.33	0.22	0.27	0.84	0.75	0.17	0.09	0.22	0.33
Gd	0.62	1.34	0.69	0.92	3.14	2.97	0.62	0.38	0.79	1.02
Tb	0.1	0.2	0.13	0.16	0.55	0.53	0.11	0.06	0.12	0.17
Dy	0.52	1.06	0.76	0.88	3.16	2.83	0.72	0.45	0.62	0.96
Ho	0.11	0.23	0.16	0.18	0.62	0.62	0.12	0.09	0.13	0.2
Er	0.3	0.62	0.47	0.51	1.73	1.63	0.37	0.25	0.38	0.51
Tm	0.04	0.08	0.07	0.07	0.23	0.23	0.05	0.04	0.05	0.08
Yb	0.28	0.57	0.45	0.49	1.65	1.53	0.37	0.25	0.32	0.43
Lu	0.045	0.09	0.07	0.07	0.24	0.23	0.05	0.04	0.05	0.07
La_N/Sm_N	4.42	3.34	3.71	3.63	3.35	3.62	4.87	5.05	4.09	5.24
Gd_N/Yb_N	1.81	1.91	1.25	1.52	1.54	1.57	1.36	1.23	1.99	1.92
Eu/Eu*	0.69	0.79	0.96	0.88	0.79	0.77	0.83	0.8	0.87	1.01
Σ REE	18.05	29.22	18.14	23.59	82.92	81.1	18.57	9.4	20.65	30.77

Table (3.4) A Correlation coefficient matrix and scatter diagram of major elements in the Tanjero samples

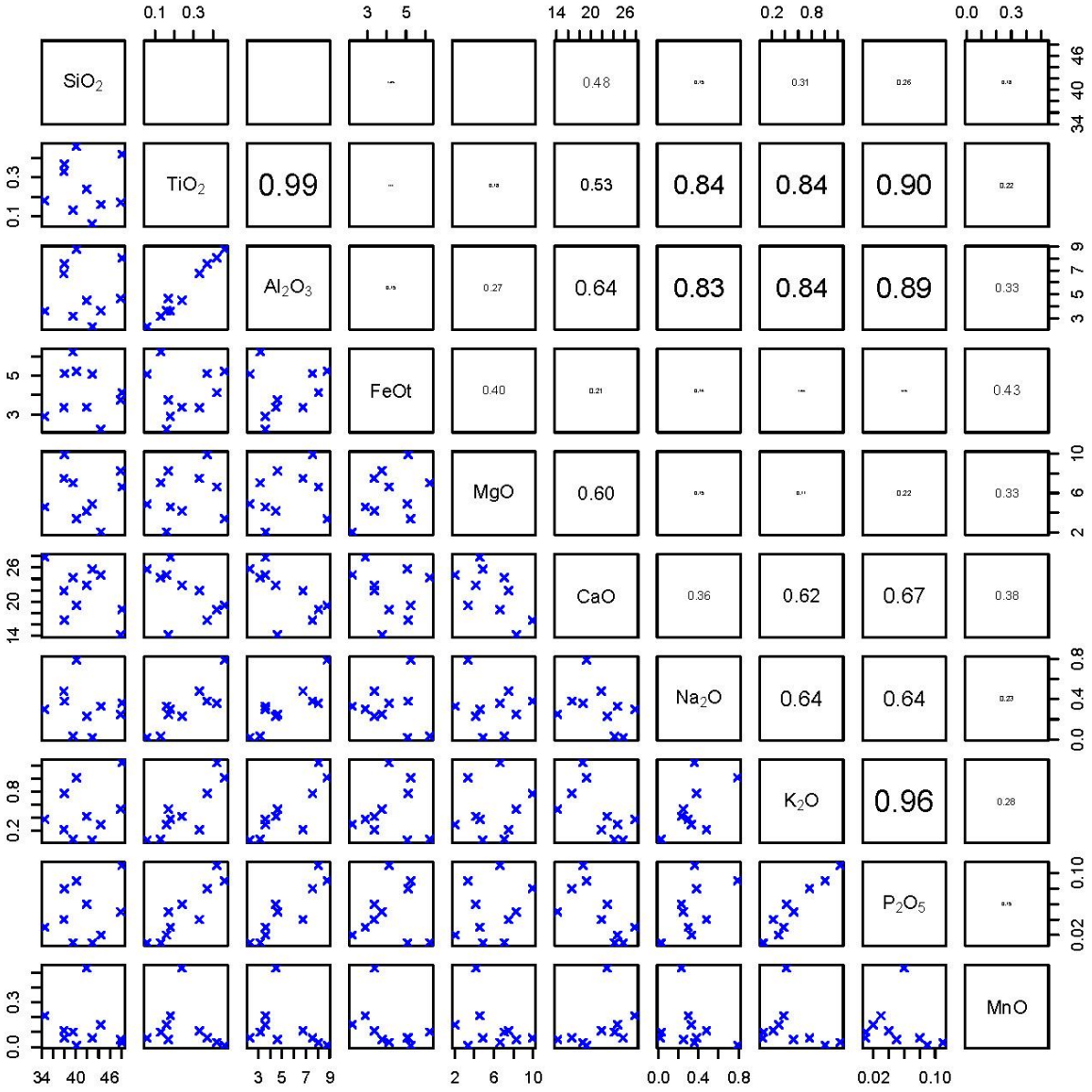

Table 3.4 B Correlation coefficient matrix and scatter diagram of major elements in the Gercus samples.

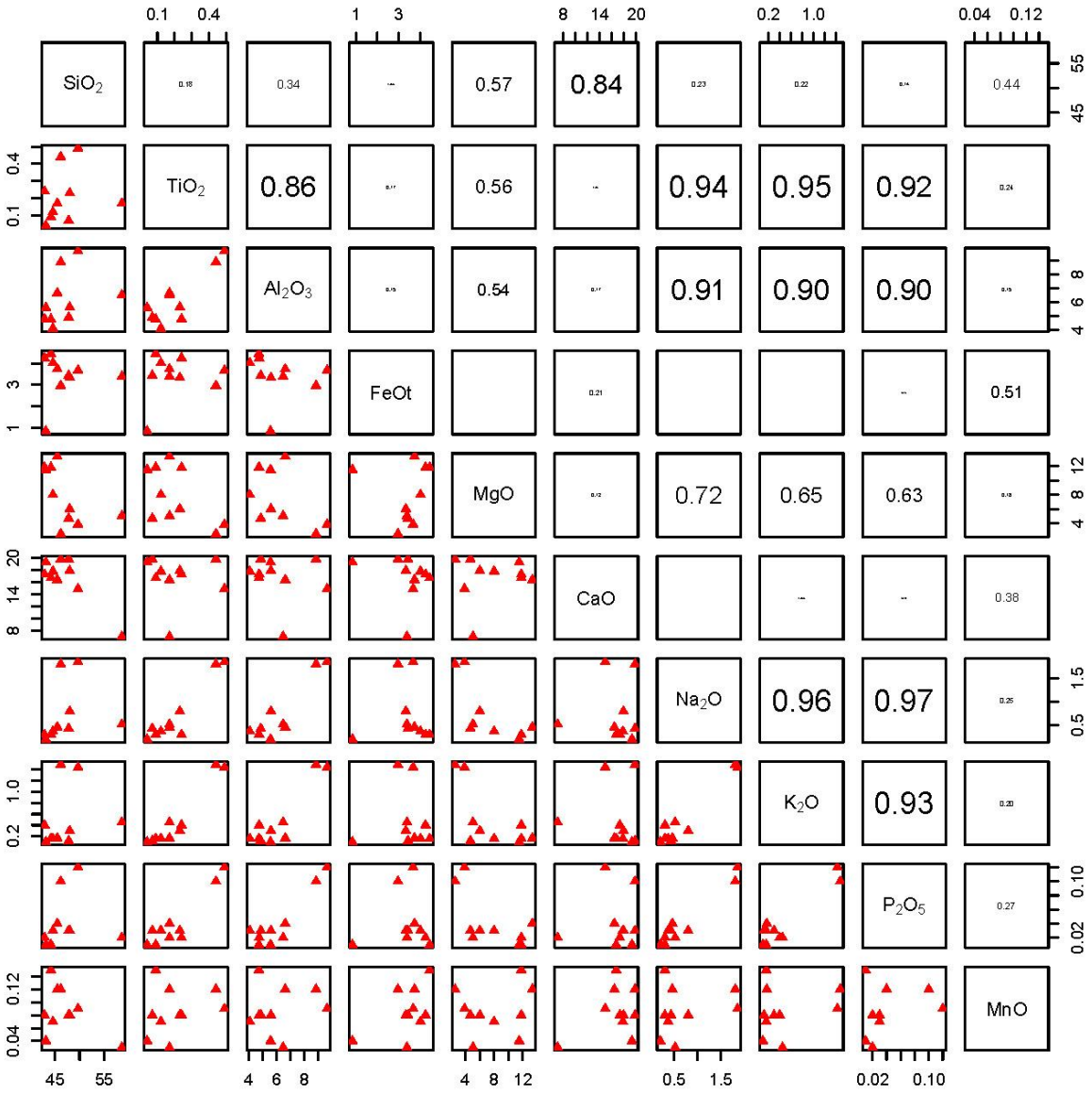

Table 3.5 A Correlation coefficient matrix and scatter diagram of major elements in the Tanjero samples.

Table 3.5 B Correlation coefficient matrix and scatter diagram of major elements in the Gercus samples.

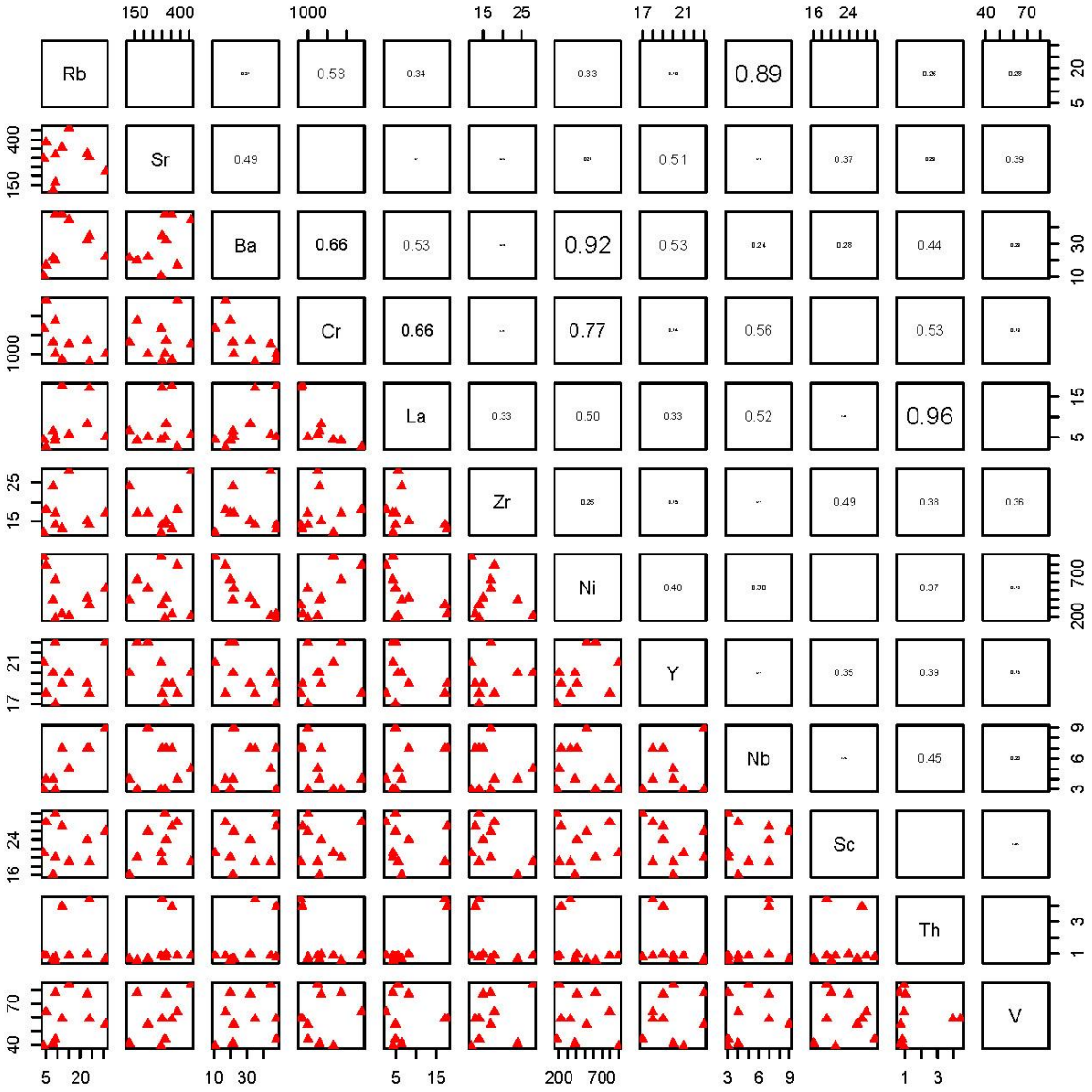

CHAPTER FOUR

GEOCHRONOLOGY

4.1 Preface

Geochronological techniques measure radioactive isotope systems in specific minerals, dating major tectonic events that affect those minerals and source rocks that feed the sedimentary basin. As a result detrital geochronology tends to produce several 'populations' of similar-aged minerals and these can be interpreted to provide highly diagnostic provenance information. Formations containing consistent populations can be correlated across a basin. Detrital zircon (DZ) U-Pb geochronology was a popular and powerful technique that has been used in most subsequent studies (e.g., Fedo et al., 2003) to identify provenance components in a sedimentary units (e.g., Haas et al., 1999). It has been successfully employed in siliciclastic sediments for mapping reservoirs in the basins, tracing sedimentary pathways, recording denudation histories and dating volcano-magmatic events (e.g., Andersen, 2005). This approach has the advantage to identify the characteristic detrital zircon age spectra if compared them with those from other stratigraphic units in the basin and to match them with potential sediment source areas.

4.2 Detrital Zircon U-Pb geochronology

Zircon is ubiquitous in a wide variety of crustal rocks and sediments. Its tendency to incorporate radioactive elements U and pb as well as low levels of Pb which enables determinations of its crystallisation age to use the U-Pb

radioactive decay systems. As zircon is a resilient mineral that can survive through prolonged weathering, sedimentary transport, metamorphism, and in some instances even mantle melting, its crystallisation age can be preserved through multiple sedimentary cycles, accordingly, single grain U–Pb dating of detrital zircon has quickly become the most popular technique for sedimentary provenance studies. Currently by far the most widespread method for visualising detrital age distributions is called Probability Density Plot (PDP), which is calculated by summing a number of Gaussian distributions whose means and standard deviations correspond to the individual ages and their respective analytical uncertainties (Vermeesch, 2012). In the context of detrital geochronology. Instead, a similar-looking but fundamentally different tool named 'Probability Density Plot' (PDP, Ludwig, 2003, also called Probability Density Distribution by Sircombe, (2004), which gained significant popularity. The PDP was first proposed by Hurford et al. (1984), in an attempt to account for the variable analytical precision of data. The PDP is also produced by stacking a Normal distribution on top of each measurement whose bandwidth, however, is not determined by the density, but by the analytical precision, in order to reduce the importance of imprecise measurements and to emphasize the precise measurements. In this study, detrital zircons are extracted from bulk samples of Tanjero and Gercus sandstones using heavy liquid and Frantz magnetic separation. U-Pb ages are collected from individual zircon grains, using laser ablation inductively coupled plasma (LA-ICPMA) samples at original analytical Ltd in Welshpool, United Kingdom. In order to correct for mass and instrumental bias, analyses are corrected against Plesovice and Temora 2 standard (Concordia age of the analysed zircons standards were displayed in (Fig. 4.1). Raw data are reduced using lolite (Paton et al, 2010) software. All

zircon analyses (30 zircon grains of Tanjero and 35 zircon grains for Gercus) are displayed on Concordia diagrams. Accepted data from each grain are then displayed on probability density plots (Fig. 4.2 and 4.3).

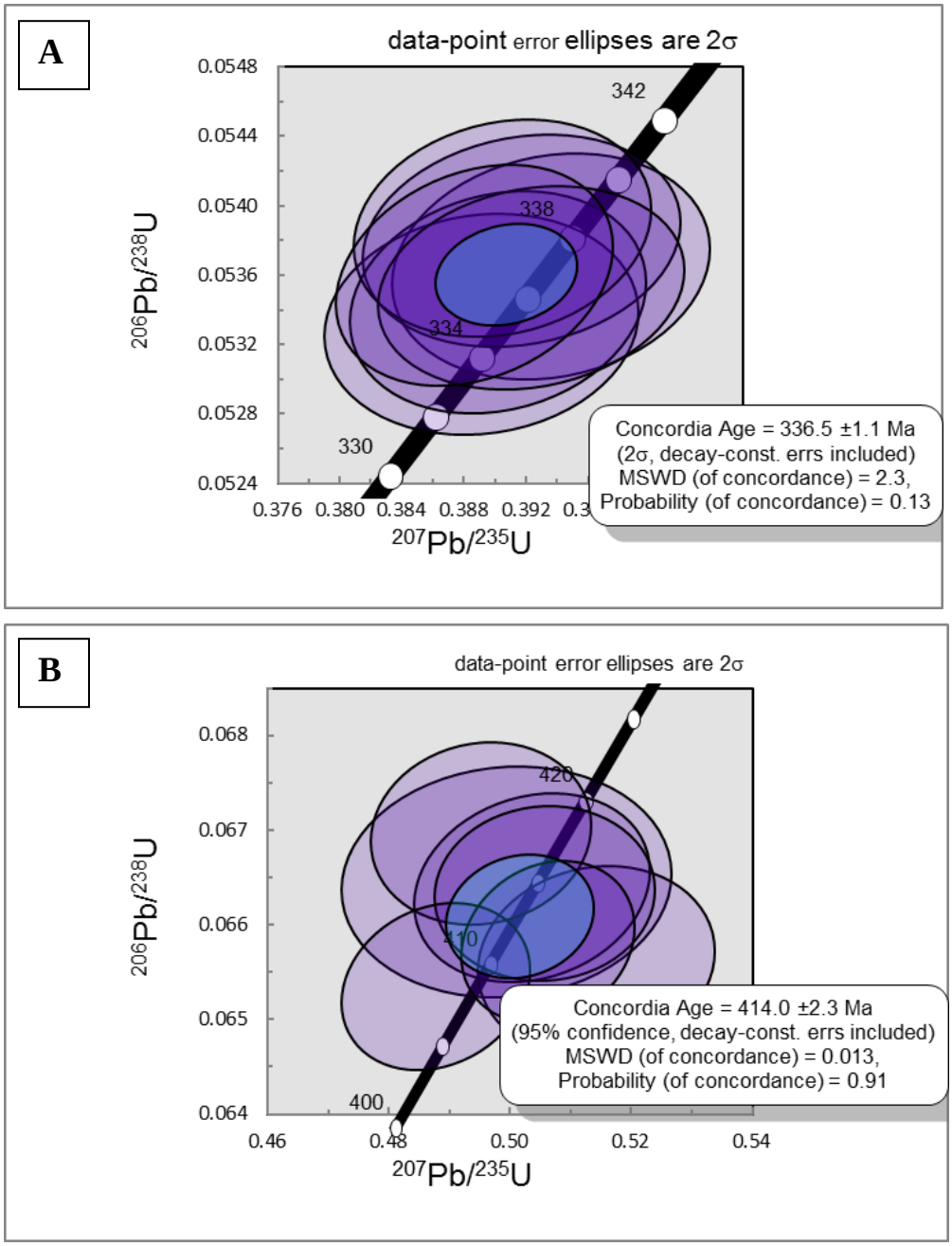

Fig. (4.1) Concordia age of the analyzed zircons standards; A- Plesovice Reference Age 337Ma and B- Temora 2 Reference Age 416 Ma

4.3 Data integration and geological implications

Recently, many detrital zircon geochronological studies have been done of the post-collisional Neogene foreland basin mega-sequences, including the Injana (Upper Fars), Mukdadiya (Lower Bakhtiari), and Bai-Hasan (Upper Bakhtiari) Formations in the Kirkuk embayment (Koshnaw et al., 2017). Few has been made to apply the detrital zircon U–Pb geochronology to assess the Late Cretaceous - Late Paleogene ages active synorogenic sedimentation records within foreland basins. As shown in this study, there are complex U–Pb age spectra (i.e., multiple age components) which are preserved in the two distinguishable formations (i.e. Tanjero flysch and Gercus molasse) within foreland basins which can prove a challenge for the forward reconstructions of the paleogeography and tectonic evolution of the foreland basin in the northeastern Iraq. These complex DZ age spectra are attributed to tectonically active terranes occurring in the east of the studied flysch and molasse outcrops. A petrologic characteristic of these terranes, which are related to passive margin settings, suggests a mixed source, between Ophiolite and an Arabian craton provenance, at least for early flysch sedimentary rock (i.e. Tanjero flysch). Noting that the subduction-related compressional tectonic was initiated during the Albian-Cenomanian (118–97 Ma; Aswad and Elias, 1988; Aswad, 1999 and 106–92 Ma; Ali et al., 2012) continued until Miocene time, when full-fledged continental collision began with final consumption of the oceanic lithosphere (Ali et al., 2013; Aswad, 1999). Thus, the parautochthonous and autochthonous terranes of the Arabian passive margin started to deform in the early Campanian. During this event, the accretion of the Qulqula Accretionary Wedge was accomplished by tectonic wedging and shortly followed by serpentinite–matrix mélanges, which incorporate old crustal components of

mixed age (Aziz et al., 2011), forming accretionary complex terrene–flexural foreland basin assemblages. Such compressional dynamics ultimately cause an oscillatory deformation against Arabian continental margin deposits, forming peripheral foreland basin (refer to as Kurdistan foreland basin, Ali et al., 2014). In such a case, the accretionary complex has accommodated a zircon-bearing detrital supply may be seen as an infinite reservoir of detrital zircons for its adjacent foreland basin systems, resulting in an invariant detrital zircon provenance trend through time (Fig. 4.2 and Fig. 4.3).

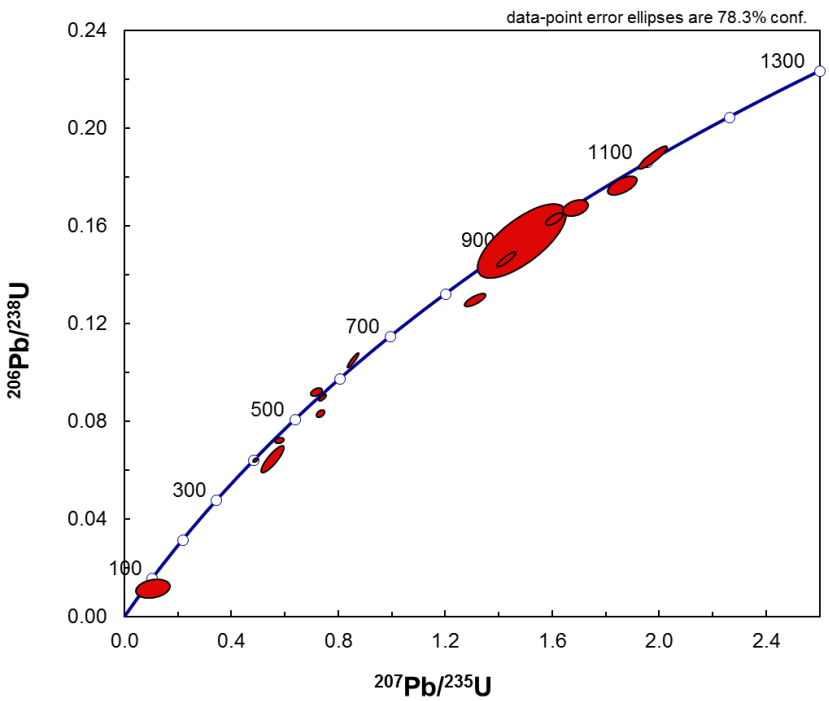

Fig. (4.2) Concordia diagram of dated detrital zircons from Tanjero Formation shows different concordant points indicates a wide spectrum of Concordia age (Ma). These data excluded the highly discordant analyses.

The U–Pb age distributions (30 grains; Fig.4.2) of Tanjero flysch reflect that the input of detrital material of the parautochthonous sediment of Qulqula within this formation likely reflects not only the cratonic influence of an Arabian passive margin, but also the denudation of an arc built (Albian-Cenomanian active magmatic arc) upon a Mid-oceanic crust of about 93-94Ma. In addition to later age, Tanjero flysch has pronounced 398- 448, 511-570, 646-690, 779, 878-880, 910-996 and 1045-1181 Ma ages; see Fig. 4.4, highlighting the cratonic influence of both the Neoproterozoic and a Mesoproterozoic ages, and therefore, the zircon age populations of the flysch units studied here can be easily correlated with those of the source-rock distribution of Qulqula Rise that show recycled DZ age contributions from erodible Arabian craton sources which can also be correlated with the results of Garzanti et al., 2013 which show that the samples of beach sands from Arabian passive margin is dominated by Pan-African source with subordinate contribution of zircon at ca. 1.0 and 2.5Ga for more information see Figure 11 in Zhang et al., 2016 . It should be noted that the accretionary mélange serpentinite sequences related to this subduction are insignificantly known, most likely because high erosion with much erosional denudation and exhumation rates took place during the Late Cretaceous and through most of the Paleogene period. The evidence from petrogenetically-related serpentinite imbricates suggest that there are sporadic exotic blocks of metabasalts and metasediments which are tectonically intermingled with the serpentinite-hosted matrix, forming a serpentinite mélange (Aziz et al., 2011a). The Rb-Sr age data of the serpentinite imbricates yielded an age ranging from150 to 770 Ma (Aziz et al., 2011b), confirming the heterogeneity of these rocks. U-Pb dating of inherited zircons undertaken by Sarmad and Aswad (2013) who reveal two episodes of Palaeoproterozoic

inherited zircon growth: (1) 1953±39 Ma cores and (2) 1777±28 Ma rims, suggesting that these analyses is interpreted as indicating that the zircons are xenocrysts in the Paleogene magma derived from Arabian crystalline basement.

Table (4.1) DZ U–Pb isotopes of the Sandston samples in Tanjero Formation

Analysis No.	**U ppm**	**Th ppm**	**Th/U**	**$^{207}Pb/^{206}Pb$**	**± 2 σ, Ma**	**$^{206}Pb/^{238}U$**	**± 2 σ Ma**	**$^{207}Pb/^{235}U$ Age Ma**	**± 2 σ, Ma**	**$^{206}Pb/^{238}U$ Age Ma**	**± 2 σ Ma**
1	200	130	0.65	70	200	92	3	87	9	93	3
2	258	250	0.97	0	110	93	2	92	6	93	2
3	97	210	2.16	200	96	96	2	102	2	94	2
4	118	130	1.1	128	118	96	2	101	4	94	2
5	94	400	4.26	690	94	401	43	440	35	398	5
6	30	1400	46.67	440	30	401	7	406	8	400	11
7	50	390	7.8	360	41	410	4	410	4	410	4
8	67	134	2	544	67	449	10	464	13	448	3
9	38	2540	66.84	738	38	516	11	560	11	511	14
10	26	1970	75.77	611	26	554	11	565	11	553	10
11	69	111	1.61	446	69	568	13	548	17	570	5
12	42	1200	28.57	610	42	644	22	628	15	646	3
13	80	110	1.37	880	82	678	19	736	22	670	17
14	57	392	6.87	689	57	693	27	690	222	697	30
15	48	338	7.04	1010	48	787	21	846	23	779	9
16	41	498	12.15	979	41	881	22	900	20	878	4
17	44	351	7.98	970	31	880	21	900	20	880	21
18	34	315	9.26	950	29	960	30	910	16	910	16
19	290	74	0.26	950	290	960	130	905	82	916	2
20	33	313	9.48	971	34	944	18	965	16	942	18
21	27	760	28.15	984	27	973	18	974	16	973	7
22	29	295	10.17	1020	30	997	24	995	21	990	20
23	60	79	1.32	1026	60	997	24	1004	23	996	9
24	35	308	8.8	1121	49	1049	28	1066	25	1045	29
25	45	301	6.69	1100	45	1119	27	1112	20	1100	16
26	29	307	10.58	1110	29	1150	20	1152	18	1111	29
27	31	300	9.68	1100	45	1119	27	1112	20	1112	35
28	49	247	5.04	1121	49	1049	28	1066	25	1121	11
29	39	308	7.89	1120	35	1150	16	1150	16	1125	20
30	30	496	16.53	1181	28	1224	23	1220	15	1181	28

The Gercus Formation (35 grains; Fig. 4.3**)** displays complex distributions that includes all age signatures from oldest to youngest (1) Paleoproterozoic 1622, 1865, 1991 Ma) ;(2)) Mesoproterozoic (1100- 1504 Ma) ; (3) Neoproterozoic rocks(697-943 Ma) ; and (4) (92-102, 221, 395-415Ma; Albian-Cenomanian, Upper Triassic and Cambrian; see Fig. 4.5). The results confirmed that the old crustal blocks of the Neoproterozoic - Mesoproterozoic and Palaeoproterozoic zircon age may be correlated with the Khida terrane (1800-1650 Ma), in the north-westernmost portion of the ‘‘Arabian Craton’’ in Saudi Arabia (Ali and Aswad, 2013) or could be the main components in the accretionary mélange serpentinite. The abundance of clasts related to the old crustal components among the detritic molasses (i.e. Gercus Formation) highlighted the impact of DZ age signatures of the accretionary mélange serpentinite on the petrogenesis of the pre-collisional molasses. To better constrain on the evolution of the flexural foreland basin, DZ U-Pb age spectra suggest that the foreland sediments either influx from multiple provenances. The active accretionary prism is composed of Pliensbachian-Turonian Qulqula radiolarite (Gharib & De Wever, 2010) and serpentinite-matrix mélange of mixed ages (150 and 200 Ma) (Aziz et al., 2011b). During pre-accretion, however, the radiolarite basin located along the Arabian passive margin, likely acted as an intermediate sediment repository of mostly Neoproterozoic DZ. It also hosts a significant fraction of the DZ transported directly from the contemporaneously active magmatic arc. In contrast, the serpentinite-matrix mélange was largely composed of post-Cenomanian mantle exhumation (Wrobel-Daveau et al., 2010). Varying volumes of exotic blocks are detached and are drifted from the Palaeoproterozoic crystalline basement fragment, as well as exhumed oceanic crustal sequence, assigning it approximately to the Late Triassic age

(Aziz et al., 2011b). It has been noted that the DZ U-Pb age spectra in the underlying Tanjero Formation show nearly exclusive derivation from the uplift Qulqula Formation (i.e. Qulqula Rise). Our results indicate that a feasible paleogeographic reconstruction of the time of Gercus sedimentation (Middle Eocene) would include a biased distribution of detrital materials in the Gercus molasse. Here, the serpentinite-matrix mélange underwent pervasive pre-Middle Eocene erosion in which the serpentinite matrix was substantially removed by erosion, leaving exotic blocks of different sources amenable to DZ U-Pb dating.

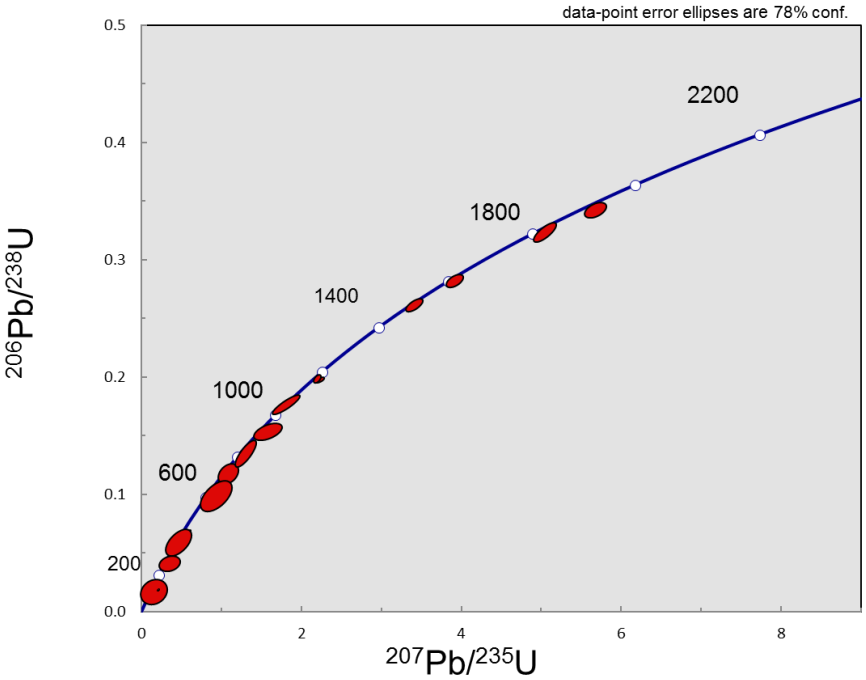

Fig. 4.3 Concordia diagram of dated detrital zircons from Gercus Formation shows different concordant points indicate a wide spectrum of Concordia age (Ma). These data excluded the highly discordant analyses.

Table (4.2) DZ U–Pb isotopes of the Sandston samples in Gercus Formation

Analysis No.	**U ppm**	**Th ppm**	**U/Th**	**$^{207}Pb/^{206}Pb$**	**± 2 σ Ma**	**$^{206}Pb/^{238}U$**	**± 2 σ Ma**	**$^{207}Pb/^{235}U$ Age Ma**	**± 2 σ Ma**	**$^{206}Pb/^{238}U$ Age Ma**	**± 2 σ Ma**
1	190	99.2	0.52	20	190	92	3	93	9	92	3
2	175	125	0.71	630	188	93	3	88	9	93	3
3	260	257	0.99	0	110	95	3	91	5	95	3
4	G 20	93	242	2.60	30	93	96	2	95	96	5
5	83	328	3.95	47	83	97	2	98	4	97	2
6	120	138	1.15	130	120	98	2	103	6	98	2
7	98	212	2.16	202	98	100	2	108	5	99	2
8	130	173	1.33	160	130	102	3	109	8	101	3
9	85	237	2.79	67	85	101	2	101	4	101	2
10	53	950	17.92	65	53	102	3	103	4	102	3
11	62	277	4.47	174	62	221	5	223	7	221	5
12	92	388	4.21	680	93	389	40	440	30	395	4
13	31	1395	45.0	438	28	400	6	405	7	400	10
14	49	392	8.00	368	49	415	8	412	10	415	8
15	66	135	2.04	542	65	445	10	465	15	444	3
16	38	2540	66.84	738	38	516	11	560	11	511	14
17	25	1950	78.0	610	25	550	10	565	10	550	10
18	68	109	1.60	440	68	565	11	540	15	570	10
19	41	1150	28.04	605	40	640	20	625	15	645	3
20	82	112	1.37	880	82	678	19	737	23	672	19
21	58	394	6.79	690	58	695	29	691	23	697	30
22	50	340	6.8	1012	45	785	20	845	20	780	10
23	40	495	12.37	975	40	880	20	900	20	875	4
24	34	315	9.26	971	34	944	18	966	16	943	19
25	30	765	25.5	985	25	975	20	975	15	975	7
26	58	75	1.29	1021	58	995	20	1005	20	996	9
27	44	298	6.77	1050	40	1110	26	1112	20	1100	10
28	29	308	10.62	1111	29	1152	21	1152	18	1111	29
29	48	241	5.02	1120	45	1048	25	1060	20	1120	10
30	40	309	7.73	1125	40	1158	24	1151	21	1125	40
31	28	498	17.79	1181	28	1224	23	1225	17	1181	28
32	28	175	6.25	1504	28	1551	29	1543	20	1504	28
33	22	422	19.18	1622	22	1653	30	1657	19	1622	22
34	36	134	3.72	1865	36	1978	43	1946	26	1865	36
35	30	141	4.70	1991	30	2072	48	2046	30	1991	30

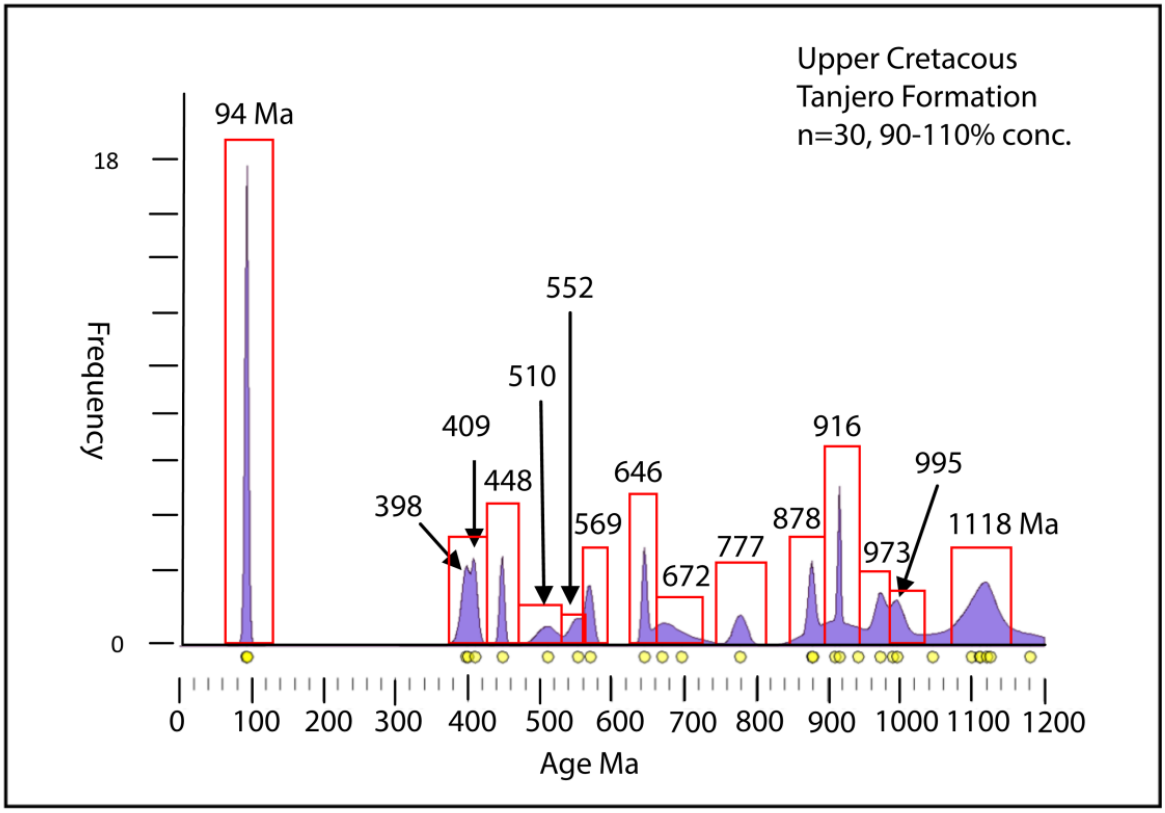

Fig. (4.4) Age probability distribution diagram depicting detrital zircon U-Pb ages of Tanjero Formation.

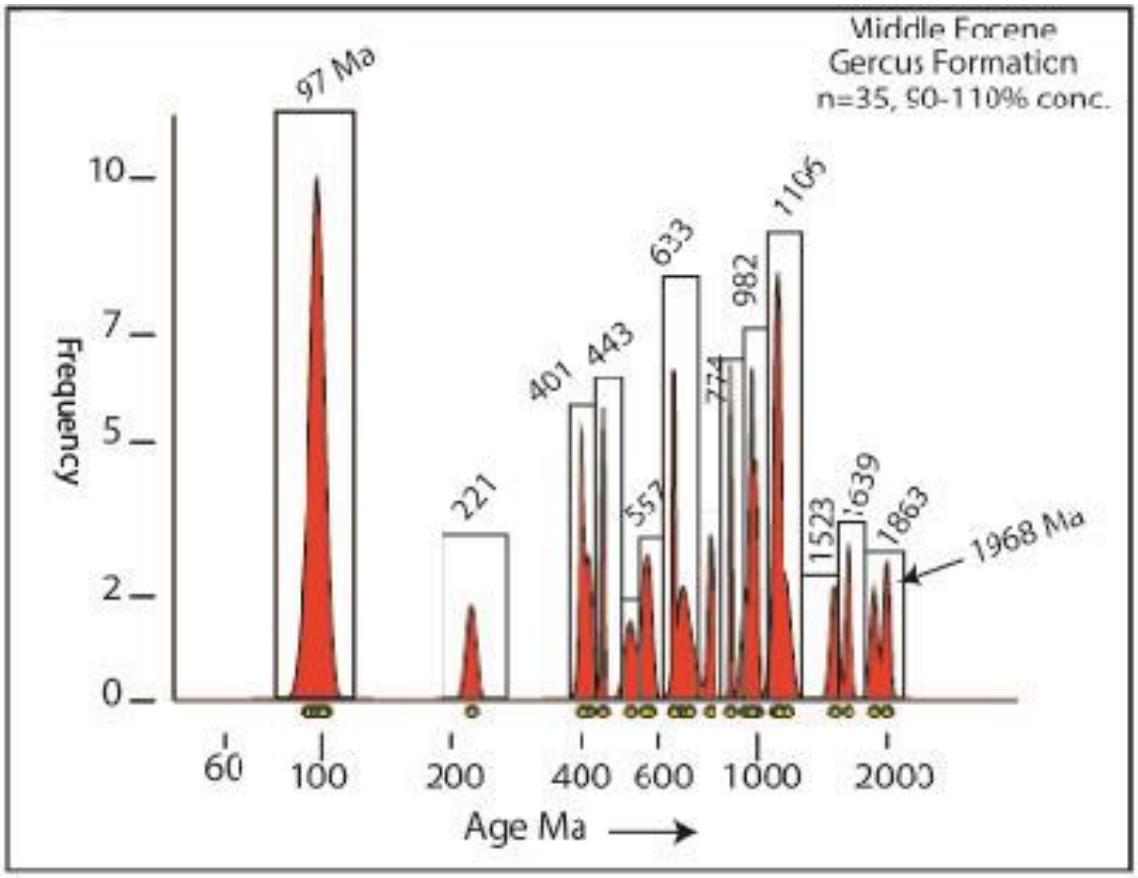

Fig. (4.5) Age probability distribution diagram depicting detrital zircon U-Pb ages of Gercus Formation.

CHAPTER FIVE

PROVENANCE

5.1 Preface

Mineralogical and chemical compositions of clastic sedimentary rocks are the products of several variables such as provenance, weathering conditions, transport, diagenesis, climate and tectonism (Johnsson and Basu, 1993). Selected immobile trace element (e.g., Th, Zr, Hf, Sc, Co, Ni, Cr, and REEs) parameters and discriminatory diagrams form a useful tool to characterize the provenance, paleo-weathering conditions and paleo-climate of the clastic sedimentary rocks and to decipher the tectonic setting of sandstones (Bhatia, 1983; Bhatia and Crook, 1986; Roser and Korsch, 1986, 1988; McLennan and Taylor, 1991; Johnsson and Basu, 1993; McLennan et al., 1993; Condie, 1993; Nesbitt et al., 1996; Fedo et al., 1997; Cullers and Podkovyrov, 2000, 2002; Bhatt and Ghosh, 2001). In this study, geochemical data are interpreted for gathering information about the provenance and are reconstructed the paleo-geographic setting of the Tanjero Flysch and Gercus Molasse of the Kurdistan foreland basin.

5.2 Provenance

5.2.1 Major elements chemistry and tectonic setting

5.2.1.1Total alkalis-Silca (TAS) diagram

The TAS diagram divides rocks into ultramafic, basic, intermediate and acidic on the basis of their silica content. In addition, this diagram subdivides volcanic rocks into alkaline and subalkaline (Rickwood, 1989). Figure (5.1A) shows the sandstone samples from Tanjero Formation mainly represent derivation from Foidite , picro

basalt and basalt whereas, the sandstone from Gercus Formation mainly represent derivation from picro basalt and basalt.

5.2.1.2 Zr/TiO_2-SiO_2

Depend on this diagram which was proposed by Winchester and Floyd (1977)most of the Tanjero samples plot in the alkaline basalt field while Gercus samples plot in the subalkaline to alkaline basalt field (5.1B).

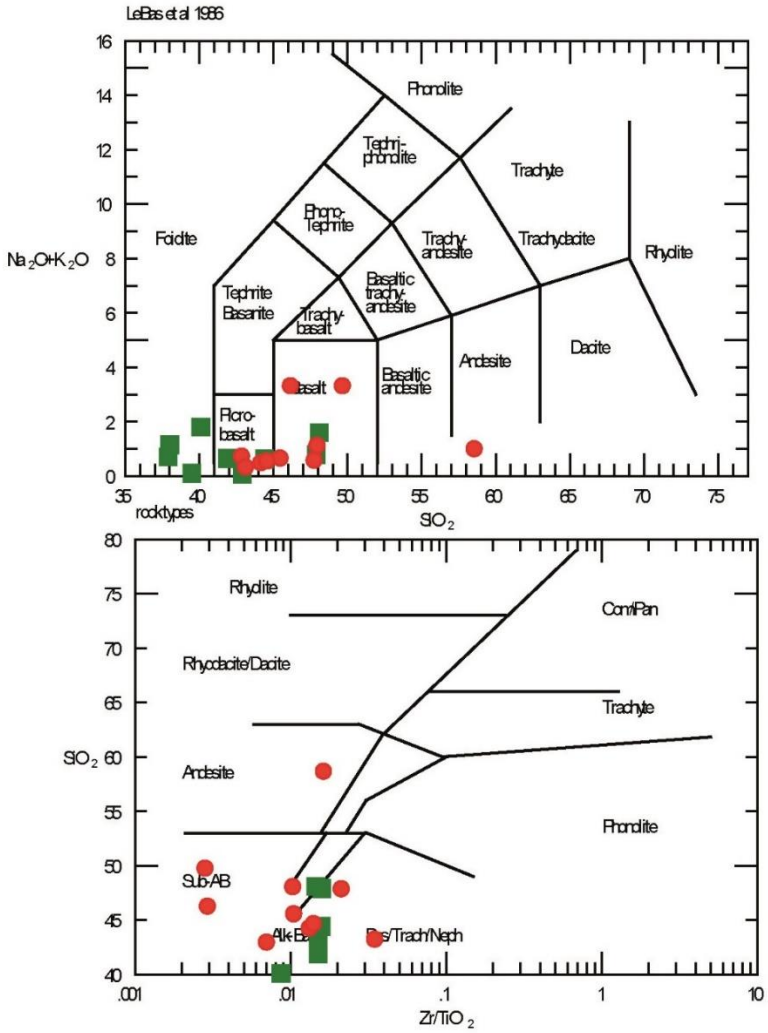

Figure (5.1 A) Total alkalis- silica shows source rock classification diagram (TAS; Lebas et al., 1986). B) Zr/TiO_2-SiO_2 (after Winchester and Floyd (1977).

5.2.2 Trace elements chemistry and tectonic setting

5.2.2.1 Y/Ni vs. Cr/V diagram

The relationships between ultramafic -mafic and felsic-derived detritus can be described by Y/Ni vs. Cr/V diagram (Hiscot, 1984; see Fig. 5.2). The plots of Y/Ni versus Cr/V ratios have been used to complement the discrimination diagrams of source area discussed above. There are two reasons to employ such ratios in this study. Firstly, the Y, Ni, Cr, and V are good indicators of sedimentary provenance, this is because they are quite insoluble and are transported almost exclusively in detritus. Secondly, the Cr/V ratios serve as an index of the enrichment of Cr which concentrates on Cr-spinel, over other ferromagnesian trace elements, whereas Y/Ni monitors the general level of proxy for heavy rare earth elements (HREE) i.e. Y, which is a proxy for heavy REE, typically hosted by zircon if compared with ferromagnesian trace element (Ni). The Cr/V vs Y/Ni diagram shows the curve model mixing between ultrabasic (Cr/V = 45; Y/Ni = 0.001), granitic (Cr/V = 0.093; Y/Ni = 8.889). Rocks (Turekian and Wedepohl 1961; Dinelli et al. 999) are characterized by the mafic to ultramafic sources that contain evidently higher Cr/V and lower Y/Ni ratios than that of the felsic rocks. Previous investigations using relations of Cr/V vs Y/Ni ratios show that the early Campanian sediments were marked by their variation in terms of the proportion of felsic and mafic components (Al-Nakib, 2013). According to the diagram of Hiscott (1984), the studied samples of Tanjero fall along the curve model intermediate between ultramafic and to a lesser extend felsic compositions (Ophiolite), that suggest heterogeneous source areas and characterized by both Radiolarite and ultramafic composition, i.e. the detritus are driven from Qulqula was intermingled with ultrabasic material. In contrast, the Gercus molasse which is characterized by overwhelming high Cr/V ratio definitely receive more Ophiolitic detritus from a belt of Ophiolitic serpentinites that accreted on top of the Qulqula accretionary

wedge and the ultramafic part of the magmatic arc. Overall the amount of the ultrabasic detritus within the Tanjero flysch is estimated to be in the range of 5–15 %. The relatively high Cr/Ni ratios (5.93 and 5.98) from Dokan Section (i.e. T1 and T9 samples) provide evidence of significant amounts of Ophiolitic mélange serpentinites (serpentinite within Qulqula Radiolarite) in the source area associated with a substantial sedimentary fractionation due to the concentration of detrital chromite in the sands.

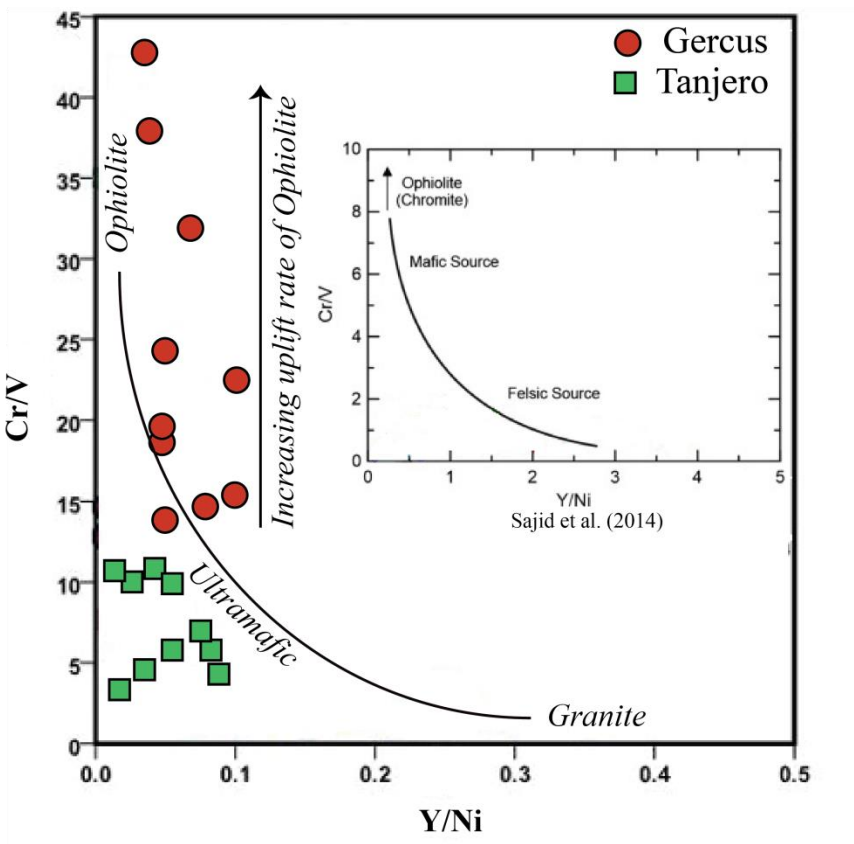

Fig. (5.2) Plot Cr/V versus Y/Ni ratios (Hiscott, 1984) showing the ultramafic and felsic sediment supply to the foreland basin. The diagram shows a mixing line of ultrabasic (Cr/V = 45; Y/Ni = 0.001) and granitic (Cr/V = 0.093; Y/Ni = 8.889) rocks (Turekian and Wedepohl 1961; Dinelli et al. 1999). Percentages show the extent of ultrabasic addition to the mixture.

5.2.2.2 Th vs. Sc diagram

Using Th vs Sc diagram for the Tanjero and Gercus clastic rocks for indication of the source rock signature (Fig. 5.3); Th is an incompatible element that is enriched in felsic rocks, and Sc is a compatible element that is enriched in mafic rocks. Th/Sc ratios near unity are typical of upper continental-crustal (UCC) derivation, and Th/Sc ratios near 0.6 suggest a more mafic component. Therefore Tanjero and Gercus clastic rocks were derived from mafic sources rather than felsic sources.

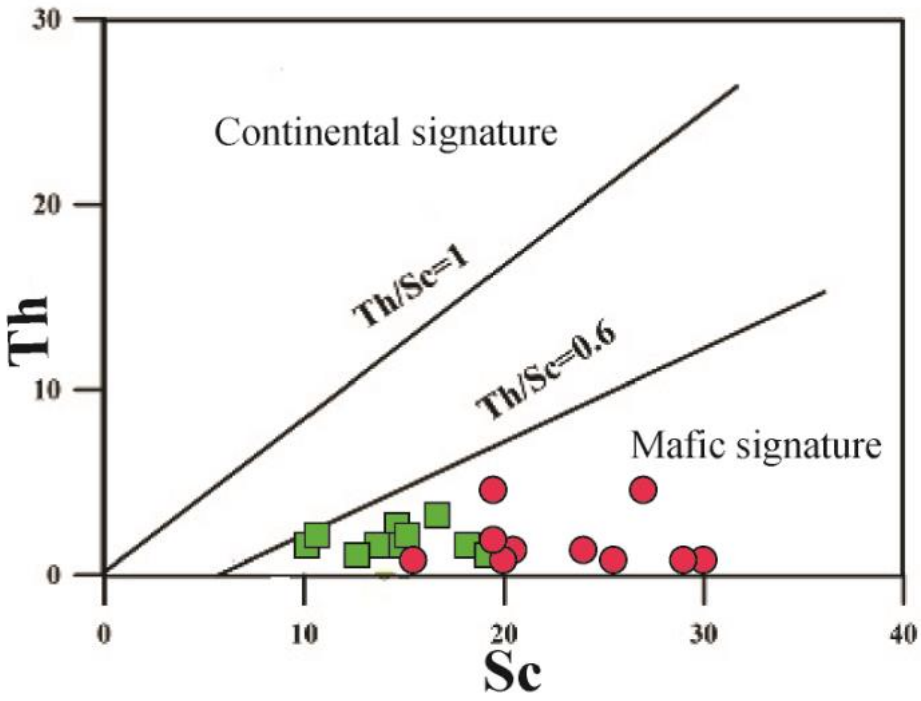

Fig. (5.3) Th vs. Sc for Tanjero and Gercus clastic samples (after McLennan et al., 1993)

The mafic-ultramafic source signature of the Tanjero and Gercus clastic rocks is also confirmed by plotting V, Ni and Th on the ternary diagram of Bracciali, et al.,

(2007) that shows most of the Gercus samples fall in ultramafic and some in the mafic source region while , most of the Tanjero samples fall in the mafic source region (Figs. 5.4A). Furthermore, same scenario has been approved in figure 5.4B CaO + MgO- Na_2O+ K_2O- SiO_2/10 after Taylor and McLenan 1985.

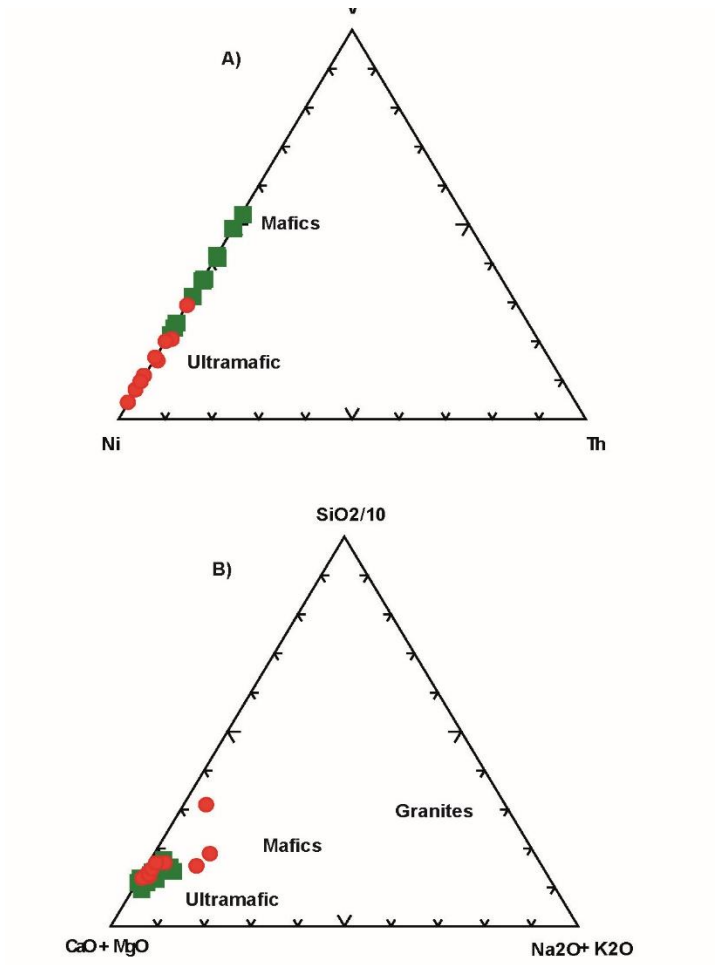

Fig. 5.4 A) V-Ni-Th ternary diagram for Tanjero and Gercus clastic rocks (from Bracciali, et al., 2007). CaO + MgO- Na2O+ K2O- SiO2/10 after Taylor and McLenan 1985.B) CaO + MgO- Na2O+ K2O- SiO2/10 after Taylor and McLenan 1985.

5-2-3 Source area weathering

The alkali and alkaline-earth contents in siliciclastic rocks can change the degree of weathering at the source site (Taylor & McLennan, 1985). In addition to that, an increase in the degree of weathering results in the depletion of alkali and alkaline earths and preferential enrichment of Al_2O_3 in sediments (Bauluz, et al., 2000; Toulkeridisa, et al., 1999). The degree of weathering of the Tanjero and Gercus clastic rocks in the studied area is assessed by using the SiO_2 versus Al_2O_3+Na_2O+ K_2O plot (Fig. 5.5A) (Suttner & Dutta, 1986), both Tanjero and Gercus samples are plotted in semi-arid region, while three samples of both areas are plotted in semi-humid region, which may reveals that both have been influenced mostly be semi-arid conditions in the source area. In addition, the Tanjero samples show slight chemical maturity than Gercus samples (Fig. 5.5A). An increase in the degree of weathering results in the depletion of alkali and alkaline earths and preferential enrichment of Al_2O_3 in sediments (Perri et al., 2016). The degree of weathering can be evaluated by using the CIW (chemical index of weathering [Al2O3/ (Al_2O_3+CaO*+ Na_2O] x 100, Harnois, 1988), and CIA (Chemical Index of Alteration [Al_2O_3/ (Al_2O_3+CaO*+Na_2O + K_2O)] x 100, Nesbitt and Young, 1982) where CaO* is the amount of CaO incorporated in the silicate fraction of the rock. All analysed Tanjero and Gercus sandstones were close to the side of the A-CN mafic rock weathering line in the Al_2O_3 - (CaO*+ Na_2O) - K_2O) (A-CN-K) diagram (Nesbitt and Young, 1984; Etemad-Saeed et al., 2011, Fig5B). All of the samples were between 52 and 87 along the A-CN line indicating moderate weathering.

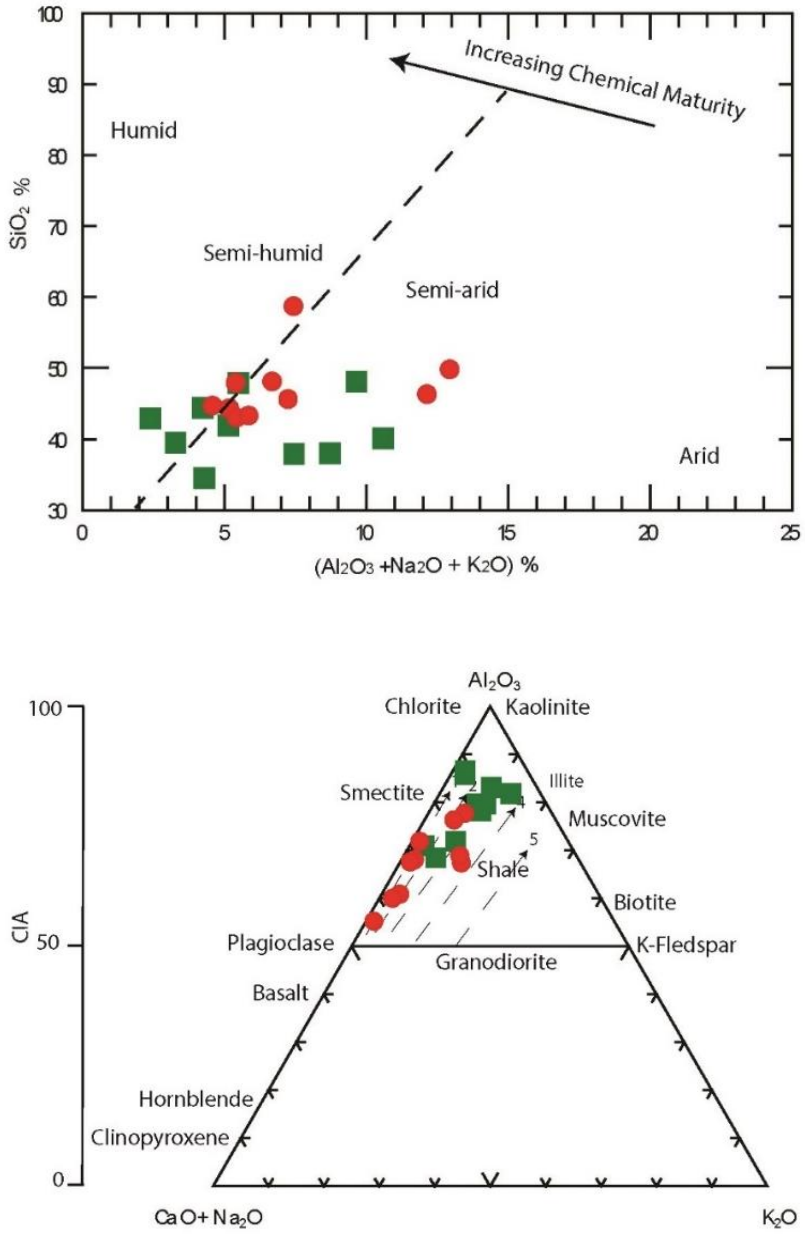

Fig.(5.5) A-Major element plots (SiO_2 vs Al_2O_3+ Na_2O+K_2O) of the Tanjero and Gercus samples to recognize chemical maturity as a function of palaeoclimatic conditions, after (Suttner & Dutta, 1986). B- Al_2O_3 - CaO + Na_2O - K_2O ternary diagram after Nesbitt and Young (1984), showing the relationship between Tanjero clastic and Gercus clastic samples. The dashed arrows 1-5 represent the weathering trends of gabbro, tonalite, granodiorite, adamellite and granite respectively. All the samples represent the weathering trends of gabbro.

5.3 Tectonic Setting

Trace elements represent a well-established provenance and tectonic setting indicators in clastic sedimentary rocks. Consequently, trace elements such as Th, Sc and Zr are considered to be immobile under conditions of weathering, diagenesis and moderate levels of metamorphism (McLennan, et al., 2001; Etemad-Saeed,et al., 2011). Ternary Th–Sc–Zr/10 diagram (Bhatia and Crook, 1986) has been used to constrain the provenance and tectonic settings for the deposition of the Tanjero and Gercus clastics. When the incompatible trace elements Th and Zr are plotted against the compatible trace elements Sc, the Tanjero and Gercus samples plotted in the oceanic island basalt (OIA) field (Fig. 5.6; after Bhatia and Crook, 1986). Using the ternary Q-F-RF tectonic discrimination diagram of (Dickinson, 1983). In Tanjero and Gercus clastic are plotted in mixed between undissected arc and the field of lithic recycle orogen (Fig. 5.7).

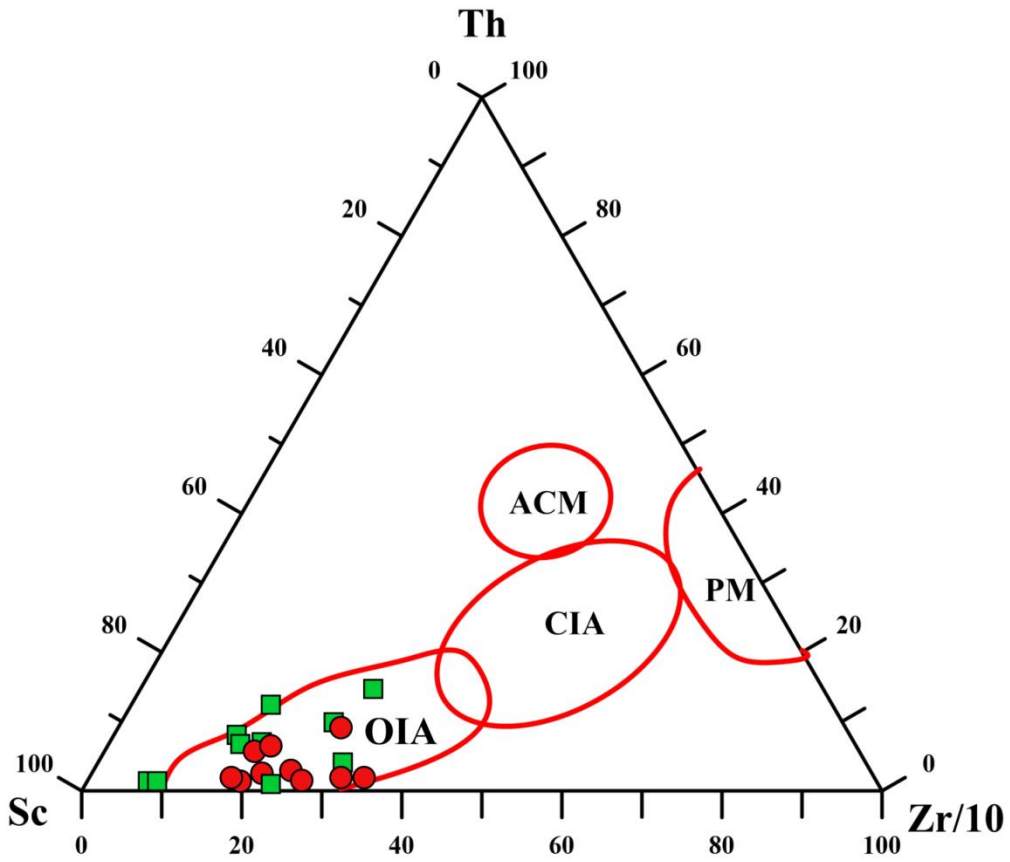

Fig. (5.6) The Plot of the trace element composition of Tanjero and Gercus clastic rocks on the Th-Sc-Zr/10 tectonic setting discrimination diagram (After Bataia and Crook, 1986). OIA: Oceanic Island Arc; CIA: Continental Island Arc; ACM: Active Continental Margin; PM: Passive continental Margin

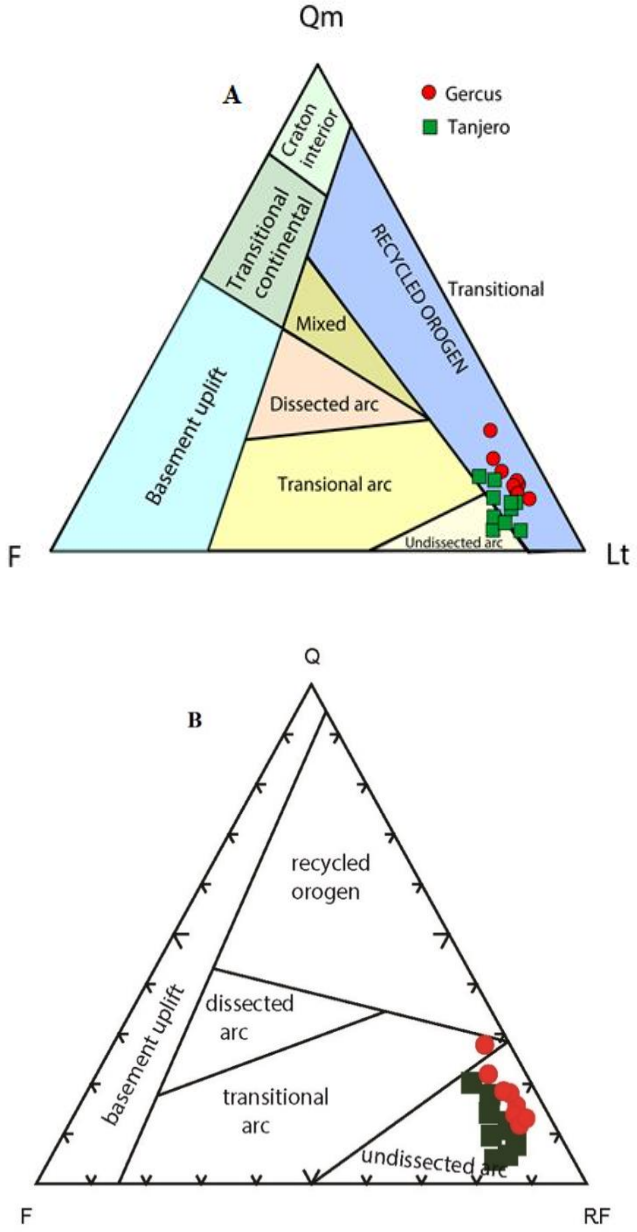

Fig. (5.7) Tectonic interpretation diagram (Ternary plots) of detrital components in Tanjero and Gercus sandstones on the tectonic provenance discrimination diagram of (Dickinson, 1983). B) Tectonic interpretation diagrams (A) Ternary plots of detrital components in the Tanjero and Gercus sandstones on the tectonic provenance discrimination diagram of Dickinson et al. (1983). Qt is the total quartz, F is the feldspar, and RF is the total rock fragments. The solid lines mark the major fields of provenance in terms of tectonic setting.

The subduction signature of the clastic rocks within the Tanjero flysch is confirmed by the Nb/Yb vs Th/Yb diagram (Fig. 5.8). According to (Pearce, 2008) Th/Yb versus Nb/Yb is another important ratio which differentiates between the volcanic, arc and MORB tectonic settings. The result shows that almost all the studied rocks fall in the compositional field of arc-related rocks-well above the field of the MORB-OIB mantle array. The subduction inputs and continental crust contamination both increase the Th content. The E-MORB and OIB source rocks in the Tanjero and Gercus clastic rocks is clear on the Nb/Yb vs.Th/Yb diagram (Fig. 5.8). Thus, it can be concluded that the deposited clastic sediments of Tanjero and Gercus in the studied areas were probably derived from their volcanic and ultramafic terrains of the Iraqi Zagros ophiolites and local Qulqula sedimentary mélange).

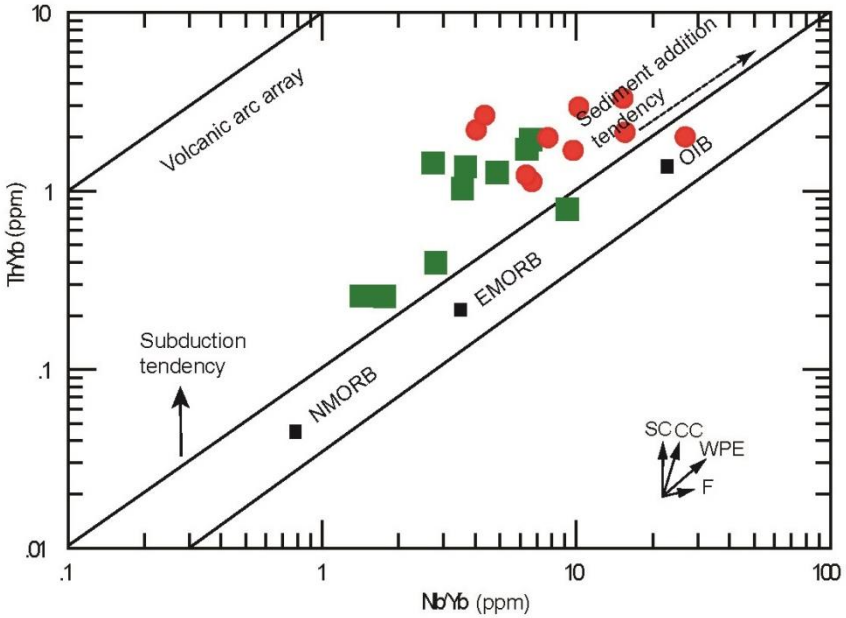

Fig. (5.8) Nb/Yb vs Th/Yb diagram for Tanjero and Gercus clastic rocks, after (Pearce, 2008). SZ-subduction zone enrichment; CC-crustal contamination; F-fractional crystallization; WPE-within plate enrichment.

5.4 Provenance demarcations

The flysch succession of Tanjero formation is exposed in front Qulqula accretionary wedge (formerly referred to as Qulqula Rise, Jassim et al., 2006) which may act as a likely source-area provenance of a definitely major input of mafic detritus for the studied succession, but the succession accommodates more variants of mineralogical and chemical compositions than those from adjacent Qulqula Radiolarite. The data collected from geochemical investigations shown above, suggest that the upper part of the Tanjero flysch succession mainly consists of mafic to ultramafic materials. The heterogeneous nature of the Flysch sediments was influenced by additional source rocks which must be involved in the delivering of the predominantly ultramafic detritus with a minor mafic contribution to the Tanjero basin. The drastic increase in detrital grains of mafic to ultramafic origin in the flysch succession points to the existence of an obducted ophiolite tectonic slice of Albian–Cenomanian age (see figures 5.2, 5.3, 5.4;e.g. Gidon et al., 1974; Ricou et al., 1977; Ravaut et al., 1997) or otherwise strongly serpentinized ophiolite-related ultramafic rocks (Aziz et al.,2011). According to these scholars, serpentinized ultramafic rocks contain sporadic exotic blocks of metabasalts and felsic rocks therefore, referred to as serpentinite-matrix mélanges. The field-based indications clearly show that the exotic blocks are tectonically intermingled up to about microscopic (millimeters) scales, forming a commonly homogeneous in appearance (Aziz et al., 2011). In other words, the accreted serpentinites–matrix mélange was not encompassed a large coherent allochthonous ophiolitic blocks. The unequivocal field-based evidence suggests that the serpentinite-matrix mélange was formerly widespread in the advancing orogenic wedge, although at the present time missing in the studied area. This is because the rocks have a weak matrix which easily erodes and seldom forms observable outcrops except certain tectonic settings (for example: within stacks of thrust nappes).

5.5 Timing and duration of Tanjero and Gercus clastic rocks.

5.5.1 Tanjero Flysch

The discussion on the U-Pb results introduces the fact that the parautochthonous radiolarite basin hosted a significant fraction of the DZ, which was derived predominantly from cratonic source-rocks of the Arabian passive margin, as well as transported directly from the contemporaneous Albian-Cenomanian active magmatic arc. The youngest peak age of DZ (93-94 Ma) obtained from the Tanjero Formation constrains the upper age limit of the stratigraphic succession of the radiolarite formation before it was accreted onto the Arabian carbonate platform (Fig 5.9). Therefore, the DZ U-Pb data indicate that the Albian-Cenomanian marked initiation of the closure of the Neotethys which means that slab pull appears to be the main driving force of extensional orogeny and the decrease in the slab pull latter (which was associated with ongoing mantle drag) leading to the cessation of subduction that was incipient during Albian-Cenomanian. In other words, the pre-orogenic extensional will collapse soon after 90 Ma (Turonian) and was caused by dramatic decrease in slab pull force leading to proto-Zagros Orogeny in the middle Campanian (≥ 80 Ma) (70 Ma, Koshnaw et al., 2017). The conclusion concerning the closure of the Neotethys, however, contradicts a common view held by geologists that the transition from autochthonous platform carbonates to neoautochthonous flysch sedimentation marked the proto-Zagros Orogeny that has been associated with the initiation of the closure of the Neotethys (Aswad, 1999). Furthermore, it has been concluded that the DZ grains acquired from the Tanjero Formation incorporation of cratonic and terrigenous materials during Early Pliensbachian-Toronian and a significant fraction of the contemporaneously Ophiolite during Albian-Cenomanian.

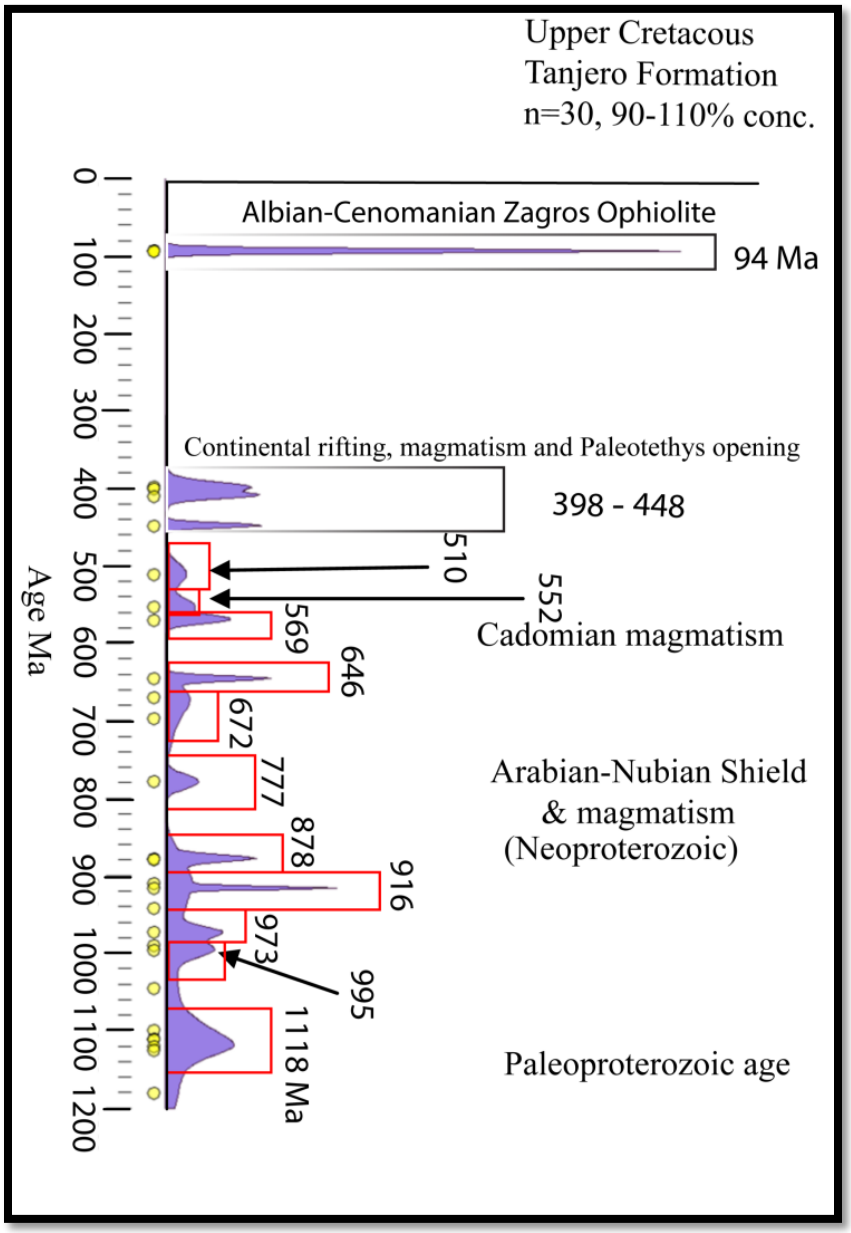

Fig. (5.9) Summary of detrital zircon age spectra of the Tanjero clastic, NE Iraq versus the main tectono-magmatic events of Arabian Plate

5.5.2 Cercus Molasse

Present-day outcrops of the serpentinite-matrix mélange can only be traced to the base of 'Lower Allochthon' (i.e. Walash–Naopurdan nappe) (Aziz, 2008; Aziz et al., 2011a) of age-dated 43-24 Ma (Ali et al., 2013; Aswad et al., 2014). It demonstrates a block-in-matrix aspect, with exotic blocks of various sizes (centimetric to hectometric) and types (meta-igneous and meta-sedimentary) locally found within the serpentinite matrix (Aziz, 2008). However, the exhumed ophiolitic mantle and associated exhumed oceanic crustal of the Late Triassic (219 Ma, see Fig. 5.10) as well as the crystalline basement sequences of the Palaeoproterozoic (1200-1968 Ma) have been dismembered and occured as fragments enclosed in the chaotic serpentinite-matrix mélange. Unlike the Harsin mélange at the southern Iraq-Iran border (Wrobel-Daveau et al., 2010), the accreted serpentinite-matrix mélange of the Iraqi segment of the NZTZ underwent pervasive pre-Middle Eocene erosion, where a substantial portion of the serpentinite matrix was removed. These left exotic blocks of the different sources amenable to DZ U-Pb dating. Three rock samples collected from the locations furthest apart revealed Sr-Nd isotopic heterogeneity (Aziz et al., 2011b). The ages obtained from these samples (i.e. Mawat, Galalah, Halsho) were 150, 200 and 770 Ma, respectively (Aziz et al., 2011b). The value of εNd = -30.0 (Mawat sample, MB) would correspond to a $^{143}Nd/^{144}Nd$ ratio of 0.5111 and could refer to a typical value for the Palaeoproterozoic crystalline basement. It is apparent that the U-Pb ages from DZ in Gercus molasse can provide key information on the serpentinite-matrix mélange. Specifically, the Late Triassic oceanic domains (219 Ma) of the GQR (Galalah, Qalander and Rayat) serpentinite–matrix mélange oceanic domains are observed through zircon age population in Gercus molasse, as the mantle floor of the Qulqula radiolarite basin between the Arabian and the Biston-Avroman

block in the south of the study area. The youngest zircon age population in Gercus molasse (93 Ma) is presumably the age of Iraqi Zagros Ophiolite sequences (Mohammad et al., 2016). This approximates the age of the contemporaneously active magmatic arc (i.e. 106–92; Ma, Ali et al., 2012, 2019; Aswad & Elias, 1988). It has been concluded Gercus Formation provides the most suitable archive to study the evolution of the foreland system of the Iraqi segment of the NZTZ with regards to the transition from passive margin to the accretionary complex terrene-flexural foreland basins setting.

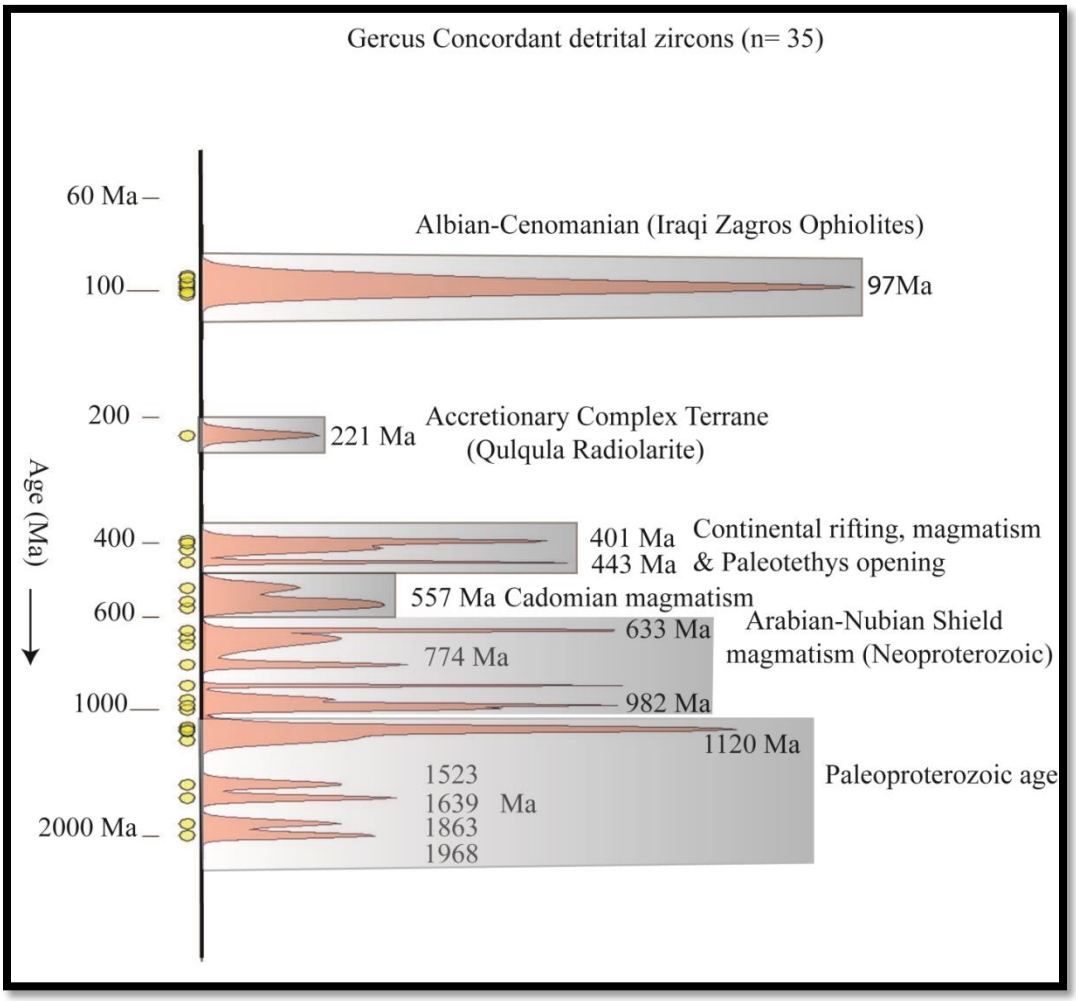

Fig. (5.10) Summary of detrital zircon age spectra of the Gercus clastic, NE Iraq versus the main tectono-magmatic events of Arabian Plate

5.6 Tectonic implication

This study present detrital zircon U-Ph data from both Cretaceous Tanjero and Tertiary Gercus Formations Northeast Iraq in the Zagros Orogen. On the basis of new field, geochronology, geochemistry combined with those published literatures, it might be able to test two hypotheses outlined below to highlight the tectonic events for only Tanjero clastic rocks because of no Tertiary ages have been determined for Gercus clastic rocks.

5.6.1Hypotheses A

Depend on the previously published scenarios (Ali et al., 2012, 2013, 2014, 2017, 2019; Agard et al., 2005, 2011; Wrobel-Daveau et al., 2010), during the Early Cretaceous subduction of the Neotethyan ocean crust toward the east and northeast developed, an ophiolite/arc complex occurred, which is represented by Hasanbag–Pushtashan–Bulfat–Mawat–Penjween– (Fig.5.11; Ali et al., 2012, 2013, 2014, 2016, 2019 ; Ismail et al., 2017) and it is located between the Sanandaj-Sirjan and Zagros thrust zones. This was distal from Eurasia which lay on the northeastern margin of Neotethys. Collision of these ophiolites onto the Arabian passive margin occurred during the Late Cretaceous. These coincide with obduction of other Ophiolites; e.g. Kermanshah–Neyriz–Haji-Abad (Mohajjel et al., 2003; Agard et al., 2005, 2011; Shafaii Moghadam and Stern, 2011; Ali et al., 2012, 2013, 2014, 2016 and 2019). Meanwhile, erosion of these obducted Ophiolites and the Quaqula radiolarian serpentinite mélange fed the detrital basins of Tanjero- Amiran basin (see Fig 5.11).

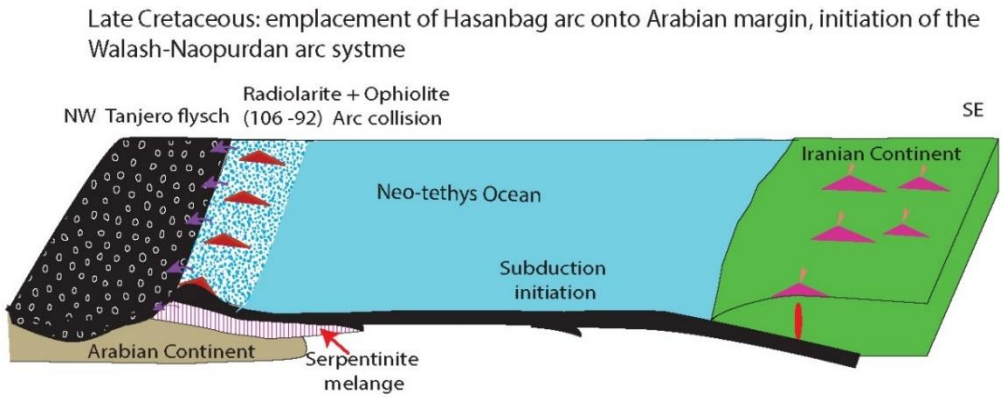

Fig. (5.11) Schematic diagram presenting the tectonic evolution model (Hypothesis A) of the Tanjero clastic rocks within the Foreland basin.

5.6.2 Hypotheses B

As a consequence of dramatic decreases of slab pull, leading to subduction cessation in the Middle Campanian which was associated with the ongoing mantle drag, causes a shift from extensional to compressional settings (Fig. 5.12). The compressional settings are generated through accretion of displaced terranes (refer to as Qulqula Accretionary Wedge and ophiolites) onto the autochthonous platform carbonates. The accreted terranes are composed of blocks of different ages and lithologies (i.e. Qulqula Radiolarite and serpentinites–matrix mélange and ophiolites). The load of the accretionary wedge controls the amount of fexural subsidence in the adjacent foreland basin. In response to dynamic loading by the adjacent accretionary wedge, the Zagros foreland basin was partitioned into

foredeep (i.e., Shiranish Fm.), forebulge “peripheral bulge” (i.e., Aqra Fm.), and marine flysch trough (Tanjero Fm.) (Fig.5.12B). Evident the dynamic loading of the orogenic wedge lags behind the initiation of subduction. An erroneous view of geologists is that the initial Neotethys closure coeval with Proto-Zagros orogeny as shown by foreland flexural subsidence. During Albian-Cenomanian subduction, however, there was extensional tectonic of the Northern Zagros Orogenic Belt which is mainly detected by the disruption of the Arabian platform carbonate. The timing of initial closure for the Neotethys Ocean is virtually synchronous with a short-lived mid-oceanic subduction. It can be concluded that the episodic nature of slab pulls geodynamic, which is thought to have triggered a short-lived extensional stresses associated with Albian–Cenomanian arc tectono-magmatism during the early stages of Neotethys closure (~100 Ma ; Fig. 5.12B). Alternatively, the ongoing mantle drag is found to induce Middle Campanian compressive deformation (~80 Ma), resulting in the formation of flysch Tanjero within foreland basin.

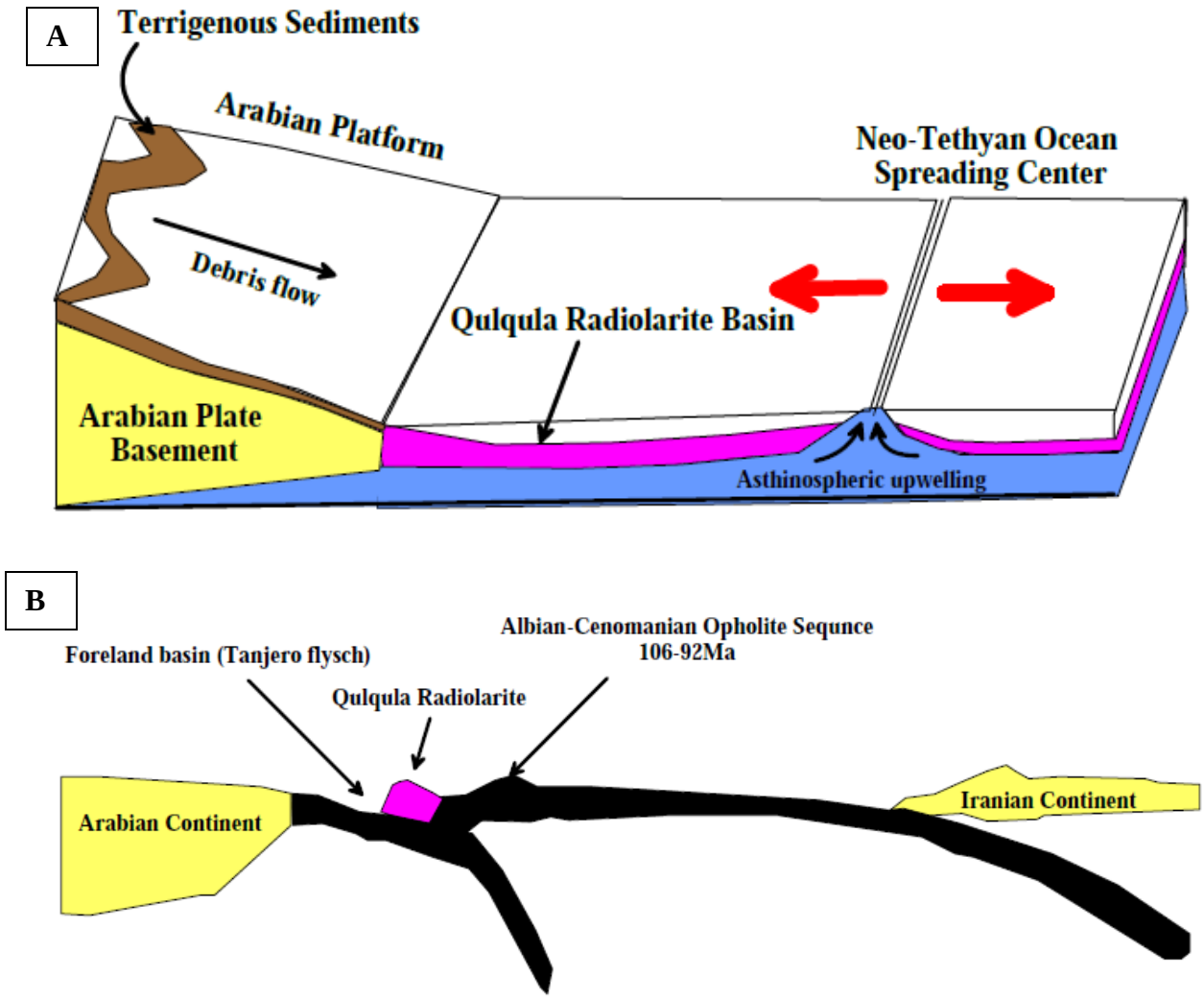

Fig. (5.12) A-Simplified tectonic evolution model (Hypothesis B) showing erosion in the both of Ophiolite material and Qulqula Radiolarite transported directly to the Tanjero flaych basin.

CHAPTER SIX:

CONCLUSIONS AND RECOMENDATIONS

6.1 Conclusions

The following conclusions have been drawn from this thesis:

1- Petrographic point count data on the Tanjero and Gercus clastic rocks indicate that the studied sandstones are lithic arenites. Depending on their mineralogical content, the lithic fragments commonly consist of sedimentary (i.e. limestone and chert), volcanic and plutonic, and low-grade metamorphic rocks, suggesting poor sorting and rapid deposition. Both Tanjero and Gercus samples are characterised by its low content of heavy minerals.

2- Geochemical studies of the Tanjero clastic rocks reveal that the sediments are mainly derived from mafic to ultramafic protoliths. Based on carefully selected major and trace elements, the results show that different trends of clastic influxes reflect the tectonic evolution of the Zagros thrust zone and the Tanjero clastics were derived mainly from the Campanian accreted terrenes (i.e. subduction-related accretionary complex). Therefore, the polymictic clasts vary considerably in the studied rock formation (i.e. Tanjero). The Gercus clastic rocks are derived from the ultramafic and some mafic terrain of Qulqula and the Iraqi Zagros Ophiolites.

3- The overall chondrite-normalized rare earth elements pattern of the Tanjero clastic rocks display one package REE variability which may reflect a single source-rock geochemistry variation (mafic rocks within Qulqula), while the Gercus pattern partitioned into three group’s package which indicates multiple source-rock geochemistry variation and exhumation of different source terrains within the uplifting of the source area.

4- Using Q-F-RF and Th-Sc-Zr/10 discrimination diagrams, Tanjero and Gercus clastics reveal mixed recycled orogen and undissected arc setting exhibitting a strong resemblance to those formed near convergent plate boundaries, were the influence of a marked subduction component that signifies the geochemical characterization of the mantle source. The subduction signature of the Tanjero and Gercus rocks is confirmed by the Nb/Yb versus Th/Yb diagram, which shows that almost all the studied rocks fall in the compositional field of arc-related rocks well above the field of the MORB-OIB mantle array.

5- The provenance of the Tanjero and Gercus clastic rocks were confirmed using Y/Ni vs. Cr/V diagram. The results may indicate heterogeneous source area for the Tanjero clastic rocks (mafic rocks associated within the Qulqula radiolarite and Zagros Ophiolites). In contrast, the Gercus molasse which is characterized by overwhelming high Cr/V ratio which indicate that may receive more Ophiolitic detritus from a belt of Ophiolitic complex that accreted on top of the Qulqula accretionary wedge and the ultramafic part of the magmatic arc (Zagros Ophiolites).

6- In the present study, an attempt has been made to apply the detrital zircon U–Pb geochronology to assess the Late Cretaceous age active syn-orogenic sedimentation records within foreland basins by two points. The study indicates that a complex U–Pb ages spectra (i.e., multiple age components) is preserved in the Tanjero flysch within foreland basin by two points: 1) incorporation of cratonic and terrigenous materials during Early Pliensbachian-Toronian .2) a significant fraction of the contemporaneously Ophiolite during Albian-Cenomanian.

7- The youngest zircon age population in the Tanjero Flysch yielded an age of 93-94 Ma which coincides closely with an Albian-Cenomanian arc -

dominated magmatic event (i.e. 106–92 Ma). In addition, the DZ U-Pb showed a strongly episodic age distribution 398- 448, 511-570, 646-690, 779, 878-880, 910-996 and 1045-1181 Ma that suggest multicycled derivation mostly from the Neoproterozoic basement of the Arabian-Nubian Shield that were at some point hosted by the Early Pliensbachian-Turonian Qulqula Radiolarite Basin which was located along the Arabian passive margin.

8- Representative DZ U-Pb measurements revealed that the Gercus Molasse fall into several separable age population ranges from 92-102 (Albian-Cenomanian), 221 (Upper Triassic), 395-511 (Cambrian), 550- 996 (Neoproterozoic), 1100-1504 (Mesoprotrozoic), and lesser numbers of Paleoproterozoic (1622-1991 Ma) ages. The source of Proterozoic detrital Zircons is enigmatic; the age peaks at 1.1, 1.5, 1.6, and 1.9 Ga (Proterozoic) does not correspond to any known outcrops of Precambrian rocks in Iraq, and it may be useful to continue to search for such basement. The detrital zircons with age populations at 0.63–0.86 Ga probably originated from the Arabian-Nubian Shield. The age peak at 0.55 Ga correlates with Cadomian Magmatism which is reported from north Gondwana. The age peaks at ~0.4 Ga is interpreted to represent Gondwana rifting and the opening of Paleotethys. The youngest age populations at 93 Ma indicate that fraction of DZ were transported directly from the contemporaneously active magmatic arc.

9- Geochemical and geochronological data suggest that the ophiolite components especially the mafic unit is the dominant supplier of sediment during disposition of Tanjero Formation, where limited contribution of Qulqula indicated.

6.2 Recommendations

To achieve a better understanding of the evolution of the Zagros Foreland basin, the following can be recommended for further studies:

1- Doing more analysis of zircon up to 110 zircon grains in a sample in particularly for Gercus clastic rocks and Tanjero and is useful to a better illustration of ages and tectonic evolutions of the Zagros foreland basin.

2- Pb-U dating of feldspar minerals required, as it contains little U or Pb, and hence, the common Pb isotope composition of unaltered K-feldspar is that of the source rock.

REFERENCES

Abdel-Kireem, M.R. (1986a) Contribution to the Stratigraphy of the Upper Cretaceous and Lower Tertiary of the Sulaimaniya – Dokan Region, Northeastern Iraq, N. Jb. Geol. Paleont., 172 (1): 121-139.

Abdel-Kireem, M.R. (1986b) Planktonic Foraminifera and Stratigraphy of the Tanjero Formation (Maastrichtian), Northeastern Iraq, Micropaleontology, 32(3): 215-231.

Alavi, M. (1994) Tectonics of the Zagros orogenic belt of Iran: new data and Interpretations, Tectonophysics, 229 (3): 211–238.

Ali, S. A. & Aswad, K. J. (2013**)** SHRIMP U-Pb dating of zircon inheritance in Walash arc volcanic rocks (Paleogene age), Zagros suture zone, NE Iraq: new insights into crustal contributions to trachytic andesite generation. Iraqi National Journal of Earth Sciences, 13 (1): 45-58.

Ali, S.A.; Buckman, S.; Aswad, K.J.; Jones, B.G.; Ismail, S.A.; Nutman, A.P. (2012) Recognition of late cretaceous Hasanbag ophiolite-arc rocks in the Kurdistan region of the Iraqi Zagros thrust zone: a missing link in the paleogeography of the closing neotethys Ocean, Lithosphere 4: 395-410.

Ali, S.A.; Buckman, S.; Aswad, K.J.; Jones, B.G.; Ismail, S.A.; Nutman, A.P., (2013) The tectonic evolution of a neo-tethyan (Eocene-Oligocene) island-arc (Walash and Naopurdan groups) in the Kurdistan region of the northeast Iraqi Zagros, Conference, Experimental Mineralogy Petrology and Geochemistry, Kiel University, Germany, 34p.

Ali, S.A., Mohajjel, M., Aswad, K.J., Ismail, S.A., Buckman, S., Jones, B.G., 2014. Tectono-stratigraphy and general structure of the northwestern Zagros collision zone across the Iraq-Iran border. J. Environ. Earth Sci. 4 (4), 92-110.

Ali, S.A., Sleabi, R.S., Talabani, M.J.A., Jones, B.G., 2017. Provenance of the Walash-Naopurdan back-arc - arc clastic sequences in the Iraqi Zagros suture zone. J. Afr. Earth Sci. 125, 73–87.

Ali, S.A., Mohammad, E.M., (2018) Geochemistry and Provenance of Sandstone Unit in Tanjero Formation in Sulimania Area, NE-Iraq, Kirkuk University Journal, 13(4): 113-126 .

Al-Kadhimi, J.A.M., V.K. Sissakian, A.S. Fattah and D.B. Deikran 1996 Tectonic Map of Iraq, State Company of Geological survey and Mining, Baghdad.

Al-Mehaidi HM. (1975) Tertiary Nappe in Mawat Range, NE Iraq, J. Geol. Soc. Iraq, 8: 31-44.

Al-Mashaikie, Z.A., Al-Azzawi, T. A., Kadum, A. K. (2014) Depositional Environment of the Gercus Formatiom in Jabal Haibat Sultan, NE Iraq; New sedimentological Approch, Iraqi Journal of Science, 55(2A): 471-483.

Al-Nakib M.A. and Dhannoun H.Y. (2013) Impact of Sharp changes in

Source Rocks on the Geochemistry of Tanjero Formation in Dokan District, Northeastern Iraq, Iraqi Bulletin of Geology and mining, 10(2): 157-172.

Al-Rawi, I.K. (1981) Sedimentology and Petrography of Tanjero Clastic Formation from north and Northeastern Iraq, Unpublished Ph.D. Thesis, University of Baghdad, 295p.

Al-Rawi, Y.T. and Al-Rawi, I.K. (2002) Tanjero Formation from northeast and North Iraq: A turbidities example of flysch type, proceeding of 15thIraqi Geological Conference, Baghdad.

Al-Qayim, B. (1993) Petrofacies Analysis and Tectonic Evolution of a Zagroside Flysch Suites from Northeastern Iraq. In Kumon and Ku (Eds.), Petrology of Sandstones in Relation to Tectonics, V.S.P., Netherlands, 33-42.

Al-Qayim, B. (1994) Evolution of Flysch Basin along the Northeastern Margin of the Arabian Plate. In Abed and Others (Eds.), Geology of Jordan and Adjacent Areas, (Geocome III), Amman, 347-372.

Al-Qayim, B. (1995) Sedimentary facies anatomy of Khurmala Formation Northern Iraq. Iraqi Geology Joiurnal, 28 (1): 36-46.

Al-Qayim, B., Al-Mutwali, M.M., Nissan, B.Y. (2007) Flysch – Molasse Sediments Of The Paleogene Foreland Basin Of North Arabia, Shiranish Area, North Iraq, Iraqi Bulletin of Geology and Mining, 4(1): 1-20.

Al-Qayim, B. and Al-Shaibani, S. (1991) A Bimodal Tidal Depositional System of the Gercus Formation, Shqlawa Area Northeastern Iraq, Salahadin University Jour. Sci.

Andersen T. (2005) Detrital Zircons as tracers of sedimentary provenance: Limiting conditions from statistics and numerical simulation, Chemical Geology, 216 (3-4):249-270.

Armstrong-Altrin, J.S.; Verma, S.P. (2005) Critical evaluation of six tectonic setting discrimination diagrams using geochemical data of Neogene sediments from known tectonic settings, Sediment. Geol., 177: 115-129.

Armstrong-Altrin; J.S.; Yong Il Lee; Surendra P. Verma; S. Ramasamy (2004) Geochemistry of Sandstones from the Upper Miocene Kudankulam Formation, Southern India: Implications for Provenance, Weathering, and Tectonic Setting, Journal of Sedimentary Research, 74 (2): 285-297.

Asadi, S.; Moore, F.; Keshavarzi, B. (2013) The nature and provenance of Golestan loess deposits in northeast Iran, Geol. J., 48: 646-660.

Ameen, B.M., (1998) Sedimentological Study of Gercus Formation in NE Iraq, Un. Pub. M. Sc. thesis Unv. Baghdad, 103p.

Ameen, B. M. (2006) Sequence Stratigraphy of Gercus Formation (Middle Eocene) in Sulaimaniya Area, Northeastern Iraq, Iraqi Journal of Earth Sciences, 6(2): 13 – 22.\

Arai, S. and Okada, H. (1991) Petrology of serpentine sandstone as a key to tectonic development of serpentine belts. Tectonophysics, 195: 65–81.

REFERENCES

Argast S. & Donnelly T.W. (1987) The chemical discrimination of clastic sedimentary components. J. Sed. Petrology 57: 813—823.

Aswad J. A.; Aziz N. R. H; Koyi H. A. (2011) Cr-spinel compositions in serpentinites and their implications for the petrotectonic history of the Zagros Suture Zone, Kurdistan Region, Iraq. Geol. Mag. 148 (5–6):802–818. DOI:10.1017/S0016756811000422.

Aswad, K.J. (1999) Arc-continent collision in northeastern Iraq as evidenced by Mawat and Penjween ophiolite complexes. Rafidain J. Sci., 10:51-61.

Aswad, K.J.; Al-Samman, A.H.; Aziz, N.R.; Koyi, A.M. (2014) The geochronology and petrogenesis of Walash volcanic rocks, Mawat nappes: constraints on the evolution of the northwestern Zagros suture zone, Kurdistan Region, Iraq. Arab. J. Geosci.**,** 7 (4): 1403–1432.

Aswad, K.J.; Elias, E.M. (1988) Petrogenesis, geochemistry and metamorphism of spilitized subvolcanic rocks of the Mawat Ophiolite Complex, NE Iraq, Ofioliti, 13 (2/3): 95–109.

Aziz, N. R.; ELIAS, E. M. and ASWAD, K. J. (2011a) Rb–Sr and Sm–Nd isotope study of serpentinites and their impact on the tectonic setting of Zagros Suture Zone, NE-Iraq. Iraqi Bulletin of Geology and Mining, 7: 67–75.

Aziz, N.R., Aswad, K.J., Koyi, H.A. (2011b) Contrasting settings of serpentinite bodies in the northwestern Zagros Suture Zone, Kurdistan Region, Iraq. Geol. Mag., 148 (5–6): 819- 837.

Bates, R.L. and Jackson, J.A. (1980) Glassary of Geology. 2nd Edition, American Geological Institute, Virginia.

Bauluz B.; Mayayo M.J. (**2000**) Fernandez-Nieto C.; Gonzalez-Lopez, J.M., Geochemistry of Precambrian and Paleozoic siliciclastic rocks from the Iberian Range (NE Spain): implications for source-area weathering, sorting, provenance, and tectonic setting, Chem. Geol. 168: 135-150.

Bellen R.C. van; Dunnington, H.V., Wetzel R. and Morton, D. (1959) Lexique Stratigraphic International, Asie, Fasc. 10a, Iraq, Paris, 333p.

Bhat, M.I., and Ghosh, S.K., 2001, Geochemistry of the 2.51 Ga old Rampur Group pelites, western Himalayas: Implications for their provenance and weathering: Precambrian Research, v. 108, p. 1–16, doi:10.1016/S0301-9268(00)00139-X.

Bhatia, M.R.(1983) Plate tectonics and geochemical composition of sandstones, J. Geol. 91: 611-627.

Bhatia, M.R.; Crook, K.A.W (1986) Trace element characteristic of greywackes and tectonic setting discrimination of sedimentary basins, Contributions to Mineralogy Petrology, 92: 181-192.

Bhatia, M. R. (1983) Plate tectonics and geochemical composition of sandstone. J. Geol., 91: 611-627.

Bhatia, M.R. (1985) Rare earth element geochemistry of Australian Paleozoic graywackes and mud rocks: provenance and tectonic control.

Sediment. Geol., 45: 97-113.

Bracciali, L., Marroni, M., Pandolfi, L. and Rocchi, S. (2007) Geochemistry and Petrography of Western Tethys Cretaceous Sedimentary Covers (Corsica and Northern Apennines): From Source Areas to Configuration of Margins, Geological Society of American Special Papers, 420: 73-93. http://dx.doi.org/10.1130/2006. 2420(06).

Buday, T. (1980) The Regional Geology of Iraq, 1, Stratigraphy, I.I.M., Kassab and S.Z., Jassim (Eds.), GEOSURV, Baghdad, Iraq, 445p.

Buday, T. and Jassim, S.Z. (1987) The Regional Geology of Iraq: Vol.II, Tectonism, Magmatisim and Metamorphism, GEOSURV, Baghdad, Iraq, 352p.

Carver, R. E. (1971) Heavy-mineral separation: ~/n Carver, R. E. (ed.), Procedures in Sedimentary Petrology, John Wiley & Sons, Inc., N. Y., 427-452.

Chaodong , W., changsong , L.,Yanping , S. and Xue , F. (2005) Compotation of Sandston and heavy minerals implies the provenance of Kuqa Depression in Jurassic , Tarim basin , China – progress in Natural Science , 15(7) : 633 – 640.

Condie, K.C. (1991) Another look to rare earth elements in mud rocks, Geochimica et Cosmochimica Acta., 55: 2527-2531.

Cookenboo, H. O.; Bustin, R. M.; and Wilks, K. R. (1997) Detrital chromian spinel compositions used to reconstruct the tectonic setting of provenance: implications for orogeny in the Canadian Cordillera. J. Sediment. Res. 67:116–123.

Cox, R. and Lowe, D.R. (1995) A Conceptual Review of Regional Scale Controls on the Compositions of Clastic Sediments and the Co-Evolution of Continental Blocks and Their Sedimentary Cover. Journal of Sedimentary Research, 65: 1-12.

Cullers R. L. and Podkovyrov, V. N. (2000) Geochemistry of the Mesoproterozoic Lakhanda Shales in Southeastern Yakutia, Russia: Implications for Mineralogical and Provenance Control, and Recycling, Precambrian Res. 104: 77–93.

Cullers R. L. and Podkovjrov, V. N. (2002) The Source and Origin of Terrigenous Sedimentary Rocks in the Mesoproterozoic Ui Group, Southeastern Russia," Precambrian Res. 117: 157–184

Deer, W. A., Howie, R. A., and Zussman, J. (1992) An Introduction to the Rock Forming Minerals, 2nd ed., Longman, London, 696p.

Degens, E. T. (1965) Geochemistry of sediments: A brioef Survey, Prentic-Hall, New Jersey, 342p.

Dercourt, J., Zonenshain, L.P., Ricou, L.E., Kazmin, V.G., Le Pichon, X., Knipper, A.L.,Grandjacquet, C.,Sbortshikov, I.M., Geyssant, J., Lepvrier, C., Pechersky, D.H., Boulin, J., Sibuet, J.-C., Savostin, L.A., Sorokhtin, O., Westphal, M., Bazhenov, M.L., Lauer, J.P., Biju-Duval, B. (1986)

Geological evolution of the Tethys belt from the Atlantic to the Pamirs since the Lias, Tectonophysics, 123: 241–315.

Dey S., Rai A.K. & Chaki A. 2009: Palaeoweathering, composition and tectonics of provenance of the Proterozoic intracratonic Kaladgi—Badami basin, Karnataka, southern India: Evidence from sandstone petrography and geochemistry. J. Asian Earth Sci. 34: 703—715.

Dhanoun H.Y. et.al.(1988) The Geochemistry of the Gercus Red Bed Formation of Northeastern Iraq Chemical Geology, Elsevier Science Publishes B.V., Amsterdam-Prited in the Netherlands, 69(1988):87-93.

Dickinson, W.R. (1970) Interpreting detrital modes of greywacke and arkose, Jour. Sed. Petrology, 40: 695-707.

Dickinson, W.R., Beard, L.S., Brakenridge, G.R., Erjavec, J.L, Ferguson, R.C., Inman, K.F., Knepp, R.A., Lindberg, F.A., Ryberg, P.T. (1983) Provenance of North American Phanerozoic sandstone in relation to tectonic setting. Geol. Soc. Am. Bull., 94: 222-235.

Dickinson, W.R.; Suczek, Ch. A. (1979) Tectonics and sandstone composition, AAPG, 63(12): 2164-2182.

Dinelli, E., Testa, G., Cortecci, G. and Barbieri, M. (1999) Stratigraphic and petrographic constraints to trace elements and isotope geochemistry of Messinian sulfates of Tuscany. Mem. Soc. Geol. Ital. 54: 61–74.

Dill, H.G. A review of heavy minerals in clastic sediments with case studies From alluvial-fan through the near-shore environments, Earth-Science Reviews, 45: 103-132.

Dott, R.H. (1964) Wacke, Greywacke and Matrix—What Approach to Immature Sandstone Classification? Journal of Sedimentary Petrology, 34: 625-632.

Dunnington, 1952 in (Bellen, 1959) Bellen RCV, Dunnington HV, Wetzel IR, Morton D (1959) Lexique startigraphique international Asie, Iraq. 3 (10a).

Etemad-Saeed, N., Hosseini-Barzi, M.,A rmstrong-Altrin, J.S. (2011) Petrography and geochemistry of clastic sedimentary rocks as evidences for provenance of the Lower Cambrian Lalun Formation, Posht-e-badam block, Central Iran. J. Afr. Earth Sci., 61: 142-159.

Falcon, N.L. (1974) Southern Iran: Zagros Mountains. Geol. Soc. Lond. Spec. Publ. 4 (1): 199–211.

Fedo C.M., Keith N.S., Robert H.R (2003) Detrital Zircon Analysis of the Sedimentary Record, Reviews in Mineralogy and Geochemistry, 53(1): 277- 303. DOI: 10. 2113/0530277.

Feng, R. and Kerrich, R. (1990) Geochemistry of Fine Grained Clastic Sediments in the Archaean Abitibi Greenstone Belt, Canada: Implications for Provenance and Tectonic Setting, Geochimica et Cosmochimica Acta, 54: 1061-1081. http://dx.doi.org/10.1016/0016-7037 (90)90439-R.

REFERENCES

Floyd PA, Kelling G, Gocken SL, Gocken N (1991). Geochemistry and tectonic environment of basaltic rocks from the Miss ophiolitic melange, south Turkey. Chem Geol 89: 263-280.

Folk , R.L. (1974) Petrology of Sedimentary rocks, Hemphill publishing Comp. Texas, 182p.

Folk, R.L (1980) Petrology of Sedimentary Rocks, Hemphill Publishing, Austin, 182p.

Garzanti, E., Limonta, M., Resentini, A., Bandopadhyay, P.C., Ando, S., Vezzoli, G. (2013) Sediment recycling at convergent plate margins (Indo-Burman ranges and Andaman-Nicobar ridge. Earth Sci. Rev., 123: 113-132.

Getaneh W. (2002) Geochemistry provenance and depositional tectonic setting of the Adigrat Sandstone northern Ethiopia. J.Afr. Earth Sci. 35:185—198.

Gidon M, Berthier F, Billiaut JP, Halbronn B, Maurizot P (1974). Sur les caractères et l'ampleur du coulissement de la "Main Fault" dans la région de Borudjerd-Dorud (Zagros oriental, Iran). Cr Acad Sci 278: 701–704 (in French).

Goldschmidt, V. M. (1962) Geochemistry, London, Oxford University press, 730p.

Grosch, E. G., A. Bisnath, H. E. Frimmel, and W. S. (2007) Board Geochemistry and tectonic setting of mafic rocks in western Dronning Maud Land, East Antarctica: Implications for the geodynamic evolution of the Proterozoic Maud Belt, J. Geol. Soc. London, 164: 465–475.

Haas GJ., Jessica V., Tom A. (1999)Detrital Zircon Geochronology: New Evidence for an old Model for Accretion of the Southwest Baltic Shield, The journal of Geology, 107(5): 569-586.

Hessami, K. (2002) Tectonic History and Present-Day Deformation in the Zagros Fold- Thrust Belt, Doctoral dissertation, University of Uppsala.

Hiscott, R., 1984. Ophiolitic source rocks for Taconic-age flysch: Trace-element evidence, Geological Society of America Bulletin, 95, 1261-1267,

Hussain S.H., Aghawan T. A., (20015) Sedimentology and evolution of a foreland desert basin, Middle Eocene Gercus Formation (North and Northeastern Iraq), Arab J Geosci, 8:2799–2830. DOI: 10.1007/s12517-014-1352-8.

Henderson P (1984) General geochemical properties and abundances of the rare earth elements. In: Henderson P (ed) Rare earth elements geochemistry. Elsevier, Amsterdam, 1–32.

Hurlbut, C. S. (1971) Dana's Manual of Mieralogy6, 18th edition, 579p.

Ingersoll, R. V., C. A. Suczek, (1979) Petrology and provenance of Neogene sand from Nicobar and Bangal Fans, DSDP sites 211 and 218, Journal of Sedimentary Petrology, 49: 1217-1228.

Ingersoll, R. V., and Suczek, C.A. (1979) Petrology and Provenance of Neogene sand from Nicobar and Bengal fans, DSDP sites 211 and 218, Journal of Sedimentary Petrology, 49(4): 1217-1228.

Ingersoll, R. V., Bullard, T. F., Ford, R. L., Grimm, J. P., Pickle, J.D., Sares, S. W. (1984) The effect of grain size on detrital modes: a test of Gazzi-Dikinson point-counting method, Jour. Sed. Petrology, 45:n 103-116.

James, G.A. and Wynd, J.G. (1965) Stratigraphic Nomenclature of Iranian Oil Consortium Agreement Area. AAPG Bulletin, 49: 2182-2245.

Jassim, S.Z. and T. Buday (2006) Tectonic framework (Chapter 4). In S.Z. Jassim and J.C. Goff, (Eds.), Geology of Iraq. Dolin, Prague and Moravian Museum, Brno, 341 p.

Jassim, S.Z. and T. Goff (2006) Phanerozoic development of the northern Arabian Plate. In S.Z. Jassim and J.C. Goff, (Eds.), Geology of Iraq. Dolin,Prague and Moravian Museum, Brno, 341 p.

Jaza, I.M. (1992) Sedimentary facies analysis of the Tanjero Clastic Formation in Sulaimaniya District, northeast Iraq. Unpublished MSc thesis, Salahaddin University, 121 p.

Karim, K.H. (2004) Basin analysis of Tanjero Formation in Sulaimaniyah Area, NE Iraq, Unpub. Ph.D Thesis, College of Science, University of Sulaimaniyah. 133p.

Kamen-Kaye, M. (1971) A review of Depositional History and Geological Structure in Turkey. In: Campbell (Ed.), Geology and History of Turkey. The Petroleum Exploration Society of Libya, Tripoli, Libya, 111 – 137.

Karim, K.H. and Surdashy, A.M. (2005) Tectonic and depositional history of Upper Cretaceous Tanjero Formation in Sulaimaniyah area, NE Iraq, Jour. Zanko Sulaimani, 8, (1): 47–62.

Karim K.H., Surdashy, A.M., Ai-Barzinji S.T. (2007) concurrent and lateral deposition of flysch and molasse in the foreland basin of upper cretaceous and paleocene from NE-Iraq, Kurdistan region, Proceeding of the Second International Conference on Geo-Recourses of the Middle East and North Africa (GRMINA II), 757-769.

Karim, K H. Baziany, M M and Khanaqa P A (2018) New Ideas and Critical review of Middle Eocene Gercus Formation, Kurdistan Region, NE-Iraq. JZS 20 – 2 (Part-A),pp.81-94.

Kassab, I.I.M. (1972) Micropaleontology of Upper Cretaceous/Lower Tertiary of north Iraq, Univ. London, Unpub. PhD. Thesis, 310p.

Kassab, I.I.M. (1975) Planktonic Foraminifera Range in the Type Tanjero Formation (Upper Campanian-Maastrichtian) of North Iraq, Journal of Geological Society, Iraq, 8: 73-86.

Keer, P.F. (1959) Optical mineralogy, (3rd ed,) Mc Graw – Hill Book Co. Inc., New York. 442p.

Koralay T. (2010) Petrographic and geochemical characteristics of upper Miocene Tekkedag volcanics (Central Anatolia—Turkey), / Chemie der

Erde 70: 335–351.

Koshnawa, R.S., Horton, BK., Stockli, D.F., Barber, D.E., Tamar-Agha, M.Y., Kendall, J.J. (2017) Neogene shortening and exhumation of the Zagros fold-thrust belt and foreland basin in the Kurdistan region of northern Iraq, Tectonophysics, 694: 332–355.

Koyi, A.M.A. (2006) Petrochemistry, Petrogenesis and Isotope Dating of Walash Volcanic Rocks at Mawat-Chowarta Area, NE Iraq, Unpublished MSc. Thesis, University of Mosul, (In Arabic), 230p.

Krauskopf, K.B. (1979) Introduction to Geochemistry. McGraw Hill, New York.

Lacassie J.P., Roser B., Solar J.R.D. & Hervé F. (2004) Discovering geochemical patterns using self-organizing neural networks: a new perspective for sedimentary provenance analysis. Sed.Geol. 165: 175—191.

Lawa, F.A., A.I. Al-Karadakhi and K.M. Ismail (1998) An interfingering of the Upper Cretaceous rocks from Chwarta-Mawat Region (NE-Iraq). Iraqi Geological Journal, 31: 13-29.

Lee, Y. (1999) Geotectonic significance of detrital chromian spinel: a review. Geosci. J. 3:23–29.

López, J. M. G., Bauluz, B., Fernández-Nieto, C., & Oliete, A. Y. (2005) Factors controlling the trace-element distribution in fine-grained rocks: the Albian kaolinite-rich deposits of the Oliete Basin (NE Spain), Chemical Geology, 214(1): 1-19. http://dx.doi.org/10.1016/j.chemgeo.2004.08.024.

Mahjoor, A.S.; Karimi, M.; Rastegarlari, A. (2009) Mineralogical and geochemical characteristics of clay deposits from south Abarkouh district of clay deposit (central Iran) and their applications. J. Appl. Sci. 9: 601-614.

Mange, M.A. and Maurer, H. (1992) Heavy Minerals in Color, Chapman and Hall, London.

Mange, M.A. and Wright, D.T. (2007) Heavy mineral in use, Amestrdam, Elsevir Science, Development of Sedimentology, 58p.

Mason, B., Moore, C.B. (1982) Principles of Geochemistry, 4th edition, John Wiley and Sons, 344p.

McLennan, S. M., Taylor, S. R. and Eriksson, K. A. (1983) Geochemistry of Archaean shales from Pilbara Supergroup, Western Australia. Geochim. Cosmochim. Acta 47, 1211–1222.

McLennan S.M., Taylor S.R. & Eriksson K.A. (1983) Geochemistry of Archean shales from the Pilbara Supergroup, Western Australia. Geochim. Cosmochim. Acta 47: 1211—1222.

McLennan and Taylor (1991) Sedimentary rocks and Crustal evolution: Tectonic setting and secular trends, Journal of Geology, 99: 1-21.

McLennan, S. M. (1989) Rare Earth Elements in Sedimentary Rocks: Influence of Provenance and Sedimentary processes. Mineralogical Society of America, reviews in mineralogy, 21: 169-200.

McLennan, S.M. (2001) Relationships between the trace element composition of sedimentary rocks and upper continental crust. Geochem. Geophys. Geosystems, 2: 18-41.

McLennan, S.M., Hemming, S., McDaniel, D.K., Hanson, G.N. (1993) Geochemical approaches to sedimentation, provenance and tectonics. In: Johnsson, M.J., Basu, A. (Eds.), Processes Controlling the Composition of Clastic Sediments. Geological Society of American Special Paper, 21-40.

Miall, A.D. (1990): Principles of Sedimentary Basin Analysis, 2nd ed., Springer- Verlag, 668 pp.

Minas, H.A.A. (1997) Sequence Stratigraphic Analysis of the Upper Cretaceous Succession of Central and Northern Iraq., Unpubl. Ph. D. Thesis, University of Baghdad, 188p.

Mohammad Y, Kareem H, Anma R (2016) The Kuradawe Granitic Pegmatite From the Mawat Ophiolite, Northeastern Iraq: Anatomy, Mineralogy, Geochemistry, and Petrogenesis, The Canadian Mineralogist, V54, 986-1019 p.

Morton, A. C., (1985) Heavy minerals in provenance studies. in: (ed: G G Zuffa): Provenance of Arenites. Reidel, Dordrecht, 249-277.

Musa, E.O. (2007) Petrography, Geochemistry and Genesis of Copper-iron Mineralization and Associated Rocks in Waraz Area, Sulaimanya, NE Iraq. Unpubl. M.Sc. thesis. University of Baghdad, 155p.

Nesbitt, H.W.; Young, G.M. (1982) Early Proterozoic climates and plate motions inferred from major element geochemistry of lutites, Nature, 299: 715-717.

Nesbitt, H.W.,Young, G.M. (1984) Prediction of some weathering trends of plutonic and volcanic rocks based on thermodynamic and kinetic considerations. Geochimica et Cosmochimica Acta, 48 (7): 1523-1534.

Nickel E. (1973) Experimental dissolution of light and heavy minerals in comparison with weathering and intrastratal solution, Contribution to Sedimentology, 1: 1-125.

Paton, C., J. D. Woodhead, J. C. Hellstrom, J. M. Hergt, A. Greig, and R Maas (2010), Improved laser ablation U-Pb zircon geochronology through robust downhole fractionation correction, Geochem. Geophys. Geosyst., 11, Q0AA06, doi:10.1029/2009GC002618.

Pearce, J.A. (2008) Geochemical fingerprinting of oceanic basalts with applications to ophiolite classification and the search for Archean oceanic crust. Lithos, 100: 14-48.

Pearce, J.A., Cann, J.R. (1973) Tectonic setting of basic volcanic rocks determined using trace element analyses, Earth Planet. Sci. Lett., 19: 290- 300.

Pearce J. A. and Peate D. (1995) Tectonic Implications of the Composition of Volcanic Arc Magmas, Annual Review of Earth and Planetary Sciences, 23: 251-285.

Peterson, J.A. (2009) Geochemical Provenance of Clastic Sedimentary Rocks in the Western Cordillera: Utah, Colorado, Wyoming, and Oregon, All Graduate Theses and Dissertations, 439p. https://digitalcommons.usu.edu/etd/439.

Pettijohn, F.J. (1975) Sedimentary Rocks, third ed. Harper and Row, New York. 628p.

Pettijohn, F.J., Potter, P.E., Siever, R. (1987) Sand and Sandstone, second ed. Springer- Verlag, New York, 553p.

Pichler, T. and Humphrey, J.D (2001) Formation of Dolomite in recent island- arc sediments due to gas-sea water interaction, Journal of sedimentary research, 71 (3): 394-399.

Potter, P. E. (1978) Petrology and chemistry of modern big river sands, J. Geol., 86, 423-449.

Pettijohn, F.J., Potter, P.E., and Siever, R. (1987) Sand and Sandstone. 2nd Edition, Springer-Verlag, New York, 553 p.

Rahman M.J.J. & Suzuki S. (2007) Geochemistry of sandstones from the Miocene Surma Group, Bengal Basin, Bangladesh: Implications for provenance, tectonic setting and weathering. Geochem. J. 41:415-428.

Ranjan, N. and Banerjee, D.M. (2009) Central Himalayan crystallines as the primary source for the sandstone-mudstone suites of the Siwalik Group: New geochemical Evidence, Gondwana Res., 16: 687-696. Rev.1998. 45, 103-132.

Ravaut, R Bayer R., Hassani R., Rousset, D., A1 Yahya'ey A. (1997) Structure and evolution of the northern Oman margin: gravity and seismic constraints over the Zagros-Makran-Oman collision zone, Tectonophysics 279: 253-280.

Roser, B. P. and Korsch, R. J. (1988) Provenance signature of sandstone-mudstone suite determined using discriminant function analysis of major element data. Chem. Geol., 67: 119-139.

Ruiz, G.M.H., Seward, D,, Winkler, W., 2007. Evolution of the Amazon Basin in Ecuador with special reference to hinterland tectonics: data from zircon fission-track and heavy mineral analysis. In: M. Mange, D.K.Wright(Eds.), Heavy Minerals in Use, Developments in Sedimentology, 58: 907-934.

Saadallah, A. and Hassan, A.H. (1987) Sedimentological study of Selected section of Tanjero Formation, Iraqi Jour. Science, 28(3 and 4): 483 – 506.

Sharbazheri, K. M. I. (2008) Biostratigraphy and Paleoecology of Cretaceous/ Tertiary Boundary in the Sulaimania Region, NE Iraq, Unpublished PhD Thesis, University of Sulaimania Iraq. 200p.

Stockmal, G.S. and Beaumont, C. (1987) Geodynamic models of convergent margin tectonics: the southern Canadian Cordillera and Swiss Alps. In C. Beaumont and A. J. Tankard eds., Sedimentary basin-forming Mechanisms,

Vol. 12 of Canadian Society of Petrolum Geologists Memoirs. Calgary: Canadian Society of Petrolum Geologists, 393-412

Sa'ad Z. A.K. Al-Mashaikie; Abbas T. ; Abbas Al-Azzawi and Ali K. Kadhum (2013) Lithofacies Architecture of the Gercus Formation in Jabal Haibat Sultan, NE Iraq; New Concept of Lithostratigraphy and Depositional Environmental, Journal of Environment and Earth Science 3(12): 97-114.

Sa'ad Z. A.K. Al-Mashaikie; Abbas T. ; Abbas Al-Azzawi and Ali K. Kadhum (2014)Depositional environment of the Gercus Formation in Jabal haobat-Sultan, NE Iraq; New sedimentological approach, Iraqi Journal of Science, 55(2A):471-483.

Saura, E.; Vergés J.; Homke S.; Blanc E.; Serra Kiel J.; Bernaola G.; Casciello E.; Fernández N.; Romaire I.; Casini G.; Embry JC.;Sharp IR.; Hunt DW. (2011) Basin architecture and growth folding of the NW Zagros early foreland basin during the Late Cretaceous and early Tertiary. J Geol Soc. 168:235–250.

Sengor, A., and Yilmaz, Y. Tethyan (1981) Evolution of Turkey: A Plate Tectonic Approach. Tectonophysics, 75: 181 – 241.

Sun, S. S., McDonough, W. E. (1989) Chemical and isotopic systematics of ocean basalt: implications for mantle composition and processes. In Magmatism in the Ocean Basins (eds A. D. Saunders & M. J. Norry), Geological Society of London, Special Publication 42: 313–45.

Suttner, L.J.; Dutta, P.K. (1986) Alluvial sandstone composition and paleoclimate Framework mineralogy. J. Sediment. Petrology, 56: 329-345.

Sugisaki R. 1984: Relation between chemical composition and sedimentationrate of Pacific ocean-floor sediments deposited since the middle Cretaceous: Basic evidence for chemical constraints on depositional environments of ancient sediments. J. Geol. 92, 235—260.

Tasman, C, E, (1949) Stratigraphy of Southeast Turkey: Bulletin of the American Association of Petroleum Geologist, 33: 22-31.

Taylor SR and McLennan SM. (1985) The continental crust: its composition and evolution. Blackwell Scientific Publication, Carlton, 312p.

Toulkeridisa, T., Clauerb, N., Kronera, A., Reimera, T., Todt, W. (1999) Characterization, provenance, and tectonic setting of fig tree greywackes from the archaean barberton greenstone belt, South Africa. Sediment. Geol, 124: 113-129.

Turekian, K. and Wedepohl, K. (1961) Distribution of the Elements in Some Major Units of the Earth's Crust , GSA Bulletin (1961) 72 (2): 175–192.

Wani, H. and Mondal M. E. (2010) Petrological and geochemical evidence of the Paleoproterozoic and the Meso-Neoproterozoic sedimentary rocks of the Bastar craton, Indian Peninsula: Implications on paleoweathering and Proterozoic crustal evolution, Journal of Asian Earth Science, 38 (5): 220-232.

White, N.M., Pringle,M., Garzanti, E., Bickle, M., Najman, Y., Chapman, H.,

Friend, P. (2002) Constraints on the exhumation and erosion of the high Himalayan slab, NW India, from foreland basin deposits, Earth Science Reviewers, 195: 25-44.

White, W.M. (2005) Geochemistry. USA, 701p.

Wilson, M. (1989) Igneous Petrogenesis. Unwin Hyman Ltd, London. 466p.

Wedepohl K. H. (1978), Handbook of Geochemistry, Vol. II/5. Berlin-Heidelberg, New York 1. Springer-Verlag.

Winter, J.D. (2001) An introduction to igneous and metamorphic petrology. Prentice-Hall, Inc., Upper Saddle River.

Wrobel-Daveau, J.-C., Ringenbach, J.-C., Tavakoli, S., Ruiz, G., Masse, P. & Frizon De Lamotte, D. (2010) Evidence for mantle exhumation along the Arabian margin in the Zagros (Kermanshah area, Iran). Arabian Journal of Geosciences 3: 499–513.

Wronkiewicz, D.J., Condie, K.C. (1987) Geochemistry of Archean shales from the Witwatersrand Supergroup, South Africa: Source-area weathering and Provenance. Geochim. Cosmochim. Acta, 51: 2401-2416.

Zurar, S. S. (2016) Petrology and Isotope Dating of Volcanic Rocks within Qulqula Radiolarite, Iraqi Kurdistan Region. Unp. MSc. Thesis, Dept. of Geology, University of Sulaimani, Iraq, 147p.

المستخلص

تم استخدام الزركون الفتاتي والزمن الجيولوجي لليورانيم –رصاص والجيوكيمياء الكاملة للصخرة لتوصيف الصخور السليكية الفتاتية لعصري الطباشيري الاعلى والايوسين الاوسط من صخور الفليش والمولاس لتكويني تانجيرو وجيركس على التوالي في شمال شرق العراق . كما تم استخدام هذه البيانات لتعيين منشأ الفتات الصخري وتقييم التطور التكتوني لحزام زاكروس الأورجيني الشمالي.

جيوكيمياء السحنات الرملية تكوين تانجيرو أظهرفرز رديئ وترسيب سريع . تركيز ايون عنصر الليثوفايل (LILE) في العينات المدروسة أقل من القيم المناظرة لها في ايون القشرة القارية العلوية وصخور شيل بعد القوس الأسترالي مما يشير على أن مصادرها هي ذات دلالات قاعدية وفوق قاعدية. مع بعض من مكونات الكرتون.

تشير نسب $(SiO_2 / (Al_2O_3 + K_2O + Na_2O$ للحالة المناخية القديمة أثناء الترسب إلى أن التغير السريع في المناخ من مناخ شبه رطب إلى مناخ شبه جاف أو مصادر متعددة ربما قد تسببت انخفاضًا في النضوج الكيميائي.

لكن المخططات التمييزية الثلاثية Q-F-RF و Th-Sc-Zr / 10 تدعم تكون فليش تانجرو وجيركس مولاس من مصادر متعددة ، مثل حقول القوس OIA ، واختراقات البازلت المحيطي والأوروجين المعاد تدويره المطابق للكراتون العربي.

تمت دراسة مجموعات بيانات العمر للزركون الفتاتي واليرانيوم – رصاص من فلش تانجيرو ببساطة لأنه يمكن إعادة تدويرها بشكل متعدد داخل الأنظمة الرسوبية. يبلغ عمر أصغر تجمع للزركون في تانجيرو فليش 93 مليون عامًا تقريبًا والذي يتزامن بشكل وثيق مع الحدث الماكماتي لقوس الالبين – سينومانين (106-92 مليونً سنة)

بالإضافة إلى العمر ألاخير ، تُظهر مجموعة بيانات الزركون الفتاتي واليورانيوم-رصاص توزيعًا عمريًا قويًا: 400 و 448 و 511 و 553 و 646 و 779 و 878 و 996 و 1121 مليون سنة والتي تشير إلى دورات متعددة مشتقة في الغالب من الدرع العربي النوبي الذي تم استضافته في وقت ما من قبل حوض قلقولا الراديولاري (بلانيشباجيان المبكر – تورونيان) الذي كان يقع على طول الحافة الخاملة للطبق العربي.

بينت قياسات الزركون الفتاتي واليورانيوم- رصاص ان جيركس مولاس يندرج في العديد من المجموعات العمرية القابلة للفصل بين 92-102 (ألبيان سينومانيان) ، 221 (الترياسي الأعلى) ، 395-511 (الكامبري)

، 570- 645 (النيوبروتروزويك) ، 1111 (ميزوبروتروزويك) ، وأعداد أقل من العصور القديمة الباليوزوك (1622-1991 مليون سنة)

مصدر البروتيروزويك زركون الفتانتي هو مبهم. اذ لا تتوافق ذروة العمر عند 1.1 و 1.5 و 1.6 و 1.9 كاما (بروتيروزويك) مع أي مكاشف صخرية معروفة من صخور ما قبل الكامبري في العراق ، وقد يكون من المفيد الاستمرار في البحث عن هكذا صخور قاعدة. من المحتمل أن نشأ الزركون الفتاتي الذي يتراوح عمره بين 0.63 و 86.86 كاما من الدرع العربي النوبي.

ذروة العمر عند 0.55 كاما ترتبط مع صهارة كادوميان والتي ذكرت من شمال كوندوانا. يتم تفسير ذروة العمر عند ~ 0.4 كاما لتمثل تصدع الكوندوانا وانفتاح الباليوثيثس. تشير الفئات العمرية الأصغر من 93 مليون سنة إلى أن جزءًا من الزركون الفتاتي تم نقله مباشرةً من القوس الصخري النشط المعاصر

تشير أطياف العمر للزركون الفتاتي واليورانيوم رصاص من الجركس مولاس إلى أن رواسب الفورلاند إما تتدفقت من منا مناشئ متعددة أو هي نتيجة لإعادة التدوير من المعقد التراكمي لتكوين (قلقلة الراديولاري 221مليون سنة). خلال مرحلة ما قبل التراكم ، من المحتمل أن يكون الحوض الراديولاري الموجود على طول الحافة الخاملة للطبق العربي بمثابة مستودع الرواسب الوسطية لمعظم أو كل الزركون الفتاتي.

تم اعادة بناء الجغرافيا القديمة والتطور التكتوني لحوض فورلاند زاجروس (نيوجين) وتم تقسيمهما إلى مرحلتين تكتونيتين. يتم تعريف المرحلة المبكرة بتكون تظاريس الكامباني (أي الاسفين الاووجيني) الذي يكون احمال كافية لإنتاج حوض منحني مع أعمق جزء يقع قريب من طرف الأحمال.

يمتلئ هذا الحوض المقوس بفتاتيات الفلش لعصر الماستريختيان - ألايوسين المبكر (المشار إليه في تتابع تانجيرو- كولوش فليش) تتميز المرحلة المتأخرة بتغيير متزامن لملئ المواد الفتاتية للحوض والتغييرات في اتجاهات وميل الحوض للتعويض عن الحد من الحمل بكل من التعرية والتمديد ، وبالتالي ، فقد تم ختم الحوض بالتضحل التتابعي نحو الاعلى منتهيا بتكوين جيركس القاري.

مصدر و الوضع التكتوني لوحدات الصخور الرملية
لتكويني تانجير و جيركس:
بتطبيقات جيوكيميائيه و عمرية , اقليم كردستان,
شمال شرق العراق

اطــروحــة

مقدمة الى مجلس كلية العلوم – جاميعة السليمانية

كجزء من المتطلبات نيل درجة دكتورا فلسفة

في علم الارض – الرسوبيات

مـن قـبـل

ديــريــن مـحـمـد صديق

بكالوريوس-جامعة السليمانية ١٩٩٨

ماجستير-جامعة السليمانية ٢٠١٠

بــأشــراف

د.نةبةز رشيد حمة عزيز

اســتــاذ مســاعــد

شباط ٢٠٢٠ **فيبراير ٢٠٢٠**

پوختە

تەمەنزانی یۆرانیۆم-قورقوشم لە پارچە زرکۆنەکان و جیۆکیمیای بەردەکان بەکار هاتووە دیاریکردنی سیفەتاکانی بەردە پارچەبووە سیلیکاتیەکانی بەشی سەرەوەی تەمەنی کریتاشیەس و ناوەندی ئیۆسین لە پێکهاتووەکانیی فلێشی تانجەرۆ و مۆڵاسی جێرکەس، لە باکووری خۆرهەڵاتی عێراق.

هەروەها ئەم زانیاریانە بەکارهاتووە بۆ دیاریکردنی بنەچەی پارچە بەردەکان و وە پەرەسندنی تێکتۆنی پشتێنەی ئۆرۆجێنی باکوری زاگرۆس. جیۆکیمیای بەردە لمینەکەی پێکهاتووی تانجەرۆ نا چونیەکەی لە قەبارەی دەنکۆڵەکان و خێرا نیشتنی بەردە لمینەکەی پشتڕاستکردەوە.

چڕی ئایۆنە گەورەکانی توخمە لیسۆفایلەکان لە نمونە لێکۆڵینەوە لەسەرکراوەکاندا کەمترە لەو نرخەی لە بەشی سەرەوەی توێکڵی کیشوەری و قوڕی ئوسترالی دوای ئەرکایەن هەیە و سەرچاوە سەرەکیەکەی مافیک و ئولترا مافیکە لەگەڵ هەندێ مادەی ناو کراتۆن.

باری کەش و هەوای کۆن لەمیانەی نیشتندا بە گوێرەی ڕێژەی ($SiO_2/(Al_2O_3+K_2O+Na_2O)$) گۆڕانی خێرا پیشان ئەدات لە نیمچە شیدارەوە بۆ نیمچە وشک یان فرە سەرچاوەیی بوەتە هۆی کەمبونەی ناپاکی کیمیایی.

بەڵام کڵێشەی جیاکەرەوەی سێگۆشەیی (Q-F-RF and Th-Sc-Zr/10) ئەوە پشت ڕاست ئەکاتەوە کە فلێشی تانجەرۆ لە سەرچاوەی جیاوازەوە هاتووە، وەک مەیدانی نێوەندی ئارک و دورگەی ئوقیانوسی بازەڵتی و کراتۆنی عەرەبی چەندبارەبووەوە.

زانیاری تەمەنی پارچە زرکۆنەکانی فلێشی تانجەرۆ لێکۆڵینەوەی لەسەرکراوە و ئەوە پیشان ئەدات کە چەندبارە بووەتەوە لە ناو سیستەمێکی نیشتندا. تازەترین کۆمەڵە زرکۆن لە فلێشی تانجەرۆ ئەگەڕێتەوە بۆ ٩٣ ملیۆن ساڵ بەر لە ئێستا و هەمەن تەمەنی ڕوداوی ئارکی بورکانی تەمەنی ئەلبیان-سینۆمانیان (٩٢-١٠٦ ملیۆن ساڵ لەمەو پێش).

لەگەڵ ئەوەشدا زانیاری تەمەنی پارچە زرکۆنەکان دابەشبونێکی جیای هەیە: (٤٠٠،٤٤٨،٥١١،٥٥٣،٦٤٦،٧٧٩،٨٧٨،٩٩٦،١١٢١ ملیۆن ساڵ لەمەو پێش) ئەم پێشنیازی چەنبارەبونەوە سەرچاوەی بنکەی نیۆپرۆتیرۆزۆیک ئەکات لە قەڵغانی عەرەبی-نوبیان کە لە هەندێ شوێندا خانەخوێکەی بریتی یە لە ڕادیۆلاریای قوڵقوڵەی تەمەنی پلێنسباچیان-تورۆنیان کە دەکەوێنات کەناری ناچالاکی عەرەبی یەوە.

پێوانە کردنی یۆرانیۆم-قوڕوقوشم لە پارچە زرکۆنەکانی مۆڵاسی جێرکەس ئەوە دەردەخات کە تەمەنەکان ئەبنە چەند کۆمەڵەیەکەوە: ٩٢-١٠٢ (ئەلبیان-سینۆمانیان)، ٢٢١(سەرەوەی جوراسیک)، ٣٩٥-٥١١(کامبریان)، ٥٧٠-٦٤٥(نیۆپرۆتیرۆزۆیک)، ١١١١(میزۆپرۆتیرۆزۆیک)، وە هەندێکی کەم لە پالیۆپرۆتیرۆ زۆیک (١٦٦٢-١٩٩١) ساڵ لەمەو پێش.

سەرچاوەی پارچە زرکۆنەکانی تەمەنی پرۆتیرۆ زۆیک وەک مەتەڵ وایە، تەمەنەکان لە نێوان 1.1, 1.5, 1.6, 1.9 ملیار ساڵدان، وە هیچ دەرکەوتەیەکی تەمەنی پریکامبریان لە عێراق نی یە، لەوانەیە بە سودبێت ئەگەر بەردەوام بۆ بنچینە بگەڕێین. ئەو کۆمەڵە پارچە زرکۆنەی تەمەنیان لە نێوان 0.63–0.86 ملیار ساڵدایە لەوانیە بنەچەکەی قەڵغانی عەرەبی-نوبیان بێت. ئەوانەی تەمەنی 0.55 ملیار ساڵن بەروارد ئەکرێت بە چالاکی بورکانی کادۆمیان لە باکووری گۆندوانا. ئەوانەی تەمەنی نزیکەی 0.4 ملیار ساڵن بە کاتی شکانی کیشوەری گۆندوانا و کردنەوەی دەریان تێتیسی کۆن دادەنرێت. تازەترین کۆمەڵە تەمەنی ٩٣ ملیۆن ساڵە کە ئەوە دەنوێنێت ڕاستەوخۆ لە چالاکی بورکانی ئارکەوە هاتووە.

تەمەنە جیاوازەکانی پارچە زرکۆنەکانی مۆڵاسی جێرکەس ئەوە دەخاتە ڕوو کە نیشتووەکانی فۆرلاند یان لە سەرچاوەی جیاوازەوە هاتوون یان چەند بارەبووەوەی ناوچەی کەڵەکەبووی ئاڵۆزە (ڕادیۆلارایتی قوڵقوڵە، ٢٢١ ملیۆن ساڵ). لە میانەی پێش-کەڵەکەبوون هەرچەندە حەوزی ڕادیۆلارایت کەوتۆتە کەناری ناچالاکی عەرەبیەوە و وەک کۆگایەکی نیشتوو نێوەنگیر بووە بۆ هەموو پارچە زرکۆنەکان.

جیۆگرافیای کۆن و پەرەسەندنی تێکتۆنی حەوزی تەکتۆنی زاگرۆس لە تەمەنی نیۆجین داڕێژراوەتەوە و دابەشکراوە بۆ دوو قۆناغ. قۆناغی سەرەتایی کە ئەناسرێت بە کەڵەکەبووی کەمپانیان (پوازی ئۆرۆجێنی) بەو قورساییەی کە هەیبووە بووەتە هۆی بەرهەم هێنانی حەوزی شەپۆلی کە قوڵترین شوێنی ئەکەوێتە ڕێکی زۆرترین قورسایی. ئەم حەوزە شەپۆلی یە پڕبۆتەوە بە کلاستیکی فلێشی تەمەنی ماستریختیان-سەرەتای ئیۆسین (پێکهاتووی تانجەرۆ و کۆڵۆش).

قۆناغی درەنگ کە بەوە جیا دەکرێتەوە کە هەردوو گۆڕانی پڕبونەوەی حەوزی کلاستیکی و گۆڕان لە ئاڕاستەی لاری بەیەکەوە ڕویانداوە کە بۆتە هۆی کەمبونەوەی قورسایی لە ئەنجامی رووداني ڕوتانەوە و کشاندا. لەبەر ئەوە قوڵی حەوزەکە کەمی کردووە و بۆتەهۆی نیشتنی پێکهاتووی جێرکەس کە نیشتووی سەر کیشوەرەکانە.

سەرچاوە و باری تکتۆنی یەکەی بەردە لمییەکانی هەردوو پێک هاتەی تانجەرۆ و جێرکەس: پراکتیزە کردنی جیۆ کیمیاوی و تەمەنزانی . هەرێمی کوردستان . باکوری رۆژهەلاتی عێراق

نامەیەکە

پێشکەش کراوە بە کۆلێژی زانست لەزانکۆی سلێمانی وەک بەشی تەواوکەر بۆ بەدەست هێنانی پلەی دکتۆرا لەزانستی جیۆلۆجی (چینە نیشتوەکان) .

لەلایەن

دێرین محمد صدیق

بەکالویورس لە زانستی جیۆلۆجی (١٩٩٨)

ماستەر لەزانستی جیۆلۆجی (٢٠١٠)

بەسەرپەرشتی

د.نەبەز رەشید حەمە عەزیز

پرۆفیسۆری یاریدەدەر

٢٧١٩رەشەمێ **٢٠٢٠ زاینی**